TALLINN UNIVERSITY OF TECHNOLOGY
DOCTORAL THESIS
44/2018

Effects of Zn^{2+} Ions and Environmental Conditions on the Fibrillization of Insulin

ANDRA NOORMÄGI

TTÜ PRESS

TALLINN UNIVERSITY OF TECHNOLOGY
School of Science
Department of Chemistry and Biotechnology

Dissertation was accepted for the defense of the degree of Doctor of Philosophy in Gene Technology on June 21, 2018.

Supervisors: Prof. Peep Palumaa, PhD,
Department of Chemistry and Biotechnology,
Tallinn University of Technology, Estonia

Vello Tõugu, PhD,
Department of Chemistry and Biotechnology,
Tallinn University of Technology, Estonia

Adviser: Andres Salumets, PhD,
Institute of Biomedicine and Translational Medicine,
University of Tartu, Estonia

Opponents: Sebastian Wärmländer, PhD,
Department of Biochemistry and Biophysics,
Stockholm University, Sweden

Erki Enkvist, PhD,
Institute of Chemistry,
University of Tartu, Estonia

Defense of the thesis: August 23, 2018 Tallinn University of Technology

Declaration:
Hereby I declare that this doctoral thesis, my original investigation and achievement, submitted for the doctoral degree at Tallinn University of Technology has not been submitted for any academic degree.

Andra Noormägi

ISSN 2585-6898 (publication)
ISBN 978-9949-83-293-4 (publication)
ISSN 2585-6901 (PDF)
ISBN 978-9949-83-294-1 (PDF)

TALLINNA TEHNIKAÜLIKOOL
DOKTORITÖÖ
44/2018

Zn^{2+} ioonide ja keskkonnatingimuste mõju insuliini fibrillisatsioonile

ANDRA NOORMÄGI

TTÜ KIRJASTUS

Contents

List of Publications 6
Author´s Contribution to the Publications 7
Introduction 9
Abbreviations 11
1. Review of literature 12
1.1 Insulin 12
1.2 Insulin Signaling 12
1.3 Insulin Synthesis 14
1.4 Diabetes mellitus 15
1.4.1 Type 1 diabetes mellitus 15
1.4.2 Type 2 diabetes mellitus 17
1.5 Structure of Insulin 18
1.6 Mechanism of Insulin Fibrillization 20
1.7 Monitoring of Insulin Fibrillization 23
1.8 Factors Affecting Fibril Formation 24
1.8.1 Effect of pH on Insulin Fibril Formation 24
1.8.2 Interaction of Insulin with Zn^{2+} Ions 25
1.8.3 Effect of Temperature on Insulin Fibril Formation 27
1.8.4 Effect of Insulin Concentration on Fibril Formation 27
1.8.5 Effect of Ionic Strength on Insulin Fibril Formation 29
1.8.6 Effect of Denaturants on Insulin Fibril Formation 29
1.8.7 Effect of Agitation on Insulin Fibril Formation 30
1.9 Morphology of Insulin Fibrils 31
2. Aims of the study 33
3. Materials and methods 34
4. Results 35
5. Discussion 37
Conclusions 40
References 41
Acknowledgement 51
Abstract 52
Kokkuvõte 53
Appendix 55
Publication I 57
Publication II 67
Publication III 75
Publication IV 83
Curriculum vitae 91
Elulookirjeldus 93

List of Publications

This thesis is based on the following publications, which will be referred to in the text by their Roman numerals.

I Noormägi, A., Gavrilova, J., Smirnova, J., Tõugu, V., Palumaa, P. "Zn(II) ions co secreted with insulin suppress inherent amyloidogenic properties of monomeric insulin" (2010) Biochem J.; 430(3): 511-518

II Noormägi, A., Primar, K., Tõugu, V., Palumaa, P. "Interference of low-molecular substances with the thioflavin-T fluorescence assay of amyloid fibrils" (2011) J Pept Sci.; 18(1): 59-64

III Tiiman, A., Noormägi, A., Friedemann, M., Krishtal, J., Palumaa, P., Tõugu, V. "Effect of agitation on the peptide fibrillization: Alzheimer´s amyloid-β peptide 1-42 but no amylin and insulin fibrils can grow under quiescent conditions" (2013) J Pept Sci.; 19(6): 386-391

IV Noormägi, A.; Valmsen, K.; Tõugu, V.; Palumaa, P. "Insulin fibrillization at acidic and physiological pH values is controlled by different molecular mechanisms" (2015) The Protein Journal.; 34(6): 398-403

Author´s Contribution to the Publications

I The author participated in experimental design, performed the experimental work, analyzed the data and participated in the manuscript preparation.

II The author participated in experimental design, performed the experimental work, analyzed the data and participated in the manuscript preparation.

III The author participated in experimental design and in conduction of the fluorimetric experiments and analyzed the data.

IV The author participated in experimental design, performed the experimental work, analyzed the data and participated in the manuscript preparation.

Introduction

Before the discovery of insulin, diabetes was a fatal disease and it was exceptional for people with diabetes to live for more than a year or two. The big breakthrough that led to the use of insulin to treat diabetes occurred in 1922, when Frederick G. Banting, Charles H. Best, J.J.R. Macleod removed dog´s pancreases and made them diabetic. Subsequently, the fluid from healthy dog´s islets of Langerhans was isolated and injected into the diabetic dogs. It was noted that the glucose levels of the dogs decreased, after the injections with the extract. These historical events represent the most important breakthrough in medicine and therapy of patients with diabetes, saving millions of lives for almost a century.

In 1955, Frederick Sanger determined the primary structure of insulin, which was the first peptide to be sequenced. Because of this discovery, it is known that every protein/peptide in living organisms has a unique amino acid sequence. Moreover, in 1969, Dorothy Hodgkin determined the 3D structure of insulin as the $2Zn^{2+}$-stabilized hexamer. Since that, the role of insulin actions from the molecular to the whole body level has been studied intensively. Despite a large amount of medical and biochemical research, the mechanisms of insulin action and insulin resistance are incompletely understood.

One of the most common physical instability problems of proteins and peptides is the tendency to form amyloid fibrils. Protein fibrillization is associated with more than 40 human pathologies, including the most common neurodegenerative diseases and type 2 diabetes mellitus. Moreover, the formation of amyloid is assumed to be a generic property of a polypeptide chain. Although these diseases-associated proteins and peptides are not related in sequence and structure, their fibrils are characterized by a common structural motif, the cross-β structure in which individual strands of the β-sheets run perpendicular to the long axis of the fibrils. This indicates that the fundamental mechanism of fibrillization in different pathologies may be common.

Insulin is one of the peptides that forms easily amyloid-like fibrils *in vitro*. The most challenging problem with insulin fibrillization is in the production, storage and delivery of the artificially produced hormone. However, pathological conditions related to insulin fibrils formation are relatively uncommon. Small amounts of insulin fibrils have been observed after continuous subcutaneous insulin infusion and after repeated insulin injections. From a physiological point of view, insulin fibrillization is undesirable process because it removes monomeric insulin out of secretion and prevents its interaction with insulin receptors. Moreover, it is know that insulin fibrillization occurs via intermediate misfolded oligomers and prefibrillar aggregates and some of these might even be cytotoxic or immunogenic. Therefore, it is important to study the mechanisms of insulin fibrillization to further improve the therapeutic use of insulin, as well as to shed light into the basic molecular features of amyloid formation.

Insulin has become one of the best models for investigating fibrillization mechanisms in general. The fibrillization kinetics can be influenced by several environmental factors, including pH, temperature, peptide concentration, agitation, etc. It is generally believed that insulin fibrillization occurs via a uniform reaction mechanism under various conditions, however, this has been never proved experimentally. Moreover, metal ions such as Zn^{2+} and Cu^{2+} have also been demonstrated to have pronounced effects on the fibrillization of a variety of amyloidogenic peptides. It is known that in the secretory granules, insulin is densely packed together with Zn^{2+} ions into crystals of $Zn_2Insulin_6$

hexamer, which prevents fibrillization of the peptide. Therefore, injection solutions of insulin usually include well-dosed equivalents of Zn^{2+} ions. However, the question arises as to what factors prevent the fibrillization after release from the pancreatic β-cells when insulin dissociates into active monomers, which are the most aggregation-prone form of the peptide. The effect of co-secreted Zn^{2+} ions on the fibrillization of monomeric insulin is unknown, however, it might prevent insulin fibrillization.

The goal of this study was to gain more understanding about the molecular mechanism of insulin fibrillization. We examined the effect of Zn^{2+} ions on the fibrillization of monomeric insulin. Based on our results we proposed a mechanism for the assembly and fibrillization of insulin in the presence of Zn^{2+} ions. We also tested whether substances that have been studied as inhibitors of Aβ42 fibrillization compete with ThT for binding sites within insulin fibrils. It was found that several low-molecular weight compounds interfere with the fluorescence of ThT and cause false positive results. Finally, we studied and compared the kinetics of insulin fibrillization at different environmental conditions. The results indicated that fibrillization of insulin at acidic and physiological pH values occurs via different molecular mechanisms. The obtained results provide a more detailed understanding of the molecular mechanisms of amyloid formation.

Abbreviations

Aβ	Amyloid-β peptide
AAS	Atomic absorption spectroscopy
AFM	Atomic force microscopy
CPH	Carboxypeptidase H
DM	Diabetes mellitus
E_a	Enthalpy of activation
ER	Endoplasmatic reticulum
ERK	Extracellular signal-regulated protein kinase
ESI-MS	Electrospray ionisation mass spectrometry
FOXO	Forkhead box O
GdnHCl	Guanidine hydrochloride
GLUT4	Glucose transporter 4
GSK3	Glycogen synthase kinase 3
HEWL	Hen egg white lysozyme
IAPP or amylin	Islet amyloid polypeptide
IR	Insulin receptor
IRS	Insulin receptor substrate
K_d	Conditional dissociation constant
LADA	Latent autoimmune diabetes in adults
MAPK	Mitogen-activated protein kinase
MARD	Mild age-related diabetes
MOD	Mild obesity-related diabetes
mTORC1	Mammalian target of rapamycin complex 1
PC1/3 and PC2	Prohormone convertases
PDK1	Phosphoinositide-dependent kinase 1
PICUP	Photo-induced cross-linking of unmodified proteins
PI3K	Phosphatidylinositol 3-kinase
PKB	Protein kinase B
Ras	Rat sarcoma
Rheb	Ras homolog enriched in brain
SAID	Severe autoimmune diabetes
SAXS	Small angle X-ray scattering
SEC	Size-exclusion chromatography
SIDD	Severe insulin-deficient diabetes
SIRD	Severe insulin-resistant diabetes
ZnT8	Zinc transporter 8
T1DM	Type 1 diabetes mellitus
T2DM	Type 2 diabetes mellitus
TEM	Transmission electron microscopy
ThT	Thioflavin T
TSC1/2	Tuberous sclerosis complex 1,2

1. Review of literature

1.1 Insulin

Insulin, a 51-residue peptide hormone crucial for glucose metabolism, is produced and matured within the pancreatic β-cells of the islets of Langerhans. Most importantly, insulin enables blood sugar, primarily glucose to enter into the body cells where it can be used as a fuel for production of biological energy. Insulin stimulates uptake of glucose into skeletal muscle, liver and adipose tissue and storage of glucose in the form glycogen for using in the future (Shulman, Rossetti et al. 1987; Newsholme and Dimitriadis 2001). Besides its major role insulin is involved also in regulation of lipid and protein metabolism (Dimitriadis, Mitrou et al. 2011). Insulin promotes fatty acid synthesis in adipose tissue and liver along with formation and storage of triglycerides. Moreover, insulin prevents lipolysis in adipose tissue by inhibiting the intracellular lipase activity that hydrolyzes triglycerides to release fatty acids (Chakrabarti, Kim et al. 2013). Insulin also stimulates the uptake of amino acids from plasma into muscle, adipose tissue, liver and other tissues, which, in turn promotes the rate of protein synthesis (Liu and Barrett 2002). At the same time insulin decreases the rate of protein degradation in muscle cells (Dimitriadis, Mitrou et al. 2011).

1.2 Insulin Signaling

Insulin mediates its actions through binding to insulin receptors (IR) on the surface of target cells. The IR signaling pathway mediates both the metabolic and the mitogenic effects of insulin. The IR is a transmembrane tyrosine kinase, which is a tetramer consisting of 2 α and 2 β glycoprotein subunits linked by disulphide bonds (Ullrich, Bell et al. 1985; Kido, Nakae et al. 2001). Insulin binds to the extracellular α subunit of the enzyme, resulting in a conformational change in the receptor that causes autophosphorylation of Tyr residues in the intracellular component of the β subunit. Phosphorylation of β subunit activates Tyr kinase activity of the receptor (Lee, Pilch et al. 1997). The activated IR kinase phosphorylates intracellular proteins known as insulin receptor substrates (IRS). Phosphorylated IRS proteins then bind other signaling molecules that activate further cellular actions of insulin (Kido, Nakae et al. 2001), including the phosphatidylinositol 3-kinase (PI3K). Activated PI3K phosphorylates membrane phospholipids and generates 3-phosphoinositides (phosphatidyl-inositol-3,4-bisphosphate (PIP2) and phosphatidyl-inositol-3,4,5-trisphosphate (PIP3)) (Alessi and Cohen 1998), which bind to the phosphoinositide-dependent kinase 1 (PDK1). PDK1 activates another kinases called protein kinase B (PKB) and protein kinase C (PKC). PKB plays an important role by linking glucose transporter (GLUT4), the insulin dependent glucose transporter protein, to the insulin signaling pathway. It activates GLUT4 which moves to the cell surface to transport glucose into the cells (Huang and Czech 2007). GLUT4 transporters are found in muscle and adipose tissue (Graham and Kahn 2007; Dimitriadis, Mitrou et al. 2011).

Activated PKB phosphorylates and inactivates glycogen synthase kinase 3 (GSK3) (Cross, Alessi et al. 1995). GSK3 phosphorylates glycogen synthase (GS) which in turn inhibits glycogen synthesis, therefore the inactivation of GSK3 by PKB promotes glucose storage as glycogen. Moreover, PKB phosphorylates and downregulates the forkhead box O (FOXO) transcription factors which regulates the expression of genes involved in cell growth, proliferation, differentiation and longevity. The inhibition of FOXO

suppresses gluconeogenesis (Zhang, Patil et al. 2006). PKB also phosphorylates and downregulates the tuberous sclerosis complex 1/2 (TSC1/2). TSC1/2 functions as a GTPase-activator protein (GAP) for the small Ras (rat sarcoma)-related GTPase Rheb (Ras homolog enriched in brain). The active, GTP-bound form of Rheb directly interacts with the mammalian target of rapamycin complex 1 (mTORC1) to stimulate its activity (Long, Lin et al. 2005). Activated mTORC1 regulates cell growth, proliferation and survival (Wullschleger, Loewith et al. 2006).

Finally, PKB deactivates of the BCL2 (B-cell lymphoma 2)-associated agonist of cell death (BAD), which inhibits the cellular apoptotic program (Datta, Dudek et al. 1997).

Phosphorylated IRS proteins also activates the growth factor receptor-bound protein 2 (GRB2). The growth factor receptor-bound protein 2-son of sevenless (GRB2-SOS) complex connects with the Ras pathway (Margolis and Skolnik 1994). Ras then activates Ser/Thr kinase Raf (named for Rapidly Accelerated Fibrosarcoma), which phosphorylates and activates Tyr/Thr kinase MEK (a MAP kinase kinase), which in turn phosphorylates and activates MAPK/ERK (mitogen-activated protein kinase/extracellular signal-regulated protein kinase) (Moodie, Willumsen et al. 1993). Activated MAPK phosphorylates different transcription factors that regulate genes involved in cell growth, proliferation, differentiation and survival (Cargnello and Roux 2011).

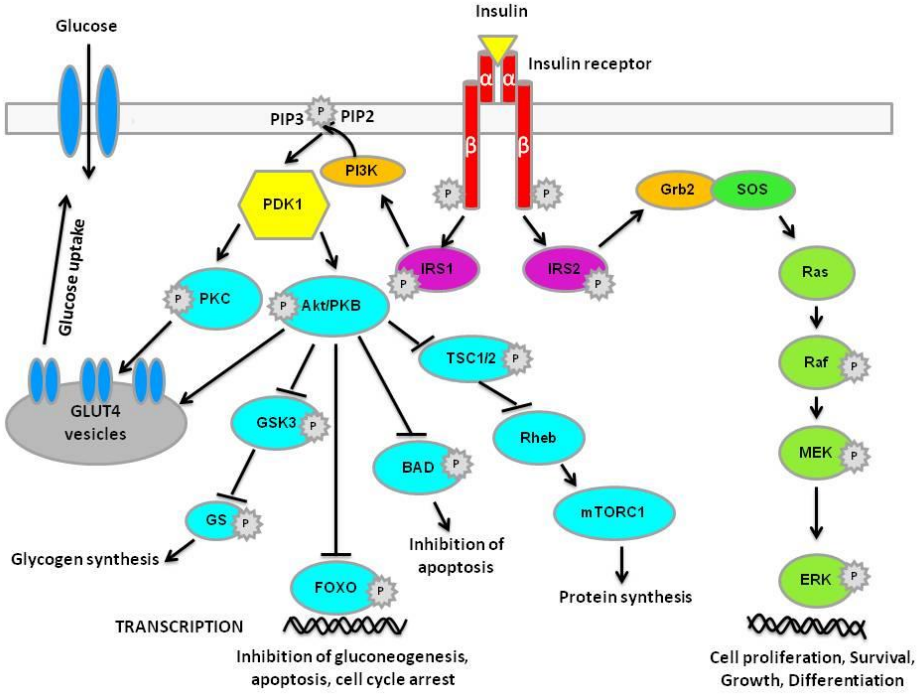

Figure 1. *Insulin signaling pathway: Binding of insulin to the insulin receptor activates a signaling cascade that involves multiple phosphorylation events (grey stars) that mediates both the metabolic and the mitogenic effects of insulin.*

1.3 Insulin Synthesis

Production of insulin involves the mRNA-directed synthesis of the insulin precursor preproinsulin, which is converted to proinsulin by the removal of its signal sequence during insertion into the endoplasmatic reticulum (ER) (Weiss, Steiner et al. 2000). Within the ER the proinsulin folds into the native three dimensional structure and three essential disulfide bonds are formed (Huang and Arvan 1995). After its assembly, the folded proinsulin is transported into secretory granules in the Golgi apparatus (Orci, Ravazzola et al. 1985), where proinsulin is cleaved endo - and exoproteolytically to yield active insulin and C-peptide. Mature insulin and free C-peptide together with islet amyloid polypeptide (IAPP or amylin) are then stored inside these secretory granules of pancreatic β-cells (Landreh, Alvelius et al. 2014).

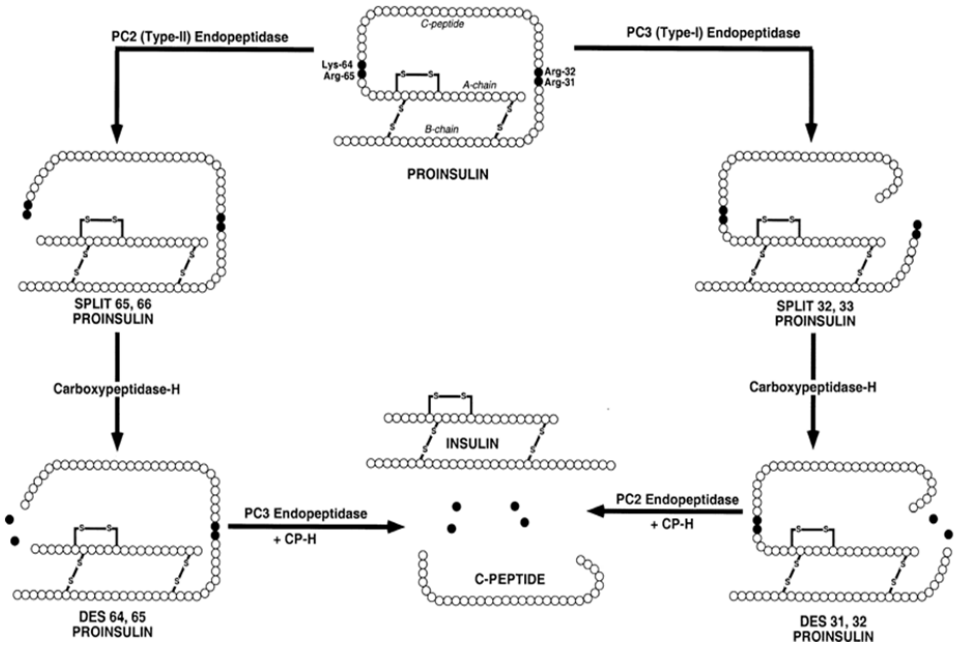

Figure 2. *Insulin Biosynthesis: Proinsulin is converted into active insulin and C-peptide through the action of cellular endopeptidases known as prohormone convertases (PC1/3 and PC2) (Creemers, Jackson et al. 1998), as well as the carboxypeptidase H (CPH). The endopeptidases cleave at 2 positions, releasing the C-peptide, and leaving 2 peptide chains, A (21 a.a.) and B (30 a.a.), linked by two disulfide bonds (Davidson 2004). For the majority of proinsulin molecules, PC1/3-mediated cleavage of the B–C junction likely occurs first, the exposed basic residues are then removed by CPH, and subsequently PC2 cleaves the A–C junction to release the mature insulin (Davidson 2004).*

1.4 Diabetes mellitus

Diabetes mellitus (DM) is a complex chronic disease characterized by hyperglycemia arising directly from insulin deficiency, resistance, insufficient insulin secretion, or excessive glucagon secretion (Blair 2016). Such metabolic imbalance can cause serious health complications including ketoacidosis, kidney failure, heart disease, stroke and blindness (van Belle, Coppieters et al. 2011). DM was first reported in Egyptian manuscript about 3000 years ago (Ahmed 2002). Diabetes is presently divided into two major forms, type 1 (T1DM) and type 2 (T2DM) diabetes mellitus. However, in a recent study by Ahlqvist et al. identified five replicable clusters of patients with diabetes, which had significantly different patient characteristics and risk of diabetic complications (Ahlqvist, Storm et al. 2018). Based on the study, DM can be divided into five subgroups: severe autoimmune diabetes (SAID), severe insulin-deficient diabetes (SIDD), severe insulin-resistant diabetes (SIRD), mild obesity-related diabetes (MOD) and mild age-related diabetes (MARD) (Ahlqvist, Storm et al. 2018). SAID overlapped with T1DM and latent autoimmune diabetes in adults (LADA), SIDD and SIRD represent two new, severe forms of diabetes previously included within T2DM.

1.4.1 Type 1 diabetes mellitus

Type 1 diabetes mellitus (T1DM) is an autoimmune disorder leading to the destruction of the insulin-producing pancreatic β-cells which in turn leads to insulin deficiency and resultant hyperglycemia (Bluestone, Herold et al. 2010). Once diagnosed, patients require lifelong insulin administration for glucose homeostasis maintenance (Kelly, Rayner et al. 2003).

T1DM is associated with genetic predisposition, unknown environmental factors, infections and stochastic events in its etiology. The symptomatic onset of T1DM occurs usually during childhood or adolescence, however new research suggests that symptoms can sometimes develop much later (Leslie 2010). Polyuria (increased urination), polydipsia (increased thirst), dry mouth, polyphagia (increased hunger), fatigue and weight loss are the classical symptoms associated with T1DM. Although the etiology of T1DM is not completely understood, the studies with non-obese diabetic (NOD) mice have demonstrated that the pathogenesis of the disease occurs through activation of the autoreactive CD4+ and CD8+ T cells (Burton, Vincent et al. 2008), which in turn causes destruction of the insulin secreting β-cells (Bluestone, Herold et al. 2010). The five most prevalent and best characterized T1DM related autoantibodies including islet cell autoantibodies (ICA), glutamic acid decarboxylase autoantibodies (GAD), autoantibodies to protein tyrosine phosphatase (IA2) (Baekkeskov, Aanstoot et al. 1990; Payton, Hawkes et al. 1995; Bonifacio, Lampasona et al. 1998) and autoantibodies to insulin itself (IAA) (Palmer, Asplin et al. 1983), as well as those against the zinc transporter 8 (ZnT8) (Wenzlau, Juhl et al. 2007).

The highest risk factor for T1DM is genetic, mainly occurring in individuals with human leukocyte antigens (HLAs) class II alleles: HLA-DR3-DQ2 or HLA-DR4-DQ8 haplotypes, or both, but a trigger from the environment is needed (Pociot and Lernmark 2016). Moreover, in a study by Padgett et al. suggested that CD4 T cells can provide “help” to B cells and stimulate antibody production, as well as promote responses by effector CD8 T cells, and stimulate islet-resident macrophages (Padgett, Anderson et al. 2015).

It is know that insulin readily forms amyloid fibrils in vitro. However, only small amounts of insulin fibrils have been observed after subcutaneous insulin infusion and

repeated injections (Storkel, Schneider et al. 1983). The reasons for absence of insulin fibrils *in vivo* is not known. Also, several studies have shown that insulin autoantibodies are the first to appear in childhood T1DM (Knip 2002), however, it is not known which are the antigenic species inducing autoantibody production. Based on our results (Publication I), we hypothesized that Zn^{2+} ions co-secreted from pancreatic β-cells protect the organism from insulin fibrillization and formation of intermediary insulin oligomers/aggregates. We also hypothesized that misfolded oligomeric intermediates occurring in the insulin fibrillation pathway, especially in zinc-deficient conditions, might induce autoantibodies against insulin, which leads to β-cell damage and autoimmune T1DM (Publication I).

1.4.2 Type 2 diabetes mellitus

Type 2 diabetes mellitus (T2DM) is the most common form of DM, characterized by hyperglycemia resulting from either the deficiency in insulin secretion or the action of insulin (Olokoba, Obateru et al. 2012). It has been proposed that the pathogenesis of T2DM occurs through eight mechanisms (Defronzo 2009). These include reduced insulin secretion from pancreatic β-cells, increased glucagon secretion from pancreatic α-cells, elevated production of glucose in liver, neurotransmitter dysfunction and insulin resistance, accelerated lipolysis, increased kidney glucose reabsorption, incretin deficiency in the gastrointestinal tract and impaired glucose uptake in skeletal muscle, liver and adipose tissue (Defronzo 2009).

The prevalence of T2DM has been increasing permanently all over the world and is expected to increase to 366 million by 2030 (Wild, Roglic et al. 2004). Individuals with T2DM are at high risk for cardiovascular disease (CVD) (primarily heart disease and stroke) (Haffner, Lehto et al. 1998) and microvascular complications (including retinopathy, nephropathy and neuropathy). T2DM is resulting from a complex interaction between genetic, environmental and lifestyle risk factors.

A wide variety of lifestyle factors are known to be important to the development of T2DM. These are sedentary lifestyle (Zimmet, Alberti et al. 2001), physical inactivity (Hu, Manson et al. 2001), smoking (Manson, Ajani et al. 2000) and alcohol consumption (Cullmann, Hilding et al. 2012). Obesity has been found to be the most important risk factor for T2DM, which may contribute to the development of insulin resistance and disease progression (Belkina and Denis 2010).

It is known that the pathophysiology of T2DM is associated with a number of genetic components. For example, 40% of first-degree relatives of T2DM patients may develop diabetes. Moreover, segregation analysis suggests the polygenic nature of T2DM. The genome-wide association studies (GWAS) have discovered numerous genes associated to T2DM (Scott, Mohlke et al. 2007; Sladek, Rocheleau et al. 2007; Zeggini, Weedon et al. 2007). Examples of candidate genes are TCF7L2 (transcription factor 7-like 2, the strongest T2DM locus identified to date) (Saxena, Voight et al. 2007), IRS1 (insulin receptor substrate 1) (Voight, Scott et al. 2010), MTNR1B (melatonin-receptor gene) (Voight, Scott et al. 2010), PPARG (peroxisome proliferator-activated receptor gamma) (Scott, Mohlke et al. 2007), FTO (fat mass and obesity associated), KCNJ11 (potassium inwardly rectifying channel, subfamily J, member 11) (Scott, Mohlke et al. 2007), IGF2BP2 (insulin-like growth factor two binding protein 2) (Scott, Mohlke et al. 2007), CDKN2A (cyclin-dependent kinase inhibitor 2A) (Zeggini, Weedon et al. 2007) and HHEX (hematopoietically expressed homeobox) gene (Ntzani and Kavvoura 2012).

No cure has yet been found for the T2DM, however several options for therapy of lowering blood glucose are available. Examples of treatment options include lifestyle modifications (Bi, Wang et al. 2012), biguanides (Viollet, Guigas et al. 2012), sulfonylureas (Aguilar-Bryan, Nichols et al. 1995), thiazolidinedione (Yki-Jarvinen 2004), sodium-glucose cotransporter inhibitors (Madaan, Akhtar et al. 2016), dipeptidyl peptidase 4 inhibitors (Pathak and Bridgeman 2010) and α-glucosidase inhibitors (Fukase, Takahashi et al. 1992).

1.5 Structure of Insulin

The crystals of insulin were first prepared by John Jacob Abel in 1926 (Abel 1926). In the early 1950s, British biochemist Frederick Sanger determined the primary structure of bovine insulin that consists of two polypeptide chains: chain A (21 amino acids) and chain B (30 amino acids) linked by two interchain disulphide bonds (Sanger and Tuppy 1951; Sanger and Tuppy 1951; Sanger and Thompson 1953; Sanger and Thompson 1953; Ryle, Sanger et al. 1955).

In the T-state conformation, the A-chain contains an amino-terminal α-helix (residues A1-A8) followed by a noncanonical turn, second helix (A12-A18) and carboxy-terminal segment (A19-A21) (Adams 1969; Bentley, Dodson et al. 1976; Baker, Blundell et al. 1988; Olsen, Ludvigsen et al. 1996). B chain can exist in two distinct conformations. In the T-state conformation, the B-chain forms an amino-terminal strand (residues B1-B6), a β-turn (B7-B10), a single α-helix (B9-B19) followed by a second β-turn (B20-B23) and a carboxy-terminal β-strand (B24-B28), extended by less well-ordered terminal residues B29 and B30 (Bentley, Dodson et al. 1976; Baker, Blundell et al. 1988; Brader and Dunn 1991). In the R-state, an additional α-helix appears between the residues B1-B8 to form a region of helix contiguous from B1 to B19 (Derewenda, Derewenda et al. 1989).

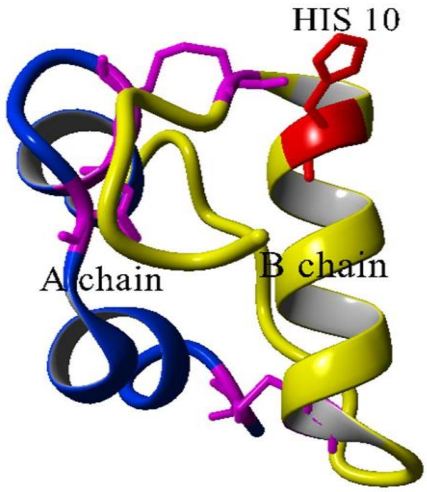

Figure 3. *Crystal structure of insulin monomer. The structure of the insulin monomer consists of a helix in the B chain, (yellow) and two shorter helices in the A chain (blue). The A chain containing an intrachain disulfide bond, and the B chain with two intermolecular disulfide bonds linking the chains (S-S bonds are marked in purple). This figure was generated using Yasara (http://www.yasara.org/).*

The 3D structure of the insulin molecules in its hexameric state has been determined by X-ray crystallography in 1969 by Dorothy Hodgkin and colleagues (Adams 1969). The hexamer is assembled from three insulin dimers, which are linked together by two Zn^{2+} ions (Hodgkin 1971; Baker, Blundell et al. 1988). Zn^{2+} ions are coordinated by three His imidazole rings (HisB10) as well as three water molecules (Frankaer, Knudsen et al. 2012). The nonpolar amino acid residues like LeuA13, LeuA16, LeuB6, LeuB11, LeuB15 and ValB18 that cluster on the inside of the insulin monomers, forming a hydrophobic core that stabilizes protein 3D structure (Hodgkin 1971; Mayer, Zhang et al. 2007).

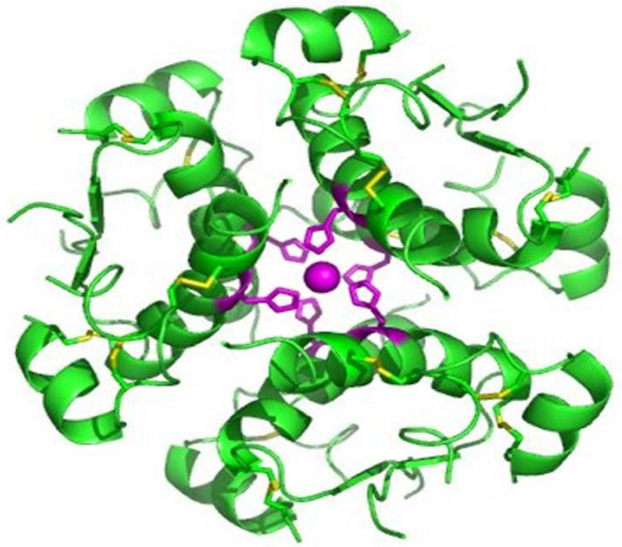

Figure 4. *Crystal structure of insulin hexamer (PDB code: 1AI0) (Chang, Jorgensen et al. 1997). The structure of the R6 insulin hexamer consists of three insulin dimers which are coordinated by two Zn^{2+} ions. The zinc ions are shown as purple spheres. Each of the two zinc ions is coordinated by three HisB10 side chains.*

In secretory granules the zinc-containing hexameric insulin forms water-insoluble crystals ($Zn_2Insulin_6$) (Orci, Ravazzola et al. 1987; Dodson and Steiner 1998). It is believed that the hexamer formation protects insulin from fibrillization during *in vivo* storage and is exploited in clinical formulations of insulin for the same purpose (Brange, Havelund et al. 1986; Rasmussen, Kasimova et al. 2009). For transfer into the blood, insulin hexamers must first dissociate into dimers, and then into Zn^{2+}-free monomers, which can now penetrate into the bloodstream (Ahmad, Millett et al. 2003).

Insulin can be present also in other oliomeric forms depending on the environmental conditions (Bryant, Spencer et al. 1993; Brange, Andersen et al. 1997). The protein is hexameric in the presence of Zn^{2+} ions at neutral pH, monomeric in 20% acetic acid (Weiss, Nguyen et al. 1989; Hua and Weiss 1991) and dimeric in 20 mM HCl (Ahmad, Millett et al. 2004). However, the native structure of insulin can be destabilized by various effectors such as high temperature, pH, organic solvents, agitation, chemical additives or hydrophobic surfaces leading to formation of amyloid-like fibrils (Brange, Andersen et al. 1997). The structure of the insulin fibrils at the atomic level is not known.

1.6 Mechanism of Insulin Fibrillization

Protein aggregation, and amyloid formation are associated with more than forty human pathologies, including Alzheimer´s disease, Parkinson´s disease, Creutzfeldt-Jakob disease and Type 2 diabetes (Castillo and Ventura 2009). During amyloid fibril formation native soluble proteins/peptides aggregate into insoluble fibrils which contain characteristic cross-β-sheets, in which the β-strands are aligned perpendicularly to the axis of the fibril (Blake and Serpell 1996) (Figure 5). Moreover, the formation of amyloid fibrils of proteins/peptides is assumed to be a generic property of polypeptide chains whereas the misfolded fibrillar proteins share several common structural characteristics even when the native proteins are not evolutionarily or structurally related (Dobson 1999). This indicates that the fundamental mechanism of fibrillization in different pathologies may be common (Kayed, Head et al. 2003). Furthermore, an increasing evidence supports the "generic hypothesis" that all proteins and peptides, at least in principle, are able to aggregate to form amyloid-like fibrils under appropriate conditions (Dobson 2003).

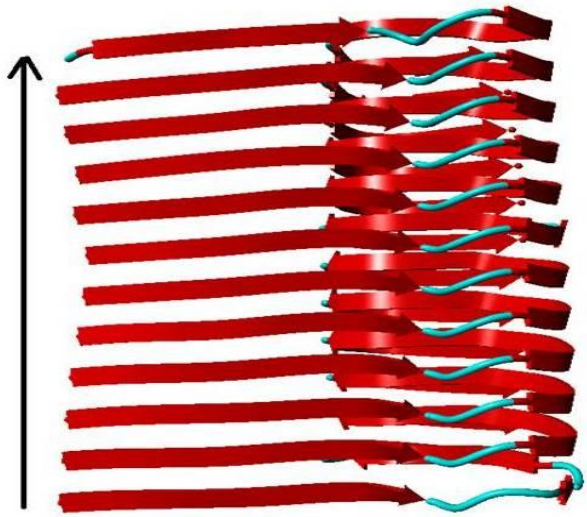

Figure 5. The three-dimensional structure of amyloid-ϐ42 (Aϐ42) fibrils based on nuclear magnetic resonance (NMR). The cross-ϐ spine consists of ϐ-sheets, which are stacked in a parallel manner (thick red arrows). This figure was generated using Yasara (http://www.yasara.org/).

It is known that insulin forms readily amyloid-like fibrils *in vitro* and it is one of the most intensively used model for studying protein fibrillization (Ivanova, Sievers et al. 2009). At the same time the formation of insulin fibrils causes also a number of concerns in the production, storage and delivery of the biotechnologically produced protein-drug, and creates many essential biomedical and biotechnological problems (Ahmad, Millett et al. 2003). However, it is relatively rare situation for insulin to form fibrils within an organism. Insulin fibrils have been found in some cases of insulin-dependent diabetes after frequent insulin injections (Dische, Wernstedt et al. 1988; Swift 2002; Shikama, Kitazawa et al. 2010), which seems to be independent of the site of injection. Insulin fibrils have been observed in shoulders (Sahoo, Reeves et al. 2003),

thighs (Dische, Wernstedt et al. 1988; Swift 2002), arms (Yumlu, Barany et al. 2009) and abdominal walls (Albert, Obadiah et al. 2007; Yumlu, Barany et al. 2009; Shikama, Kitazawa et al. 2010) of individuals around or at the site of repeated injections. Moreover, inhalation of insulin causes fibril formation in the lungs, which, in turn significantly reduces pulmonary air flow (Lasagna-Reeves, Clos et al. 2010). Examination of insulin fibrillization might therefore be also important to improve insulin therapy.

A large number of studies have been carried out to explore the mechanism of insulin fibrillization. It has been shown that both individual A and B chains can easily form fibrils (Hong and Fink 2005; Hong, Ahmad et al. 2006). Moreover, seeds of A chain or B chain can nucleate the formation of fibrils of full length insulin (Devlin, Knowles et al. 2006).

It is widely known that insulin aggregation proceeds through the dissociation of oligomers into dimers, and subsequently into monomers, which then undergo a structural change to a conformation having strong propensity to fibrillate (David F. Waugh 1953; Brange and Langkjoer 1993; Nielsen, Khurana et al. 2001). This partially misfolded intermediate then oligomerizes to form soluble oligomers that lead to the formation of the nucleus. Thus, the initial step in aggregation is probably the formation of conformationally changed monomers, in which the hydrophobic surfaces, normally buried in the dimer and hexamer, become exposed to the solvent (Millican and Brems 1994; Brange, Dodson et al. 1997). According to the literature data, the mechanism for assembly and fibrillogenesis of insulin is following: hexamer → monomer → partially misfolded monomer → oligomers/protofibrils → fibrils (Ahmad, Millett et al. 2003; Ahmad, Millett et al. 2004).

In the process of insulin fibrillization the kinetic profile are characterized by a typical sigmoidal curve, characteristic for a nucleation-dependent fibril assembly (Lee, Nayak et al. 2007) (Figure 6). The classic fibrillization process starts with a lag phase during which nucleation occurs but no fibrils are formed. In the nucleation phase, several insulin monomers assemble to produce fibril nuclei, which are precursors for fibril formation. The lag phase of fibril formation is related to the time required to form substantial amount of nuclei (Nielsen, Frokjaer et al. 2001; Nielsen, Khurana et al. 2001). The nucleation phase is followed by an elongation phase in which fibrils are formed through the addition of monomers or oligomers to preexisting nuclei (Kelly 1998; Cohen, Vendruscolo et al. 2012). Finally, the process reaches saturation where most of the protein in the solution is converted into fibrils.

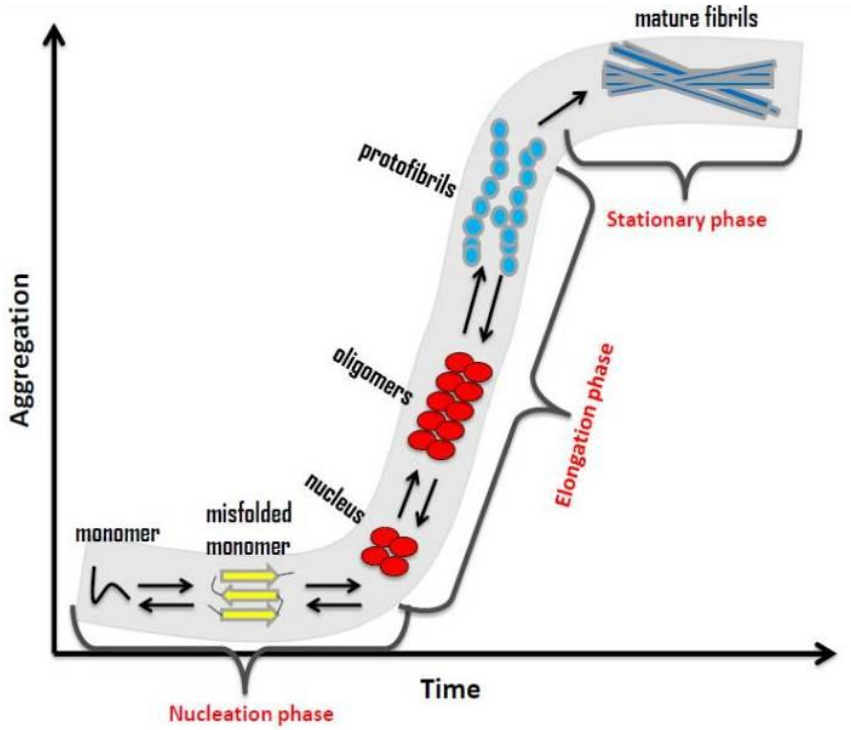

Figure 6. *Nucleation dependent fibrillization model of insulin aggregation. The kinetics of amyloid formation is well represented by a sigmoidal curve, that consists of two phases: (i) a nucleation phase in which monomers undergo conformational change and associate to form oligomeric nuclei and (ii) rapid elongation phase, in which the nuclei grow by further addition of monomers and form larger polymers/fibrils until saturation.*

Nucleation is the key stage in the fibril formation, which determines the pathway of fibrillization (Selivanova and Galzitskaya 2012). According to the published results, insulin fibril formation can occur in three pathways depending on the size of nucleus. First, it is supposed that fibrillization may start from direct assembly of insulin monomers, which denature in solution and then attach to the growing fibrils (Brange, Andersen et al. 1997; Pease, Sorci et al. 2010). Second, it is suggested that nucleus of protofibrils can be composed from three dimers (Ivanova, Sievers et al. 2009; Nayak, Sorci et al. 2009). According to the third hypothesis, the nucleus of protofibrils are oligomers, that can include different numbers of insulin monomers (from 3 to 6) and have different morphology (Nielsen, Frokjaer et al. 2001; Nielsen, Khurana et al. 2001; Ahmad, Millett et al. 2003; Vestergaard, Groenning et al. 2007).

As shown for several proteins the elongation phase may also occur via different mechanisms (Padrick and Miranker 2002; Koo and Miranker 2005; Pedersen, Dikov et al. 2006). In addition to an end-to-end attachment of protein monomers to the nucleus (homogenous nucleation), also secondary nucleation pathways may take place, involving the already formed fibrils as precursors for new fibrils (Knowles, Waudby et al. 2009). It is supposed that a fibril can catalyze the formation of other fibrils through the three distinct mechanisms: fragmentation, branching and nucleation on the already formed fibrils (heterogeneous nucleation), (Librizzi and Rischel 2005).

Fragmentation is based on the breaking of a part of the fibril. Such fragments contain additional fibril ends to start new fibril growth. Branching involves the addition of a monomer, or generally of a subunit, on a specific site already present in the growing fibril. Finally, the heterogeneous nucleation can occur when a minimum length of the polymeric chain is provided (Librizzi and Rischel 2005). Then, the heterogeneous nucleus is formed and new elongation pathway is activated resulting in a different shape of the kinetic profile (Ferrone 1999).

1.7 Monitoring of Insulin Fibrillization

The formation of amyloid fibrils can be directly monitored by Transmission Electron Microscopy (TEM), by X-ray fiber diffraction and also by Atomic Force Microscopy (AFM). However, one of the most widely used techniques for quantification and tracking of fibrillization is indirect monitoring of fibrils by using Thioflavin T (ThT) fluorescence. ThT is a fluorogenic dye that consists of a dimethylaminobenzene ring and a positively charged benzothiazole ring (Scheme 1). The conformation of the dye is defined by the torsion angle ϕ. The basis for the use of ThT is simple, it forms complexes with amyloid fibrils (LeVine 1993; LeVine 1999), connected with the increase of fluorescence intensity with excitation and emission maxima at approximately 440 and 490 nm, respectively (LeVine 1993; Nilsson 2004). In general, ThT does not affect the peptide fibrillization kinetics (Chander, Chauhan et al. 2007).

The binding mode(s) of ThT to amyloid fibrils is not fully understood, but the most widely accepted theory involves the insertion of ThT molecules into the grooves formed by side chains of the amyloid fibril that run parallel to the long axis of the fibrils (Krebs, Bromley et al. 2005; Biancalana, Makabe et al. 2009). Binding into the grooves is believed to provide rigidity of the dye and increase the quantum yield of the emission. It has been proposed that ThT incorporates into amyloid fibrils as monomer (Stsiapura, Maskevich et al. 2007; Sulatskaya, Lavysh et al. 2017). It is known that the interactions between ThT and amyloid fibrils are stoichiometric and saturates at relatively low ThT concentrations, therefore the fluorescence signal from the amyloid-ThT complex provides a simple tool for the quantification of amyloid fibrils (Bolder, Sagis et al. 2007).

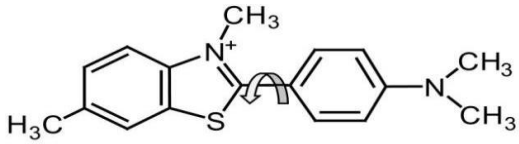

Scheme 1. *Molecular structure of Thioflavin T with the torsion angle φ between the benzothiazole and the aminobenzene fragments.*

However, this method has also some disadvantages. It has been shown that low molecular weight compounds interfere with the fluorescence of ThT bound to fibrils of other amyloidogenic peptide - Alzheimer´s amyloid β, which may lead to false positive results in the screening of fibrillization inhibitors (Hudson, Ecroyd et al. 2009; Zovo, Helk et al. 2010). We demonstrated that the same putative fibrillization inhibitors also decrease the fluorescence signal of ThT bound to insulin fibrils (Publication II). These compounds (Basic Blue 41, Basic Blue 12, Azure C and Tannic acid) were similar to the structure of ThT, and, therefore, it can be conclude that they compete with ThT for

common binding sites on amyloid fibrils. Our results showed that interference with ThT test is a general phenomenon and more attention has to be paid to the interpretation of kinetic results of protein fibrillization obtained by using fluorescent dyes.

1.8 Factors Affecting Fibril Formation

The duration of initial lag phases and fibril growth rates depend upon multiple factors such as the peptide concentration, temperature, the ionic strength of the solution and pH (Burke and Rougvie 1972; Nielsen, Khurana et al. 2001). Presence of denaturants (urea, guanidine chloride [GdnHCl]) and the intensity of agitation also contribute to the kinetics of fibril formation.

1.8.1 Effect of pH on Insulin Fibril Formation

Insulin is hexameric in the presence of zinc ions at pH 7.4, tetrameric at pH 3.0, dimeric at pH 1.6 in HCl and monomeric in 20% acetic acid at pH 1.6 (Nielsen, Khurana et al. 2001; Frankaer, Sonderby et al. 2017). It is not clear why insulin is dimeric at pH 1.6 in HCl, and monomeric in acetic acid (Nielsen, Frokjaer et al. 2001).

However, in a recent study Mawhinney et al. showed that at concentrations below 50 μM, oligomers comprise up to 40% and 70% of soluble insulin at acidic and neutral pH, respectively (Mawhinney, Williams et al. 2017). They also demonstrated that the highest oligomer formation increases with insulin concentration at acidic pH, the opposite propensity was observed at neutral pH, where oligomers up to heptamers are formed in case of 10 μM insulin (Mawhinney, Williams et al. 2017).

It is generally believed that the formation of fibrils most likely proceeds from the monomer (Brange, Andersen et al. 1997), and the propensity of insulin to fibrillate is expected to increase in acetic acid. The fibrillization rate of insulin decreases at acidic pH and high peptide concentrations with increasing pH values (Brange, Andersen et al. 1997); (Publication IV). This was opposite to the pH effect observed in 2.5 μM insulin solutions, where the rate constant increased and the duration of the lag phase decreased with increasing pH (Publication IV). We also demonstrated, that in 2.5 μM insulin solutions, the ThT fluorescence were higher at elevated pH values (Publication IV), which is in good agreement with literature, where the fluorescence of ThT bound to insulin fibrils was tenfold lower at acidic pH values (Mishra, Sjolander et al. 2011). The inhibition of fibrillization at low pH also indicates involvement of His residue(s) in the nucleation of monomeric insulin.

It has been shown that HisB5 of insulin participates in the hexamer assembly and contributes to the foldability and functioning of insulin (Tang, Whittingham et al. 1999; Wan, Huang et al. 2008). Moreover recent results suggested that ethyloxyformylation of imidazole ring of HisB5 accelerated the fibrillization of insulin at neutral pH, whereas in acidic condition, a reverse trend was observed (Yang, Li et al. 2014). The authors proposed that modification of HisB5 prevents the exposure of the hydrofobic residues during the fibrillization at pH 2.0 more than at pH 7.4 (Yang, Li et al. 2014). However, under physiological conditions at pH 7.4 insulin fibrillization is a much more complicated process than in acidic solution (Brange, Andersen et al. 1997). This is because the dissociation of insulin hexamers is the rate-limiting step in fibril formation at neutral pH (Ahmad, Millett et al. 2003; Ahmad, Millett et al. 2004) and oligomeric forms have to dissociate into monomers before fibrillization.

1.8.2 Interaction of Insulin with Zn^{2+} Ions

As mentioned above, in pancreatic β-cells insulin is stored inside secretory vesicles, in which Zn^{2+} ions coordinate and stabilize the hexameric forms of insulin (Brange, Havelund et al. 1986; Rasmussen, Kasimova et al. 2009). Zn^{2+} content in the pancreatic β-cells is among the highest in the body and reaches 10 millimoles per liter (Clifford and MacDonald 2000). Analyses of islets from Zn^{2+}-treated rats have shown that one-third of the total β-cell zinc content is present within insulin granules (Figlewicz, Forhan et al. 1984). Zn^{2+} is uploaded to the granules with the assistance of a pancreas-specific zinc transporter ZnT8 localized in the membranes of the granules (Chimienti, Devergnas et al. 2006).

Zinc plays a crucial role in many cell functions; as a result, both zinc deficiency and excess of free zinc ions are toxic to mammalian cells (Lemaire, Ravier et al. 2009). Extra-granular zinc may act as a reservoir for granular zinc and may regulate insulin synthesis, storage and secretion (Figlewicz, Forhan et al. 1984).

It is known that Zn^{2+} supplementation is effective in preventing type 1 and type 2 diabetes in several rodent models and it is possible that Zn^{2+} ions can protect against progressive β-cell injury in type 2 diabetes (Taylor 2005). Moreover, several studies demonstrated that metal ions like Zn^{2+}, Cu^{2+}, Fe^{3+} have pronounced effects on the fibrillization of amyloidogenic peptides like Alzheimer's amyloid peptide (Bush, Pettingell et al. 1994), synuclein (Bharathi, Indi et al. 2007; Bharathi and Rao 2008) and tau protein, whereas metal ions can enhance (Bharathi, Indi et al. 2007; Bharathi and Rao 2008) or inhibit (Tougu, Karafin et al. 2009) fibrillization. It has been demonstrated that in the case of hen egg white lysozyme (HEWL), Zn^{2+} ions inhibited the conversion of α-helix to β-sheet conformation and prevented the fibril formation (Ma, Zhang et al. 2017). However, the morphology of HEWL fibrils was not significantly varied dependent on presence of Zn^{2+} ions (Ma, Zhang et al. 2017).

In Publication I we have demonstrated that Zn^{2+} ions inhibit fibrillization of monomeric insulin at pH 7.3 by forming a soluble Zn^{2+}-insulin complex. Furthermore, it has been shown in our laboratory that the dissociation constant value of the monomeric 1 : 1 Zn^{2+}-insulin complex is equal to 0.40 μM (Gavrilova, Tougu et al. 2014). The inhibitory effect of Zn^{2+} ions was very strong (IC50 = 3.5 μM) and the addition of a 4-fold excess of Zn^{2+} almost completely suppressed the fibrillization of insulin (Figure 7a, [Publication I]). At pH 5.5, the inhibitory effect of Zn^{2+} ions was much weaker, pointing towards participation of the His residue(s) in the complex formation (Figure 7b, [Publication I]).

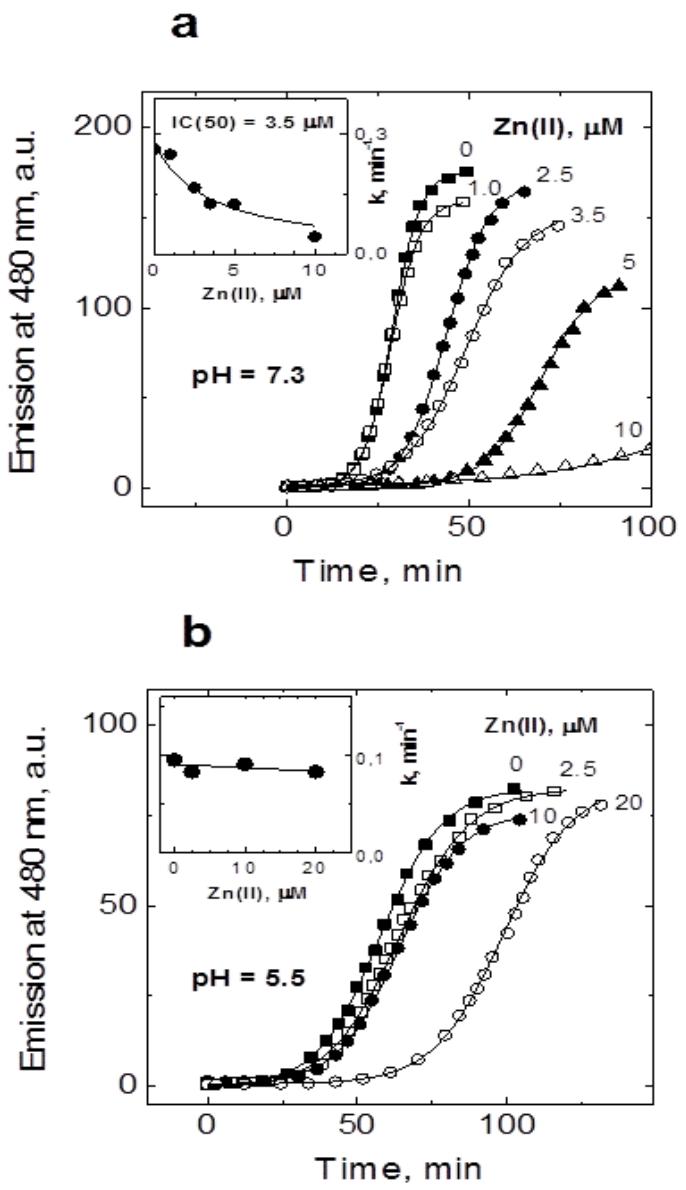

Figure 7. *Effect of Zn^{2+} ions on fibrillization of insulin. Conditions: 2.5 μM of insulin in 20 mM Hepes and 100 mM NaCl at (a) pH 7.3 and (b) pH 5.5 was incubated at 50°C in a quartz cell with continuous agitation in the presence of 2.5 μM ThT and various concentrations of Zn^{2+} as shown in the Figure. Solid lines correspond to fits of the data to the Boltzmann equation (eqn 1). Insets: dependence of the fibrillization rate constant on the concentration of Zn^{2+}. a.u., arbitrary units. From (Noormagi, Gavrilova et al. 2010) with permission.*

Moreover, in a recent study by Frankaer et al. showed that at pH 7.3 Zn^{2+} ions bind to the fibrils of insulin (Frankaer, Sonderby et al. 2017). Zn^{2+} coordinates to His residues in an environment, which is very similar to the coordination seen in the insulin R6

hexamers, where three His residues and a chloride ion is coordinating the Zn^{2+} ions (Frankaer, Sonderby et al. 2017). It was shown that Zn^{2+} ions have the effect also on the morphology of the insulin fibrils (Frankaer, Sonderby et al. 2017).

These results indicate that Zn^{2+} ions might prevent fibrillization of insulin at its release sites and in circulation.

1.8.3 Effect of Temperature on Insulin Fibril Formation

The classical method to induce insulin fibrillization is to heat insulin in a relatively strong acid solution. In these, the most common fibrillization conditions for the studies of insulin fibrillization, the lag phase decreases and the fibrillization rate constant values increases with increasing temperature (Brange, Andersen et al. 1997); (Publication IV). Moreover, experiments conducted at physiological pH showed that the lag phase decreases and the fibrillization rate constant increases with increasing temperature (Publication I). It has been reported that increase in temperature helps unfold monomeric mouse prion protein and thus accelerate elongation (Milto, Michailova et al. 2014). Application of elevated temperatures accelerates also unfolding of insulin monomers that induces fibrillization (Arora, Ha et al. 2004; Huus, Havelund et al. 2005). It has been speculated that with increasing temperature the formation of covalent polymerization products via thiol-catalysed disulfide exchange becomes significant and causes fibril formation (Costantino, Langer et al. 1994).

Frankaer et al. also examined the influence of temperature on insulin fibril formation (Frankaer, Sonderby et al. 2017). In the absence of Zn^{2+} ions the enthalpy of activation E_a was increasing at elevated protein concentrations. The increase in E_a indicated that there exists an equilibrium between hexamers and dimers that will be shifted more towards dimers at lower protein concentrations (Frankaer, Sonderby et al. 2017). In the presence of Zn^{2+} ions the fibrillization starts from hexamers, and the E_a was more or less independent from the protein concentration (Frankaer, Sonderby et al. 2017).

We have demonstrated that the E_a of the fibril growth at pH 7.3 equals to 84 kJ/mol (Publication I), which was significantly larger than 33.8 kJ/mol at pH 2.5 (Publication IV). This result indicates that the conformational changes necessary for the formation of β-sheet rich structure are much more substantial at neutral pH values.

1.8.4 Effect of Insulin Concentration on Fibril Formation

Despite of intensive studies of insulin fibrillization, the effect of insulin concentration on the fibrillization is rarely investigated. Most of the studies are performed in acidic solution, where insulin is monomeric (Nielsen, Khurana et al. 2001). According to the literature, insulin is also monomeric at low peptide concentrations (Nettleton, Tito et al. 2000). It is known that insulin dimers begin to dissociate at concentrations below 100 μM (Roy, Lee et al. 1990). Our electrospray ionisation mass spectrometry (ESI-MS) measurements at 50°C and pH 7.3 yielded a K_d of 18.9 μM for dimerization of insulin (Publication I).

Generally, the propensity for fibrillization of the amyloidogenic peptides increases at elevated concentrations, which can be explained by the formation of on-pathway oligomers and fibril nuclei/ends. It has been shown that at acidic pH the duration of lag phase of fibrillization decreases and the rate of fibril formation increases with increasing of insulin concentration (Mawhinney, Williams et al. 2017); (Publication IV). At the same time under physiological pH values a ‘‘reverse’’ dependence on peptide concentration was observed, the rate of fibrillization decreases and lag phase increases with increasing concentration of insulin (Nielsen, Frokjaer et al. 2001; Nielsen, Khurana

et al. 2001; Frankaer, Sonderby et al. 2017); (Figure 8, [Publication I]). This phenomenon can be explained by insulin oligomerization and formation of off-pathway oligomers (Publication I), which must dissociate to monomers before fibrillization (Ahmad, Millett et al. 2003).

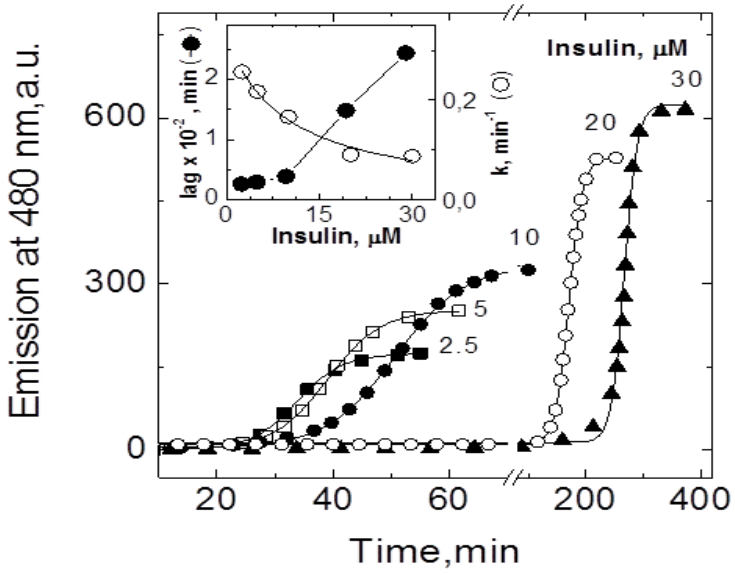

Figure 8. *Effect of insulin concentration on its fibrillization. Conditions: 2.5 μM (black squares), 5 μM (white squares), 10 μM (black circles), 20 μM (white circles) and 30 μM (black triangles) insulin in 20 mM Hepes, pH 7.3, and 100 mM NaCl were incubated at 50°C in a quartz cell with continuous agitation in the presence of 2.5 μM ThT. Solid lines correspond to fits of the data to the Boltzmann equation (eqn 1). Inset: dependence of the fibrillization rate constant on the insulin concentration. a.u., arbitrary units. From (Noormagi, Gavrilova et al. 2010) with permission.*

Furthermore, Frankaer and coworkers showed that at pH 7.3 in the presence of Zn^{2+} insulin was only in the hexameric form, but in the absence of Zn^{2+} ions a concentration dependent equilibrium between dimeric and hexameric insulin was observed (Frankaer, Sonderby et al. 2017). However, recent study by Mawhinney et al. showed that under physiological conditions the lag phase of insulin decreases and the rate of fibrillization increases with insulin concentration in the concentration range 2.5–50 μM (Mawhinney, Williams et al. 2017).

It has been demonstrated that at pH 1.6 in the presence of HCl the increase of insulin concentration produces drastic changes in the kinetics profile, ThT emission showed a biphasic temporal behavior in the intermediate range of concentration investigated (0.6 and 0.7 mM) (Fodera, Cataldo et al. 2009). The authors proposed a scheme in which formation of an intermediate species may determine the first increase of ThT intensity (pre transition) and afterward the cooperative mechanism leads to the formation of mature fibrils (main transition) (Fodera, Cataldo et al. 2009). At the same time, in solutions at pH 1.6 in the presence of acetic acid, insulin displays a classical sigmoidal curve in a wide range of protein concentrations (0.2–3.5 mM) (Librizzi and Rischel 2005). However, we have shown that at low pH fibrillization curves

demonstrated clear systematic deviation of residuals from the Boltzmann curve, contrary to the physiological pH, where the fibrillization curves were symmetrical and well fitted to the Boltzmann equation (Publication IV).

It is also known that insulin concentration has an influence on the physical appearance of the insulin fibrils. For concentrations of ≥ 0.9 mM, the end state of the fibrillated insulin solutions consisted of a firm, turbid gel (Nielsen, Khurana et al. 2001). At concentrations of ≤ 0.4 mM, the fibrillated insulin solution was viscous containing visible aggregates (Nielsen, Khurana et al. 2001).

1.8.5 Effect of Ionic Strength on Insulin Fibril Formation

The effect of salts have been observed to mediate through ionic interactions - Debye-Hückel screening (Debye P 1923) or electroselectivity series (Gjerde, Schmuckler et al. 1980), or by influencing water-solute interactions - Hofmeister series (Collins and Washabaugh 1985; Baldwin 1996). According to Munishkina et al., (Munishkina, Henriques et al. 2004), the salt effects are a combination of the electrostatic and solvent interactions in addition to the other exogenous and endogenous factors.

According to the literature, at pH 7.4 the increasing salt concentration seems to induce structural rigidity around the disulfide bonds whereas at pH 2.0 the structure seems to get loosened around the disulfides with an increase in the salt concentration (Muzaffar and Ahmad 2011). This is typical of the Hofmeister effect where ions reverse the effect as a function of pH.

The pronounced influence of ionic strength on the rate of insulin fibril formation was demonstrated by Waugh et al., (David F. Waugh 1953) who showed that increasing the ionic strength increased substantially the rate of nucleation. Nielsen et al., (Nielsen, Khurana et al. 2001) also showed that increased ionic strength led to shorter lag phases, but there was no clear correlation between the rate constant for fibril growth and ionic strength. The fibrillization induced by salts like NaCl can be explained by the property of NaCl to induce structural changes in the molecule that push aside the N- and C-terminal segments leading to the exposure of highly hydrophobic inner core of insulin (Muzaffar and Ahmad 2011).

It has been also shown that solution ionic strength plays an important role in determining the type of structures generated during insulin fibril formation (Emily Ha 2012). At elevated ionic strength conditions AFM (Emily Ha 2012) and time-dependent small angle X-ray scattering (SAXS) (Chatani, Inoue et al. 2015) measurements revealed formation of prefibrillar intermediate species including oligomers and protofibrils. These early prefibrillar aggregates further coalesce mutually and form larger clusters (Chatani, Inoue et al. 2015). When exposed to lower ionic strength, no significant aggregation would occur (Emily Ha 2012; Chatani, Inoue et al. 2015). The effect of ionic strength on prefibrillar intermediate formation are generally explained with formation of a molten globule conformation of proteins in the presence of high salt concentrations (Goto, Takahashi et al. 1990; Goto and Fink 1994; Sinibaldi, Howes et al. 2003).

1.8.6 Effect of Denaturants on Insulin Fibril Formation

Denaturants like GdnHCl and urea, affect the structure of insulin. As a result of denaturants an aggregation-prone intermediate species form that stimulate the kinetics of insulin fibrillization (Ahmad, Millett et al. 2003; Ahmad, Millett et al. 2004). It has been shown that addition of increasing concentrations of urea to insulin at pH 7.4 resulted in shortening of lag phase and slightly increasing fibrillization rate constants

(Nielsen, Khurana et al. 2001). The effect of urea can be explained with the fact that urea destabilizes the conformation of insulin and promotes the formation of the partially misfolded intermediate, which will lead to a decrease in the lag phase (Nielsen, Khurana et al. 2001).

The GdnHCl-induced denaturation of insulin is a multistage process, where the compact dimer is the major species at low GdnHCl concentrations (< 2 M) (Ahmad, Millett et al. 2003). In the range of 1.5–5M GdnHCl, the major species are the partially misfolded dimer and monomer (Ahmad, Millett et al. 2003). High concentrations of GdnHCl resulted in misfolded monomers with some residual structure (Ahmad, Millett et al. 2003). The addition of very low concentrations of GdnHCl resulted in substantially accelerated fibrillization. Accelerated fibrillization correlated with the population of the partially misfolded monomer, which existed in the presence of up to > 6 M GdnHCl, accounting for the formation of substantial amounts of fibrils under such conditions (Ahmad, Millett et al. 2003).

There are substantial differences between the effects of urea and GdnHCl on insulin fibrillization; it is possible that these differences are caused by increased ionic strength that occurs when GdnHCl is used as a denaturant (Ahmad, Millett et al. 2004). These differences are most obvious in the case of the helix-rich monomeric insulin (Ahmad, Millett et al. 2003), that forms fibrils very slowly in the presence of urea but not in the presence of GdnHCl (Ahmad, Millett et al. 2004). Moreover, in a solution with very high denaturant concentrations, the structure of the fibrils can be altered (Kim, Muresan et al. 2004).

1.8.7 Effect of Agitation on Insulin Fibril Formation

It is well-known that the agitation of the solution accelerates fibrillization of the amyloidogenic peptides and proteins. The first explanation for this effect was that agitation causes the fragmentation of fibrils and increases the number of fibril ends that serve as the growth centers where the growing occurs. This explanation links the acceleration with a phenomenon called secondary nucleation that is crucial for explanation of the exponential phase in the fibrillization kinetics (Librizzi and Rischel 2005; Knowles, Waudby et al. 2009).

The fibril fragmentation is not the only mechanism that can accelerate the fibrillization when the solution is agitated. Agitation also enhance the interactions of peptide/protein fibrils with hydrophobic surfaces, in particular air-water and solid-water (container walls) interfaces, which may accelerate the fibrillization (Sluzky, Tamada et al. 1991; Morinaga, Hasegawa et al. 2010). The most reasonable explanation for the role of the air-water interface in fibrillization is that it promotes the denaturation and aggregation of the protein. Agitation allows a continuous creation of new interface and thus provides a large surface area for adsorption of insulin (Brange, Andersen et al. 1997). Monomers as well as dimers and hexamers of insulin can reversibly adsorb to the surface. However, monomers are the least stable species and therefore they can more easily undergo conformational changes after interaction with hydrophobic interfaces than dimers and hexamers (Sluzky, Tamada et al. 1991). This leads to the buildup of partially misfolded intermediates that are critical species in the fibrillization pathway (Nielsen, Frokjaer et al. 2001; Nielsen, Khurana et al. 2001).

It has been shown that in the absence of agitation at neutral pH, fibrils form very slowly, confirming that agitation is necessary for building up the fibrillization intermediates (Nielsen, Khurana et al. 2001). In a recent study Mawhinney et al. showed that under physiological conditions agitation increases fibrillar mass by an order

of magnitude (Mawhinney, Williams et al. 2017). However, it is not known what happens if the agitation is stopped during the elongation phase of fibrillization. In Publication III we demonstrated that when the mixing was stopped during the fibril elongation phase, the fibrillization of amylin and insulin at pH 7.3 was stopped and the rate for Aβ40 fibrillization was substantially decreased. At the same time, after discontinuation of the agitation the fibrillization of insulin at low pH (Publication IV) and the fibrillization of Aβ42 at pH 7.3 (Publication III) continued to proceed with almost the same rate as in the agitated conditions. The different sensitivity of the fibrillization towards agitation of these peptides remains elusive.

1.9 Morphology of Insulin Fibrils

The morphology of insulin fibrils depends on the conditions of their formation. Insulin fibrils are characterized by a cross-β structure in which the β-strands are aligned perpendicularly to the fibril axis, with a layer structure involving interchain hydrogen bonds (Burke and Rougvie 1972). The β-sheet structure results from the alignment of β-strands into parallel (Burke and Rougvie 1972) or antiparallel manner (Yu, Jo et al. 1974). Both types of structure occur in the native state of globular proteins although the antiparallel arrangement is more common (Bouchard, Zurdo et al. 2000). For insulin fibrils the presence of parallel β-sheets has been suggested from X-ray diffraction studies (Burke and Rougvie 1972) and antiparallel structure from analysis by Raman spectroscopy (Yu, Jo et al. 1974).

It has been shown that in the presence of HCl, insulin generally forms bundles of two or five fibers twisted together at 60-100 nm intervals into filaments with a gross diameter of 15-25 nm (Brange, Andersen et al. 1997). A similar pattern was observed in the presence of acetic acid but with a lower tendency for twisting (Nielsen, Frokjaer et al. 2001). However, in the presence of acetic acid and salt, laterally associated insulin fibrils are formed that are associated in thicker bundles with diameter 60-80 nm (Nielsen, Frokjaer et al. 2001).

Furthermore, it has been shown that the morphology of insulin fibrils changes with increasing the temperature (Arora, Ha et al. 2004). At 50^{o}C the shape of the fibrils was straight and demonstrated distinct nodes suggestive of intertwined protofibrils (Jimenez, Nettleton et al. 2002). At 100^{o}C, the fibrils were more curvilinear, indicating increased flexibility (Arora, Ha et al. 2004).

Freeze-thawing cycles also dramatically affects the morphology of insulin fibrils. The cycles broke the fibrils into shorter segments with lengths ranging from 30 to 200 nm (Nielsen, Frokjaer et al. 2001).

The AFM studies show that the morphology of insulin fibrils differs depending on the presence of dye. Insulin fibrils formed in the absence of 1-anilinonaphthalene-8-sulfonate or ThT were finer, whereas fibrils formed in the presence of dyes appeared thicker, reflecting a higher degree of lateral association (Bekard and Dunstan 2009).

Recently, Frankaer et al. showed that Zn^{2+} also affects the morphology of insulin fibrils. According to the size distribution the Zn^{2+} containing fibrils were larger and less frayed compared to Zn^{2+} free fibrils (Frankaer, Sonderby et al. 2017). They also showed that pH had a large effect on the fibril morphology, fibrils formed at pH 2.0 were more elongated and had a better alignment in the fiber diffraction patterns than fibrils at pH 7.3 (Frankaer, Sonderby et al. 2017). According to our TEM analysis (Publication IV), the morphology of insulin fibrils formed at neutral and acidic pH values was also different.

At acidic pH short fibrils were formed whereas “networks” of longer fibrils were detected at physiological pH.

Moreover, Fourier transform infrared spectroscopy (FTIR) analysis indicated a more loosely packed β-sheet structure in insulin fibrils formed at neutral pH compared to the samples formed at acidic pH (Iannuzzi, Borriello et al. 2017).

2. Aims of the study

The aim of this study was to investigate and compare the effect of different environmental conditions, agitation, Zn^{2+} ions and low-molecular substances on the kinetics of insulin fibrillization. For this purpose, the following studies were performed:

- Determination of the effect of Zn^{2+} ions, C-peptide and amylin on the fibrillization of monomeric insulin.

- Investigation of the kinetics of insulin fibrillization at different pH values, temperatures, agitation conditions and peptide concentrations.

- Testing of substances that have been studied as inhibitors of Aβ42 fibrillization (Tannic acid, Basic Blue 41, Basic Blue 12, Azure C, riboflavin, imidazole, ascorbic acid, phenolphtalein and Zn^{2+}) as competitors with ThT for binding sites on insulin fibrils.

3. Materials and methods

Publication I

- Insulin fibrillization monitoring by ThT fluorescence
- Calculation of kinetic parameters
- Determination of oligomeric composition of insulin using size-exclusion chromatography (SEC)
- Determination of oligomeric composition of insulin using ESI-MS
- Equilibrium dialysis
- Atomic absorption spectroscopy (AAS) measurements of Zn^{2+} binding to insulin
- Determination of Zn^{2+} binding affinity of insulin
- TEM visualization of fibrils

Publication II

- Monitoring of insulin fibrillization by ThT fluorescence
- Calculation of kinetic parameters
- Determination of concentration of soluble insulin by using SEC

Publication III

- Monitoring of Aβ40, Aβ42, amylin and insulin fibrillization by ThT fluorescence
- Calculation of kinetic parameters
- Determination of soluble peptide using Bicine/Tris SDS-PAGE

Publication IV

- Monitoring of insulin fibrillization by ThT fluorescence
- Calculation of kinetic parameters
- TEM visualization of fibrils

4. Results

Publication I

- It was shown that at pH 7.3 the lag phase of insulin fibrillization decreases and the fibrillization rate constant increases with increasing temperature.
- It was shown that the enthalpy of activation of the insulin fibrillization E_a at pH 7.3 is equal to 84 kJ/mol.
- It was demonstrated that at pH 7.3 fibrillization of insulin depends only slightly on the insulin concentration in the range 2.5–10 μM, whereas at higher concentrations the fibrillization lag phase increases and the fibrillization rate decreases.
- It was determined by SEC and ESI-MS studies that at 2.5 μM insulin is prevalently monomeric.
- It was determined by ESI-MS that the K_d value for insulin dimers is equal to 18.9 μM.
- It was shown that micromolar concentrations of C-peptide and amylin do not affect fibrillization of monomeric insulin.
- Zn^{2+} exhibited an inhibitory effect on the fibrillization of monomeric insulin at pH 7.3 by forming a soluble Zn^{2+}-insulin complex (K_{Zn} = 7.5 μM).
- It was demonstrated that the inhibitory effect of Zn^{2+} (IC50 = 3.5 μM) was very strong at pH 7.3.
- It was demonstrated that the inhibitory effect of Zn^{2+} was much weaker at pH 5.5, as 20 μM Zn^{2+} did not affect the fibrillization rate constant and caused only a slight increase of the lag pahase.
- Based on the effects of Zn^{2+} ions a model of assembly and fibrillogenesis of insulin was suggested.

Publication II

- The effect of several low-molecular weight compounds on the fibrillization of monomeric insulin was demonstrated.
- It was shown that Basic Blue 41, Basic Blue 12, Tannic acid and Azure C interfere with ThT emission in the ThT based fibrillization assay.
- It was demonstrated that the same selected substances did neither decrease the fibrillization rate nor increase the lag phase at low micromolar concentrations.
- Absence of soluble insulin in the end of the experiment was determined by SEC analysis, which confirms that these compounds do not disaggregate the insulin fibrils.
- It was shown that Zn^{2+} ions did not decrease the fluorescence of preformed insulin fibrils.
- It was shown that riboflavin, imidazole, ascorbic acid and phenolphthalein had no effect on the fibrillization and ThT fluorescence.

Publication III

- The effect of agitation on the fibrillization of Aβ40, Aβ42, amylin and insulin was demonstrated.
- It was shown that Abβ2 does not require agitation during this elongation phase as stopping of the agitation did not affect fibril elongation rate.

- It was demonstrated that the rate for Aβ40 fibrillization significantly decreases when agitation was stopped during the fibril elongation phase.
- It was shown that the fibrillization of insulin and amylin stops when agitation was stopped during the fibril elongation phase.

Publication IV

- It was shown that at pH 2.5 the lag phase of insulin fibrillization decreases and the rate constant increases with increasing temperature.
- It was shown that the enthalpy of activation of the insulin fibrillization E_a at pH 2.5 is equal to 33.8 kJ/mol.
- It was demonstrated that at pH 2.5 under the final ThT florescence levels increases with increasing peptide concentration.
- It was demonstrated that at pH 2.5 fibrillization of insulin depends only slightly on the insulin concentration in the range 50–250 μM, whereas, at low (2.5 μM) insulin concentration no amyloid formation was observed.
- It was shown that the fibrillization of 2.5 μM insulin exposes shorter lag phases and faster growth of fibrils at physiological pH range compared to those measured at acidic pH values.
- It was shown that the fibrillization of 250 μM insulin, on the contrary, exposes shorter lag phases and faster growth of fibrils at acidic pH values compared to those measured at physiological pH values.
- It was demonstrated that at pH 2.5 the fibrillization of insulin continues to proceed with the same rate, after stopping the agitation.
- It was demonstrated that the morphology of fibrils formed at physiological and acidic pH is also different.

5. Discussion

In the secretory granules, insulin is densely packed together with Zn^{2+} into crystals of $Zn_2Insulin_6$ hexamers, which prevents fibrillization of the peptide (Orci, Ravazzola et al. 1987). In addition to Zn^{2+} ions, insulin is stored in these secretory granules together with C-peptide and amylin, which are present in equimolar and approx. 10-fold lower amounts than insulin, respectively (Westermark, Li et al. 1996). Previous studies have shown that insulin interferes with amylin fibrillization (Cui, Ma et al. 2009), at the same time it has been also demonstrated that C-peptide affects the pattern of insulin oligomerization (Shafqat, Melles et al. 2006) and inhibits amylin aggregation (Westermark, Li et al. 1996). The influence of Zn^{2+} ions, C-peptide and amylin on fibrillization of insulin have not been studied. Moreover, fibrillization of insulin has been intensively studied at acidic pH values and high peptide concentrations and only few studies have been performed at physiological pH values.

In the first set of experiments, we investigated the effects of Zn^{2+} ions, C-peptide and amylin on the fibrillization of monomeric insulin (2.5 μM) at physiological pH values (Publication I). We demonstrated that micromolar concentrations of C-peptide (2.5 μM) and amylin (1 μM) did not affect fibrillization of monomeric insulin (Figure 5 in [Publication I]). At the same time Zn^{2+} ions inhibited fibrillization of monomeric insulin at pH 7.3 by forming a soluble Zn^{2+}-insulin complex. The inhibitory effect of Zn^{2+} ions was very strong (IC50 = 3.5 μM) (Figure 7a, [Publication I]), indicating that Zn^{2+} ions inhibit fibrillization of insulin at low micromolar concentrations. Later, Frankaer et al. also confirmed that the presence of Zn^{2+} ions generally impedes the fibril formation seen as a prolonged lag phase (Frankaer, Sonderby et al. 2017). However, at pH 5.5 the inhibitory effect of Zn^{2+} progressively weakens and only a slight (10%) decrease in the fibrillization rate was observed in the presence of 20 μM Zn^{2+} (Figure 7b, [Publication I]). The pH dependence points to the participation of His residue(s) in the Zn^{2+}-induced inhibition of insulin fibrillization. It has been demonstrated that the six-residue B-chain segment (B12–B17) contributes to the formation of cross-β structure of the insulin fibrils (Ivanova, Sievers et al. 2009). It is also known that the HisB10 that is located in the nearby of the segment (B12–B17), participates in the binding of Zn^{2+} ions. Therefore, it can be suggested that binding of Zn^{2+} to HisB10 may prevent the formation of a β-sheet rich conformation of adjacent segment B12–B17 compatible for fibrillization. Based on the results, we suggested that Zn^{2+} ions inhibit fibrillization through differential stabilization of the insulin monomer. In a recent study Frankaer et al., (Frankaer, Sonderby et al. 2017) showed that Zn^{2+} ions bound to the insulin fibrils are coordinated with three His residues and chloride ions. It has been shown recently that the Zn^{2+} binding affinity is higher at lower insulin concentrations, where the insulin is monomeric and the apparent binding affinity decreases drastically at higher insulin concentrations where the peptide forms dimers (Gavrilova, Tougu et al. 2014). A schematic model describing the effect of Zn^{2+} ions on the fibrillization of insulin is presented in Scheme 2.

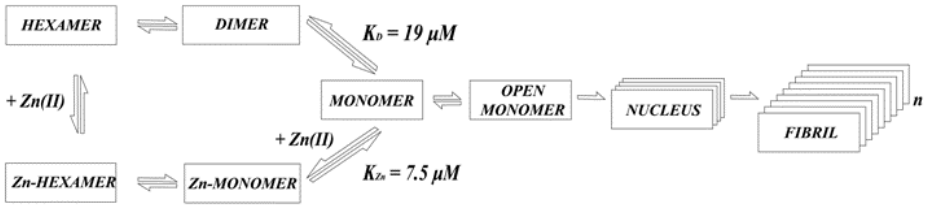

Scheme 2. *Mechanism for assembly and fibrillogenesis of insulin in the presence of Zn^{2+} ions. Insulin is hexameric at high peptide concentrations both in the presence and absence of Zn^{2+} ions. Insulin hexamers dissociate to dimers and monomers at low peptide concentrations, whereas peptide monomers can also bind Zn^{2+} ions. Monomeric insulin tends to fibrillize via a partially misfolded intermediate that is also assumed to be important for receptor binding. Zn^{2+}-insulin-monomer formation is off-pathway for fibrillization as it prevents opening of the conformation of monomeric insulin. From (Noormagi, Gavrilova et al. 2010) with permission.*

It is generally believed that insulin fibrillization occurs via a uniform reaction mechanism under various environmental conditions, however, this has been never proved experimentally. In the second set of experiments, we studied the effect of different environmental conditions on the kinetics of insulin fibrillization (Publication I, IV).

Our results show that the fibrillization of insulin at pH 7.3 is characterized by a ''reverse'' dependence on the peptide concentration - the fibrillization rate increases at low peptide concentrations (2.5–5 μM) and decreases at higher peptide concentrations (10–30 μM) (Figure 8, [Publication I]). The inhibition of fibril formation at higher insulin concentrations at physiological pH values, indicates that oligomerization suppresses insulin fibrillization (Nielsen, Khurana et al. 2001). However, contrary to our results, Mawhinney et al., (Mawhinney, Williams et al. 2017), have found that at pH 7.4 the lag phase of insulin fibrillization decreases and the rate constant increases with increasing insulin concentration in the concentration range of 2.5–50 μM. They indicated by photo-induced cross-linking of unmodified proteins (PICUP) SDS-PAGE that in this concentration range, solubility of neutral insulin increases at higher concentrations, with a concomitant decrease in oligomer populations. They also showed that the highest oligomer order decreases with insulin concentration at neutral pH and was the highest for 10 μM insulin. However, our ESI-MS (Figure 3b in [Publication I]) and SEC (Figure 6a in [Publication I]) measurements showed that 10 μM insulin was mainly monomeric. Moreover, SAXS experiments also demonstrated that insulin was predominantly dimeric at low concentrations and higher oligomers appeared and dominated at higher insulin concentrations in the range of 0,2 to 2 mM (Frankaer, Sonderby et al. 2017). These inconsistencies may be due to the different insulin samples used in the studies. Mawhinney et al. examined fibril formation of human insulin, which differs from bovine insulin (used in our experiments) in three amino acid residues. It is also possible to speculate that these differences may be caused by different sample preparation procedures. Mawhinney et al. dissolved insulin in neutral buffer at 50°C by agitation at 155 rpm for 1–2 min using a magnetic stirring bar. We incubated the stock solution of insulin for 30 min at 25°C without magnetic stirring. Moreover, Mawhinney et al. used magnetic stirring at 155 rpm during the time of monitoring insulin fibrillization, which was significantly slower than the 250 rpm used in our experiments.

Our results also demonstrated that fibrillization of insulin at pH 7.3 depends only slightly on the insulin concentration in the range of 2.5–10 μM, since the rate constant for fibril growth was almost constant (Figure 8, [Publication I]). This indicates that the rate-limiting step of fibrillization is most probably connected with some intramolecular event such as conformational change. However, at pH 2.5 the duration of lag phase and rate constants did not significantly change in the concentration range of 50–250 μM, whereas formation of fibrils was not observed at low (2.5 μM) peptide concentrations (Figure 2 in [Publication IV]). These results clearly demonstrate that the effects of peptide concentration were opposite at pH 2.5 and pH 7.3. It is know that IC50 for insulin dimerization is approx. 30 μM at pH 3.3 (Nettleton, Tito et al. 2000), therefore it is possible to speculate that at low pH insulin dimerization is required for fibrillization. Thus, we suggest that the mechanisms of insulin fibrillization at physiological and acidic pH values may proceed through different molecular events. Furthermore, in a recent study by Frankaer et al., (Frankaer, Sonderby et al. 2017), it was suggested that the structure of the fibril nucleus could be different depending on whether the starting insulin is hexameric, dimeric or monomeric.

In a recent study by Iannuzzi et al., (Iannuzzi, Borriello et al. 2017), it was demonstrated that insulin fibrils formed at neutral pH are morphologically different from those obtained at lower pH, which is in good agreement with our results. In order to determine when the ‘‘high pH’’ fibrillization mechanism is replaced by a ‘‘low pH’’ mechanism we studied the pH effects on the insulin fibrillization at low (2.5 μM) and high (250 μM) peptide concentrations. We demonstrated that the fibrillization curves of 2.5 μM insulin exposed shorter lag phases and faster growth rates at physiological pH values as compared to those measured at acidic pH values (Figure 3a in [Publication IV]). It is know that insulin is partially misfolded at acidic pH values (Hua and Weiss 2004), however, it seems that the stabilization of partially misfolded forms on the peptide does not result in higher fibrillization rate. Moreover, the maximal ThT fluorescence values were also higher at higher pH values (Figure 3a in [Publication IV]). We suggested that the pH dependence of maximal ThT level changed due to different ThT binding or spectral properties of ThT bound to ‘‘high pH’’ and ‘‘low pH’’ fibrils. The opposite pH effect was obtained at high, 250 μM insulin: the growth rate decreased and the duration of the lag phase increased with increasing pH (Figure 3b in [Publication IV]).

This difference indicates that protonation of His residues seems to be involved in the fibrillization of monomeric insulin. It is known that the HisB10 contributes to the formation of cross-β structure of the insulin fibrils (Ivanova, Sievers et al. 2009). It has also been shown that His18 participates in the formation of intermolecular β-sheet structure of amylin fibrils (Alexandrescu 2013). The lowered pK_a of His18 in the amylin fibrils indicates that positive charges at the His residues inhibit fibrillization (Jha, Snell et al. 2014). This led the authors to the suggestion that the protonation of HisB10 plays a similar role in insulin: HisB10 protonation at low pH results in electrostatic repulsion between positive charges in neighboring monomers in fibril. We also suggest that the pH effect at high insulin concentration may result from off-pathway oligomerization propensity.

Conclusions

- Zn^{2+} ions inhibit fibrillization of monomeric insulin at physiological pH values by forming a soluble Zn^{2+}-insulin complex. The results obtained indicate that Zn^{2+} ions that are co-secreted together with insulin might prevent fibrillization of insulin at its release sites and in circulation (Publication I).
- The effects of peptide concentration on the fibrillization of insulin are opposite at pH 2.5 and pH 7.3. The fibrillization of insulin at pH 7.3 is characterized by a ''reverse'' dependence on the peptide concentration - the fibrillization rate increases at low peptide concentrations (2.5–5 μM) and decreases at higher peptide concentrations (10–30 μM), whereas at acidic pH values the insulin fibrillization occurs only at high (> 10 μM) peptide concentrations. The inhibition of fibril formation at higher insulin concentrations at physiological pH values, indicates that oligomerization suppresses insulin fibrillization (Publication I, IV).
- The fibrillization rate of insulin decreases with increasing pH at high, 250 μM concentration, which was opposite to the pH effect observed at low, 2.5 μM insulin solutions. The latter effect indicates that protonation of histidine residues seems to be involved in the fibrillization of monomeric insulin, whereas the pH effect at high concentration may be caused by the formation of off-pathway oligomers (Publication IV).
- The enthalpy of activation Ea of the fibril growth at acidic pH is considerably lower than at physiological pH, which indicates that fibrillization mechanisms are different under the acidic conditions and at the physiological pH values. It can be assumed that the conformational changes necessary for the formation of fibrillization-competent structure are much more substantial at physiological pH values (Publication I, IV).
- The effects of agitation on the fibrillization of insulin are different at pH 2.5 and pH 7.3. At physiological pH insulin required agitation throughout the whole fibrillization process, whereas the fibrillization at low pH shows high fibrillization rate in the absence of agitation in the fibril growth phase (Publication III, IV).
- Taken together, the results indicate that fibrillization of insulin at acidic and physiological pH values occurs via different mechanisms, which should be considered in using of insulin fibrillization as model for fibrillization processes.
- Low-molecular weight compounds like Basic Blue 41, Basic Blue 12, Azure C and Tannic acid interfere with the fluorescence of ThT bound to insulin fibrils and cause false positive results during the screening of fibrillization inhibitors. The interference with ThT test is a general phenomenon and more attention has to be paid to interpretation of kinetic results of protein fibrillization obtained by using fluorescent dyes (Publication II).

References

Abel, J. J. (1926). "Crystalline Insulin." Proc Natl Acad Sci U S A **12**(2): 132-136.

Adams, M. J., Blundell, T. L., Dodson, E. J., Dodson, G. G., Vijayan, M., Baker, E. N., Harding, M. M., Hodgkin, D. C., Rimmer, B., and Sheat, S (1969). "Structure of Rhombohedral 2 Zinc Insulin Crystals." Nature **224**: 491-495.

Aguilar-Bryan, L., C. G. Nichols, et al. (1995). "Cloning of the beta cell high-affinity sulfonylurea receptor: a regulator of insulin secretion." Science **268**(5209): 423-426.

Ahlqvist, E., P. Storm, et al. (2018). "Novel subgroups of adult-onset diabetes and their association with outcomes: a data-driven cluster analysis of six variables." Lancet Diabetes Endocrinol.

Ahmad, A., I. S. Millett, et al. (2003). "Partially folded intermediates in insulin fibrillation." Biochemistry **42**(39): 11404-11416.

Ahmad, A., I. S. Millett, et al. (2004). "Stimulation of insulin fibrillation by urea-induced intermediates." J Biol Chem **279**(15): 14999-15013.

Ahmed, A. M. (2002). "History of diabetes mellitus." Saudi Med J **23**(4): 373-378.

Albert, S. G., J. Obadiah, et al. (2007). "Severe insulin resistance associated with subcutaneous amyloid deposition." Diabetes Res Clin Pract **75**(3): 374-376.

Alessi, D. R. and P. Cohen (1998). "Mechanism of activation and function of protein kinase B." Curr Opin Genet Dev **8**(1): 55-62.

Alexandrescu, A. T. (2013). "Amide proton solvent protection in amylin fibrils probed by quenched hydrogen exchange NMR." PLoS One **8**(2): e56467.

Arora, A., C. Ha, et al. (2004). "Insulin amyloid fibrillation at above 100 degrees C: New insights into protein folding under extreme temperatures." Protein Science **13**(9): 2429-2436.

Baekkeskov, S., H. J. Aanstoot, et al. (1990). "Identification of the 64K autoantigen in insulin-dependent diabetes as the GABA-synthesizing enzyme glutamic acid decarboxylase." Nature **347**(6289): 151-156.

Baker, E. N., T. L. Blundell, et al. (1988). "The structure of 2Zn pig insulin crystals at 1.5 A resolution." Philos Trans R Soc Lond B Biol Sci **319**(1195): 369-456.

Baldwin, R. L. (1996). "How Hofmeister ion interactions affect protein stability." Biophysical Journal **71**(4): 2056-2063.

Bekard, I. B. and D. E. Dunstan (2009). "Tyrosine autofluorescence as a measure of bovine insulin fibrillation." Biophys J **97**(9): 2521-2531.

Belkina, A. C. and G. V. Denis (2010). "Obesity genes and insulin resistance." Curr Opin Endocrinol Diabetes Obes **17**(5): 472-477.

Bentley, G., E. Dodson, et al. (1976). "Structure of insulin in 4-zinc insulin." Nature **261**(5556): 166-168.

Bharathi, S. S. Indi, et al. (2007). "Copper- and iron-induced differential fibril formation in alpha-synuclein: TEM study." Neurosci Lett **424**(2): 78-82.

Bharathi and K. S. Rao (2008). "Molecular understanding of copper and iron interaction with alpha-synuclein by fluorescence analysis." J Mol Neurosci **35**(3): 273-281.

Bi, Y., T. Wang, et al. (2012). "Advanced research on risk factors of type 2 diabetes." Diabetes Metab Res Rev **28 Suppl 2**: 32-39.

Biancalana, M., K. Makabe, et al. (2009). "Molecular mechanism of thioflavin-T binding to the surface of beta-rich peptide self-assemblies." J Mol Biol **385**(4): 1052-1063.

Blair, M. (2016). "Diabetes Mellitus Review." Urol Nurs **36**(1): 27-36.
Blake, C. and L. Serpell (1996). "Synchrotron X-ray studies suggest that the core of the transthyretin amyloid fibril is a continuous beta-sheet helix." Structure **4**(8): 989-998.
Bluestone, J. A., K. Herold, et al. (2010). "Genetics, pathogenesis and clinical interventions in type 1 diabetes." Nature **464**(7293): 1293-1300.
Bolder, S. G., L. M. Sagis, et al. (2007). "Thioflavin T and birefringence assays to determine the conversion of proteins into fibrils." Langmuir **23**(8): 4144-4147.
Bonifacio, E., V. Lampasona, et al. (1998). "IA-2 (islet cell antigen 512) is the primary target of humoral autoimmunity against type 1 diabetes-associated tyrosine phosphatase autoantigens." J Immunol **161**(5): 2648-2654.
Bouchard, M., J. Zurdo, et al. (2000). "Formation of insulin amyloid fibrils followed by FTIR simultaneously with CD and electron microscopy." Protein Sci **9**(10): 1960-1967.
Brader, M. L. and M. F. Dunn (1991). "Insulin hexamers: new conformations and applications." Trends Biochem Sci **16**(9): 341-345.
Brange, J., L. Andersen, et al. (1997). "Toward understanding insulin fibrillation." Journal of Pharmaceutical Sciences **86**(5): 517-525.
Brange, J., G. G. Dodson, et al. (1997). "A model of insulin fibrils derived from the x-ray crystal structure of a monomeric insulin (despentapeptide insulin)." Proteins-Structure Function and Genetics **27**(4): 507-516.
Brange, J., S. Havelund, et al. (1986). "Neutral insulin solutions physically stabilized by addition of Zn2+." Diabet Med **3**(6): 532-536.
Brange, J. and L. Langkjoer (1993). "Insulin structure and stability." Pharm Biotechnol **5**: 315-350.
Bryant, C., D. B. Spencer, et al. (1993). "Acid stabilization of insulin." Biochemistry **32**(32): 8075-8082.
Burke, M. J. and M. A. Rougvie (1972). "Cross- protein structures. I. Insulin fibrils." Biochemistry **11**(13): 2435-2439.
Burton, A. R., E. Vincent, et al. (2008). "On the pathogenicity of autoantigen-specific T-cell receptors." Diabetes **57**(5): 1321-1330.
Bush, A. I., W. H. Pettingell, et al. (1994). "Rapid induction of Alzheimer A beta amyloid formation by zinc." Science **265**(5177): 1464-1467.
Cargnello, M. and P. P. Roux (2011). "Activation and function of the MAPKs and their substrates, the MAPK-activated protein kinases." Microbiol Mol Biol Rev **75**(1): 50-83.
Castillo, V. and S. Ventura (2009). "Amyloidogenic Regions and Interaction Surfaces Overlap in Globular Proteins Related to Conformational Diseases." Plos Computational Biology **5**(8).
Chakrabarti, P., J. Y. Kim, et al. (2013). "Insulin inhibits lipolysis in adipocytes via the evolutionarily conserved mTORC1-Egr1-ATGL-mediated pathway." Mol Cell Biol **33**(18): 3659-3666.
Chander, H., A. Chauhan, et al. (2007). "Binding of proteases to fibrillar amyloid-beta protein and its inhibition by Congo red." J Alzheimers Dis **12**(3): 261-269.
Chang, X., A. M. Jorgensen, et al. (1997). "Solution structures of the R6 human insulin hexamer." Biochemistry **36**(31): 9409-9422.

Chatani, E., R. Inoue, et al. (2015). "Early aggregation preceding the nucleation of insulin amyloid fibrils as monitored by small angle X-ray scattering." Sci Rep **5**: 15485.

Chimienti, F., S. Devergnas, et al. (2006). "In vivo expression and functional characterization of the zinc transporter ZnT8 in glucose-induced insulin secretion." J Cell Sci **119**(Pt 20): 4199-4206.

Clifford, K. S. and M. J. MacDonald (2000). "Survey of mRNAs encoding zinc transporters and other metal complexing proteins in pancreatic islets of rats from birth to adulthood: similar patterns in the Sprague-Dawley and Wistar BB strains." Diabetes Res Clin Pract **49**(2-3): 77-85.

Cohen, S. I., M. Vendruscolo, et al. (2012). "From macroscopic measurements to microscopic mechanisms of protein aggregation." J Mol Biol **421**(2-3): 160-171.

Collins, K. D. and M. W. Washabaugh (1985). "The Hofmeister Effect and the Behavior of Water at Interfaces." Quarterly Reviews of Biophysics **18**(4): 323-422.

Costantino, H. R., R. Langer, et al. (1994). "Solid-phase aggregation of proteins under pharmaceutically relevant conditions." Journal of Pharmaceutical Sciences **83**(12): 1662-1669.

Creemers, J. W., R. S. Jackson, et al. (1998). "Molecular and cellular regulation of prohormone processing." Semin Cell Dev Biol **9**(1): 3-10.

Cross, D. A., D. R. Alessi, et al. (1995). "Inhibition of glycogen synthase kinase-3 by insulin mediated by protein kinase B." Nature **378**(6559): 785-789.

Cui, W., J. W. Ma, et al. (2009). "Insulin is a kinetic but not a thermodynamic inhibitor of amylin aggregation." FEBS J **276**(12): 3365-3371.

Cullmann, M., A. Hilding, et al. (2012). "Alcohol consumption and risk of pre-diabetes and type 2 diabetes development in a Swedish population." Diabet Med **29**(4): 441-452.

Datta, S. R., H. Dudek, et al. (1997). "Akt phosphorylation of BAD couples survival signals to the cell-intrinsic death machinery." Cell **91**(2): 231-241.

David F. Waugh , D. F. W., Spencer L. Commerford , Muriel L. Sackler (1953). "Studies of the Nucleation and Growth Reactions of Selected Types of Insulin Fibrils." J. Am. Chem. Soc **75**(11): 2592-2600.

Davidson, H. W. (2004). "(Pro)Insulin processing: a historical perspective." Cell Biochem Biophys **40**(3 Suppl): 143-158.

Debye P, H. E. (1923). "The theory of electrolytes. I. Lowering of freezing point and related phenomena." Physikalische Zeitschrift **24**: 185-206.

Defronzo, R. A. (2009). "Banting Lecture. From the triumvirate to the ominous octet: a new paradigm for the treatment of type 2 diabetes mellitus." Diabetes **58**(4): 773-795.

Derewenda, U., Z. Derewenda, et al. (1989). "Phenol stabilizes more helix in a new symmetrical zinc insulin hexamer." Nature **338**(6216): 594-596.

Devlin, G. L., T. P. Knowles, et al. (2006). "The component polypeptide chains of bovine insulin nucleate or inhibit aggregation of the parent protein in a conformation-dependent manner." J Mol Biol **360**(2): 497-509.

Dimitriadis, G., P. Mitrou, et al. (2011). "Insulin effects in muscle and adipose tissue." Diabetes Res Clin Pract **93 Suppl 1**: S52-59.

Dische, F. E., C. Wernstedt, et al. (1988). "Insulin as an Amyloid-Fibril Protein at Sites of Repeated Insulin Injections in a Diabetic Patient." Diabetologia **31**(3): 158-161.

Dobson, C. M. (1999). "Protein misfolding, evolution and disease." Trends Biochem Sci **24**(9): 329-332.

Dobson, C. M. (2003). "Protein folding and misfolding." Nature **426**(6968): 884-890.

Dodson, G. and D. Steiner (1998). "The role of assembly in insulin's biosynthesis." Curr Opin Struct Biol **8**(2): 189-194.

Emily Ha, J. S. S., Bhaskara Jasti and Xiaoling Li (2012). "Effect of Concentration and Ionic Strength on Pathway of Bovine Insulin Fibril Formation." Indian Journals **6**(3): 290-299.

Ferrone, F. (1999). "Analysis of protein aggregation kinetics." Methods Enzymol **309**: 256-274.

Figlewicz, D. P., S. E. Forhan, et al. (1984). "65Zinc and endogenous zinc content and distribution in islets in relationship to insulin content." Endocrinology **115**(3): 877-881.

Fodera, V., S. Cataldo, et al. (2009). "Self-organization pathways and spatial heterogeneity in insulin amyloid fibril formation." J Phys Chem B **113**(31): 10830-10837.

Frankaer, C. G., M. V. Knudsen, et al. (2012). "The structures of T6, T3R3 and R6 bovine insulin: combining X-ray diffraction and absorption spectroscopy." Acta Crystallogr D Biol Crystallogr **68**(Pt 10): 1259-1271.

Frankaer, C. G., P. Sonderby, et al. (2017). "Insulin fibrillation: The influence and coordination of Zn(2)." J Struct Biol **199**(1): 27-38.

Fukase, N., H. Takahashi, et al. (1992). "Differences in glucagon-like peptide-1 and GIP responses following sucrose ingestion." Diabetes Res Clin Pract **15**(3): 187-195.

Gavrilova, J., V. Tougu, et al. (2014). "Affinity of zinc and copper ions for insulin monomers." Metallomics **6**(7): 1296-1300.

Gjerde, D. T., G. Schmuckler, et al. (1980). "Anion Chromatography with Low-Conductivity Eluents .2." Journal of Chromatography **187**(1): 35-45.

Goto, Y. and A. L. Fink (1994). "Acid-induced folding of heme proteins." Methods Enzymol **232**: 3-15.

Goto, Y., N. Takahashi, et al. (1990). "Mechanism of acid-induced folding of proteins." Biochemistry **29**(14): 3480-3488.

Graham, T. E. and B. B. Kahn (2007). "Tissue-specific alterations of glucose transport and molecular mechanisms of intertissue communication in obesity and type 2 diabetes." Horm Metab Res **39**(10): 717-721.

Haffner, S. M., S. Lehto, et al. (1998). "Mortality from coronary heart disease in subjects with type 2 diabetes and in nondiabetic subjects with and without prior myocardial infarction." N Engl J Med **339**(4): 229-234.

Hodgkin, D. C. (1971). "X rays and the structures of insulin." Br Med J **4**(5785): 447-451.

Hong, D. P., A. Ahmad, et al. (2006). "Fibrillation of human insulin A and B chains." Biochemistry **45**(30): 9342-9353.

Hong, D. P. and A. L. Fink (2005). "Independent heterologous fibrillation of insulin and its B-chain peptide." Biochemistry **44**(50): 16701-16709.

Hu, F. B., J. E. Manson, et al. (2001). "Diet, lifestyle, and the risk of type 2 diabetes mellitus in women." N Engl J Med **345**(11): 790-797.

Hua, Q. X. and M. A. Weiss (1991). "Comparative 2D NMR studies of human insulin and des-pentapeptide insulin: sequential resonance assignment and implications for protein dynamics and receptor recognition." Biochemistry **30**(22): 5505-5515.

Hua, Q. X. and M. A. Weiss (2004). "Mechanism of insulin fibrillation: the structure of insulin under amyloidogenic conditions resembles a protein-folding intermediate." J Biol Chem **279**(20): 21449-21460.

Huang, S. and M. P. Czech (2007). "The GLUT4 glucose transporter." Cell Metab **5**(4): 237-252.

Huang, X. F. and P. Arvan (1995). "Intracellular transport of proinsulin in pancreatic beta-cells. Structural maturation probed by disulfide accessibility." J Biol Chem **270**(35): 20417-20423.

Hudson, S. A., H. Ecroyd, et al. (2009). "The thioflavin T fluorescence assay for amyloid fibril detection can be biased by the presence of exogenous compounds." FEBS J **276**(20): 5960-5972.

Huus, K., S. Havelund, et al. (2005). "Thermal dissociation and unfolding of insulin." Biochemistry **44**(33): 11171-11177.

Iannuzzi, C., M. Borriello, et al. (2017). "Insights into Insulin Fibril Assembly at Physiological and Acidic pH and Related Amyloid Intrinsic Fluorescence." Int J Mol Sci **18**(12).

Ivanova, M. I., S. A. Sievers, et al. (2009). "Molecular basis for insulin fibril assembly." Proc Natl Acad Sci U S A **106**(45): 18990-18995.

Jha, S., J. M. Snell, et al. (2014). "pH dependence of amylin fibrillization." Biochemistry **53**(2): 300-310.

Jimenez, J. L., E. J. Nettleton, et al. (2002). "The protofilament structure of insulin amyloid fibrils." Proc Natl Acad Sci U S A **99**(14): 9196-9201.

Kayed, R., E. Head, et al. (2003). "Common structure of soluble amyloid oligomers implies common mechanism of pathogenesis." Science **300**(5618): 486-489.

Kelly, J. W. (1998). "The alternative conformations of amyloidogenic proteins and their multi-step assembly pathways." Curr Opin Struct Biol **8**(1): 101-106.

Kelly, M. A., M. L. Rayner, et al. (2003). "Molecular aspects of type 1 diabetes." Mol Pathol **56**(1): 1-10.

Kido, Y., J. Nakae, et al. (2001). "Clinical review 125: The insulin receptor and its cellular targets." J Clin Endocrinol Metab **86**(3): 972-979.

Kim, J. R., A. Muresan, et al. (2004). "Urea modulation of beta-amyloid fibril growth: experimental studies and kinetic models." Protein Sci **13**(11): 2888-2898.

Knip, M. (2002). "Natural course of preclinical type 1 diabetes." Horm Res **57 Suppl 1**: 6-11.

Knowles, T. P., C. A. Waudby, et al. (2009). "An analytical solution to the kinetics of breakable filament assembly." Science **326**(5959): 1533-1537.

Koo, B. W. and A. D. Miranker (2005). "Contribution of the intrinsic disulfide to the assembly mechanism of islet amyloid." Protein Sci **14**(1): 231-239.

Krebs, M. R., E. H. Bromley, et al. (2005). "The binding of thioflavin-T to amyloid fibrils: localisation and implications." J Struct Biol **149**(1): 30-37.

Landreh, M., G. Alvelius, et al. (2014). "Insulin, islet amyloid polypeptide and C-peptide interactions evaluated by mass spectrometric analysis." Rapid Commun Mass Spectrom **28**(2): 178-184.

Lasagna-Reeves, C. A., A. L. Clos, et al. (2010). "Inhaled insulin forms toxic pulmonary amyloid aggregates." Endocrinology **151**(10): 4717-4724.

Lee, C. C., A. Nayak, et al. (2007). "A three-stage kinetic model of amyloid fibrillation." Biophys J **92**(10): 3448-3458.

Lee, J., P. F. Pilch, et al. (1997). "Conformational changes of the insulin receptor upon insulin binding and activation as monitored by fluorescence spectroscopy." Biochemistry **36**(9): 2701-2708.

Lemaire, K., M. A. Ravier, et al. (2009). "Insulin crystallization depends on zinc transporter ZnT8 expression, but is not required for normal glucose homeostasis in mice." Proc Natl Acad Sci U S A **106**(35): 14872-14877.

Leslie, R. D. (2010). "Predicting adult-onset autoimmune diabetes: clarity from complexity." Diabetes **59**(2): 330-331.

LeVine, H., 3rd (1993). "Thioflavine T interaction with synthetic Alzheimer's disease beta-amyloid peptides: detection of amyloid aggregation in solution." Protein Sci **2**(3): 404-410.

LeVine, H., 3rd (1999). "Quantification of beta-sheet amyloid fibril structures with thioflavin T." Methods Enzymol **309**: 274-284.

Librizzi, F. and C. Rischel (2005). "The kinetic behavior of insulin fibrillation is determined by heterogeneous nucleation pathways." Protein Science **14**(12): 3129-3134.

Liu, Z. and E. J. Barrett (2002). "Human protein metabolism: its measurement and regulation." Am J Physiol Endocrinol Metab **283**(6): E1105-1112.

Long, X., Y. Lin, et al. (2005). "Rheb binds and regulates the mTOR kinase." Curr Biol **15**(8): 702-713.

Ma, B., F. Zhang, et al. (2017). "Investigating the inhibitory effects of zinc ions on amyloid fibril formation of hen egg-white lysozyme." Int J Biol Macromol **98**: 717-722.

Madaan, T., M. Akhtar, et al. (2016). "Sodium glucose CoTransporter 2 (SGLT2) inhibitors: Current status and future perspective." Eur J Pharm Sci **93**: 244-252.

Manson, J. E., U. A. Ajani, et al. (2000). "A prospective study of cigarette smoking and the incidence of diabetes mellitus among US male physicians." Am J Med **109**(7): 538-542.

Margolis, B. and E. Y. Skolnik (1994). "Activation of Ras by receptor tyrosine kinases." J Am Soc Nephrol **5**(6): 1288-1299.

Mawhinney, M. T., T. L. Williams, et al. (2017). "Elucidation of insulin assembly at acidic and neutral pH: Characterization of low molecular weight oligomers." Proteins **85**(11): 2096-2110.

Mayer, J. P., F. Zhang, et al. (2007). "Insulin structure and function." Biopolymers **88**(5): 687-713.

Millican, R. L. and D. N. Brems (1994). "Equilibrium intermediates in the denaturation of human insulin and two monomeric insulin analogs." Biochemistry **33**(5): 1116-1124.

Milto, K., K. Michailova, et al. (2014). "Elongation of mouse prion protein amyloid-like fibrils: effect of temperature and denaturant concentration." PLoS One **9**(4): e94469.

Mishra, R., D. Sjolander, et al. (2011). "Spectroscopic characterization of diverse amyloid fibrils in vitro by the fluorescent dye Nile red." Mol Biosyst **7**(4): 1232-1240.

Moodie, S. A., B. M. Willumsen, et al. (1993). "Complexes of Ras.GTP with Raf-1 and mitogen-activated protein kinase kinase." Science **260**(5114): 1658-1661.

Morinaga, A., K. Hasegawa, et al. (2010). "Critical role of interfaces and agitation on the nucleation of Abeta amyloid fibrils at low concentrations of Abeta monomers." Biochim Biophys Acta **1804**(4): 986-995.

Munishkina, L. A., J. Henriques, et al. (2004). "Role of protein-water interactions and electrostatics in alpha-synuclein fibril formation." Biochemistry **43**(11): 3289-3300.

Muzaffar, M. and A. Ahmad (2011). "The mechanism of enhanced insulin amyloid fibril formation by NaCl is better explained by a conformational change model." PLoS One **6**(11): e27906.

Nayak, A., M. Sorci, et al. (2009). "A universal pathway for amyloid nucleus and precursor formation for insulin." Proteins **74**(3): 556-565.

Nettleton, E. J., P. Tito, et al. (2000). "Characterization of the oligomeric states of insulin in self-assembly and amyloid fibril formation by mass spectrometry." Biophys J **79**(2): 1053-1065.

Newsholme, E. A. and G. Dimitriadis (2001). "Integration of biochemical and physiologic effects of insulin on glucose metabolism." Exp Clin Endocrinol Diabetes **109 Suppl 2**: S122-134.

Nielsen, L., S. Frokjaer, et al. (2001). "Probing the mechanism of insulin fibril formation with insulin mutants." Biochemistry **40**(28): 8397-8409.

Nielsen, L., S. Frokjaer, et al. (2001). "Studies of the structure of insulin fibrils by Fourier transform infrared (FTIR) spectroscopy and electron microscopy." Journal of Pharmaceutical Sciences **90**(1): 29-37.

Nielsen, L., R. Khurana, et al. (2001). "Effect of environmental factors on the kinetics of insulin fibril formation: elucidation of the molecular mechanism." Biochemistry **40**(20): 6036-6046.

Nilsson, M. R. (2004). "Techniques to study amyloid fibril formation in vitro." Methods **34**(1): 151-160.

Noormagi, A., J. Gavrilova, et al. (2010). "Zn(II) ions co-secreted with insulin suppress inherent amyloidogenic properties of monomeric insulin." Biochem J **430**(3): 511-518.

Ntzani, E. E. and F. K. Kavvoura (2012). "Genetic risk factors for type 2 diabetes: insights from the emerging genomic evidence." Curr Vasc Pharmacol **10**(2): 147-155.

Olokoba, A. B., O. A. Obateru, et al. (2012). "Type 2 diabetes mellitus: a review of current trends." Oman Med J **27**(4): 269-273.

Olsen, H. B., S. Ludvigsen, et al. (1996). "Solution structure of an engineered insulin monomer at neutral pH." Biochemistry **35**(27): 8836-8845.

Orci, L., M. Ravazzola, et al. (1985). "Direct identification of prohormone conversion site in insulin-secreting cells." Cell **42**(2): 671-681.

Orci, L., M. Ravazzola, et al. (1987). "Proteolytic Maturation of Insulin Is a Post-Golgi Event Which Occurs in Acidifying Clathrin-Coated Secretory Vesicles." Cell **49**(6): 865-868.

Padgett, L. E., B. Anderson, et al. (2015). "Loss of NOX-Derived Superoxide Exacerbates Diabetogenic CD4 T-Cell Effector Responses in Type 1 Diabetes." Diabetes **64**(12): 4171-4183.

Padrick, S. B. and A. D. Miranker (2002). "Islet amyloid: phase partitioning and secondary nucleation are central to the mechanism of fibrillogenesis." Biochemistry **41**(14): 4694-4703.

Palmer, J. P., C. M. Asplin, et al. (1983). "Insulin antibodies in insulin-dependent diabetics before insulin treatment." Science **222**(4630): 1337-1339.

Pathak, R. and M. B. Bridgeman (2010). "Dipeptidyl Peptidase-4 (DPP-4) Inhibitors In the Management of Diabetes." P T **35**(9): 509-513.

Payton, M. A., C. J. Hawkes, et al. (1995). "Relationship of the 37,000- and 40,000-M(r) tryptic fragments of islet antigens in insulin-dependent diabetes to the protein tyrosine phosphatase-like molecule IA-2 (ICA512)." J Clin Invest **96**(3): 1506-1511.

Pease, L. F., 3rd, M. Sorci, et al. (2010). "Probing the nucleus model for oligomer formation during insulin amyloid fibrillogenesis." Biophys J **99**(12): 3979-3985.

Pedersen, J. S., D. Dikov, et al. (2006). "The changing face of glucagon fibrillation: structural polymorphism and conformational imprinting." J Mol Biol **355**(3): 501-523.

Pociot, F. and A. Lernmark (2016). "Genetic risk factors for type 1 diabetes." Lancet **387**(10035): 2331-2339.

Rasmussen, T., M. R. Kasimova, et al. (2009). "The chaperone-like protein alpha-crystallin dissociates insulin dimers and hexamers." Biochemistry **48**(39): 9313-9320.

Roy, M., R. W. Lee, et al. (1990). "1H NMR spectrum of the native human insulin monomer. Evidence for conformational differences between the monomer and aggregated forms." J Biol Chem **265**(10): 5448-5452.

Ryle, A. P., F. Sanger, et al. (1955). "The disulphide bonds of insulin." Biochem J **60**(4): 541-556.

Sahoo, S., W. Reeves, et al. (2003). "Amyloid tumor: a clinical and cytomorphologic study." Diagn Cytopathol **28**(6): 325-328.

Sanger, F. and E. O. Thompson (1953). "The amino-acid sequence in the glycyl chain of insulin. I. The identification of lower peptides from partial hydrolysates." Biochem J **53**(3): 353-366.

Sanger, F. and E. O. Thompson (1953). "The amino-acid sequence in the glycyl chain of insulin. II. The investigation of peptides from enzymic hydrolysates." Biochem J **53**(3): 366-374.

Sanger, F. and H. Tuppy (1951). "The amino-acid sequence in the phenylalanyl chain of insulin. 2. The investigation of peptides from enzymic hydrolysates." Biochem J **49**(4): 481-490.

Sanger, F. and H. Tuppy (1951). "The amino-acid sequence in the phenylalanyl chain of insulin. I. The identification of lower peptides from partial hydrolysates." Biochem J **49**(4): 463-481.

Saxena, R., B. F. Voight, et al. (2007). "Genome-wide association analysis identifies loci for type 2 diabetes and triglyceride levels." Science **316**(5829): 1331-1336.

Scott, L. J., K. L. Mohlke, et al. (2007). "A genome-wide association study of type 2 diabetes in Finns detects multiple susceptibility variants." Science **316**(5829): 1341-1345.

Selivanova, O. M. and O. V. Galzitskaya (2012). "Structural polymorphism and possible pathways of amyloid fibril formation on the example of insulin protein." Biochemistry (Mosc) **77**(11): 1237-1247.

Shafqat, J., E. Melles, et al. (2006). "Proinsulin C-peptide elicits disaggregation of insulin resulting in enhanced physiological insulin effects." Cell Mol Life Sci **63**(15): 1805-1811.

Shikama, Y., J. Kitazawa, et al. (2010). "Localized Amyloidosis at the Site of Repeated Insulin Injection in a Diabetic Patient." Internal Medicine **49**(5): 397-401.

Shulman, G. I., L. Rossetti, et al. (1987). "Quantitative analysis of glycogen repletion by nuclear magnetic resonance spectroscopy in the conscious rat." J Clin Invest **80**(2): 387-393.

Sinibaldi, F., B. D. Howes, et al. (2003). "Anion concentration modulates the conformation and stability of the molten globule of cytochrome c." J Biol Inorg Chem **8**(6): 663-670.

Sladek, R., G. Rocheleau, et al. (2007). "A genome-wide association study identifies novel risk loci for type 2 diabetes." Nature **445**(7130): 881-885.

Sluzky, V., J. A. Tamada, et al. (1991). "Kinetics of insulin aggregation in aqueous solutions upon agitation in the presence of hydrophobic surfaces." Proc Natl Acad Sci U S A **88**(21): 9377-9381.

Storkel, S., H. M. Schneider, et al. (1983). "Iatrogenic, insulin-dependent, local amyloidosis." Lab Invest **48**(1): 108-111.

Stsiapura, V. I., A. A. Maskevich, et al. (2007). "Computational study of thioflavin T torsional relaxation in the excited state." J Phys Chem A **111**(22): 4829-4835.

Sulatskaya, A. I., A. V. Lavysh, et al. (2017). "Thioflavin T fluoresces as excimer in highly concentrated aqueous solutions and as monomer being incorporated in amyloid fibrils." Sci Rep **7**(1): 2146.

Swift, B. (2002). "Examination of insulin injection sites: an unexpected finding of localized amyloidosis." Diabet Med **19**(10): 881-882.

Zeggini, E., M. N. Weedon, et al. (2007). "Replication of genome-wide association signals in UK samples reveals risk loci for type 2 diabetes." Science **316**(5829): 1336-1341.

Zhang, W., S. Patil, et al. (2006). "FoxO1 regulates multiple metabolic pathways in the liver: effects on gluconeogenic, glycolytic, and lipogenic gene expression." J Biol Chem **281**(15): 10105-10117.

Zimmet, P., K. G. Alberti, et al. (2001). "Global and societal implications of the diabetes epidemic." Nature **414**(6865): 782-787.

Zovo, K., E. Helk, et al. (2010). "Label-free high-throughput screening assay for inhibitors of Alzheimer's amyloid-beta peptide aggregation based on MALDI MS." Anal Chem **82**(20): 8558-8565.

Tang, L., J. L. Whittingham, et al. (1999). "Structural consequences of the B5 histidine --> tyrosine mutation in human insulin characterized by X-ray crystallography and conformational analysis." Biochemistry **38**(37): 12041-12051.

Taylor, C. G. (2005). "Zinc, the pancreas, and diabetes: insights from rodent studies and future directions." Biometals **18**(4): 305-312.

Tougu, V., A. Karafin, et al. (2009). "Zn(II)- and Cu(II)-induced non-fibrillar aggregates of amyloid-beta (1-42) peptide are transformed to amyloid fibrils, both spontaneously and under the influence of metal chelators." J Neurochem **110**(6): 1784-1795.

Ullrich, A., J. R. Bell, et al. (1985). "Human insulin receptor and its relationship to the tyrosine kinase family of oncogenes." Nature **313**(6005): 756-761.

van Belle, T. L., K. T. Coppieters, et al. (2011). "Type 1 diabetes: etiology, immunology, and therapeutic strategies." Physiol Rev **91**(1): 79-118.

Wan, Z. L., K. Huang, et al. (2008). "The structure of a mutant insulin uncouples receptor binding from protein allostery. An electrostatic block to the TR transition." J Biol Chem **283**(30): 21198-21210.

Weiss, M., D. F. Steiner, et al. (2000). "Insulin Biosynthesis, Secretion, Structure, and Structure-Activity Relationships."

Weiss, M. A., D. T. Nguyen, et al. (1989). "Two-dimensional NMR and photo-CIDNP studies of the insulin monomer: assignment of aromatic resonances with application to protein folding, structure, and dynamics." Biochemistry **28**(25): 9855-9873.

Wenzlau, J. M., K. Juhl, et al. (2007). "The cation efflux transporter ZnT8 (Slc30A8) is a major autoantigen in human type 1 diabetes." Proc Natl Acad Sci U S A **104**(43): 17040-17045.

Vestergaard, B., M. Groenning, et al. (2007). "A helical structural nucleus is the primary elongating unit of insulin amyloid fibrils." PLoS Biol **5**(5): e134.

Westermark, P., Z. C. Li, et al. (1996). "Effects of beta cell granule components on human islet amyloid polypeptide fibril formation." FEBS Lett **379**(3): 203-206.

Wild, S., G. Roglic, et al. (2004). "Global prevalence of diabetes: estimates for the year 2000 and projections for 2030." Diabetes Care **27**(5): 1047-1053.

Viollet, B., B. Guigas, et al. (2012). "Cellular and molecular mechanisms of metformin: an overview." Clin Sci (Lond) **122**(6): 253-270.

Voight, B. F., L. J. Scott, et al. (2010). "Twelve type 2 diabetes susceptibility loci identified through large-scale association analysis." Nat Genet **42**(7): 579-589.

Wullschleger, S., R. Loewith, et al. (2006). "TOR signaling in growth and metabolism." Cell **124**(3): 471-484.

Yang, X., Y. Li, et al. (2014). "Diethylpyrocarbonate modification reveals HisB5 as an important modulator of insulin amyloid formation." J Biochem.

Yki-Jarvinen, H. (2004). "Thiazolidinediones." N Engl J Med **351**(11): 1106-1118.

Yu, N. T., B. H. Jo, et al. (1974). "Single-crystal Raman spectra of native insulin. Structures of insulin fibrils, glucagon fibrils, and intact calf lens." Arch Biochem Biophys **160**(2): 614-622.

Yumlu, S., R. Barany, et al. (2009). "Localized insulin-derived amyloidosis in patients with diabetes mellitus: a case report." Hum Pathol **40**(11): 1655-1660.

Acknowledgement

These studies were carried out between 2009-2018 at the Department of Gene Technology, Tallinn University of Technology (TUT), Estonia.

First and foremost I would like to express my sincere gratitude to my supervisor, Professor Peep Palumaa, for introducing me the world of science, for his professional guidance and encouragement during my studies.

I would especially like to thank Vello Tõugu for proofreading my thesis, and for his excellent advisements and interesting discussions throughout all the years in the Proteomics lab.

I thank Andres Salumets for his advice and guidance.

I am also grateful to all of those with whom I have had the pleasure to work during these years in the Proteomics lab. I especially thank Merlin and Julia for being such a great colleagues. It has been a pleasure to work with you.

I must also acknowledge Valdek Mikli and Kairit Zovo for all their help with the transmission electron microscopy experiments.

I thank Professor Nigulas Samel for reviewing the thesis.

I am sincerely thankful to my family and friends for all the support and encouragement. My special thanks go to my mother for everything and more. Above all, I am grateful to my loving Sten for always being there for me and appreciating my achievements, and my son Rasmus for the happiness and inspiration.

I am indebted to the World Federation of Scientists for financial support, and also to the Archimedes Foundation and the DoRa program for the scholarship and for enabling me to introduce my results and broaden my knowledge at conferences and seminars.

Abstract

Effects of Zn^{2+} Ions and Environmental Conditions on the Fibrillization of Insulin

Protein and peptide fibrillization is obtaining much attention because it is connected with more than 40 human pathologies, including the most common neurodegenerative diseases and type II diabetes mellitus. Insulin is one of the peptides that readily forms amyloid-like fibrils *in vitro*. In relation to the therapeutic use of insulin, this fibrillization phenomenon constitutes a challenge during the production and delivery, and *in vivo* fibrillization has been observed after both insulin inhalation and injection. Therefore, it is important to study the mechanisms of insulin fibrillization to further improve the therapeutic use of insulin, as well as to shed light into the basic molecular features of amyloid formation. The aim of this study was to investigate and compare the effect of different environmental conditions, agitation, Zn^{2+} ions and low-molecular weight substances on the kinetics of insulin fibrillization using the fluorescent dye ThT.

Since the factors that prevent the fibrillization after release from the pancreatic β-cells when insulin dissociates into aggregation-prone monomers are not known, the influence of Zn^{2+} ions on the fibrillization of monomeric insulin was studied. It was demonstrated that Zn^{2+} inhibits fibrillization of monomeric insulin at physiological pH values by forming a soluble Zn^{2+}–insulin complex. It was suggested that Zn^{2+} ions that are co-secreted together with insulin might prevent fibrillization of insulin at its release sites and in circulation. Furthermore, it was found that several low molecular weight compounds that have been studied as inhibitors of Aβ42 fibrillization compete with ThT for binding sites within insulin fibrils and cause false positive results. Therefore, it is essential to pay more attention to interpretation of kinetic results of protein fibrillization obtained by using fluorescent dyes.

The effect of peptide concentration, pH, temperature and agitation on the fibrillization kinetics was examined. It was demonstrated that at acidic pH values the insulin fibrillization occurred only at high (> 10 μM) peptide concentrations, whereas at pH 7.4 the fibrillization was inhibited at higher insulin concentrations (> 10 μM). The effect of pH was also opposite at different concentrations of insulin. The fibrillization rate of insulin decreases with increasing pH at high, 250 μM concentration, whereas at low, 2.5 μM concentration the fibril formation was accelerated with increasing pH. Moreover, significant differences in the enthalpy of activation values of the insulin fibrillization were detected. Last, but not least, it was shown that at pH 7.4 the fibrillization of insulin stops when the agitation was stopped, whereas the fibrillization at pH 2.5 continues to proceed with the same rate after stopping the agitation. Together, the different effect of environmental factors on the insulin fibrillization suggest that the reaction rate is controlled by different molecular events in acidic conditions and at physiological pH values.

To sum up it can be concluded that the obtained results provide a more detailed understanding of the molecular mechanisms of amyloid formation, which should be considered in using of insulin fibrillization as model for fibrillization processes.

Kokkuvõte

Zn^{2+} ioonide ja keskkonnatingimuste mõju insuliini fibrillisatsioonile

Valkude ja peptiidide fibrillisatsioon ning amüloidsete struktuuride moodustumine on teadaolevalt seotud enam kui neljakümne inimesel esineva patoloogiaga. Nende hulgas on ka kõige levinumad neurodegeneratiivsed haigused ja II tüüpi diabeet. Insuliin on peptiidne hormoon, mis moodustab väga hõlpsasti amüloidseid fibrille *in vitro*. Insuliini terapeutilisel kasutamisel põhjustab selle fibrillisatsioon probleeme nii tootmisel kui ka käitlemisel. Insuliini fibrillid võivad moodustuda ka patsientidel pärast insulini inhalatsiooni ja süstimist. Insuliini fibrillisatsioonimehhanismide väljaselgitamine on vajalik nii selleks, et veelgi tõhustada insuliini terapeutilist kasutamist kui ka selleks, et mõista amüloidsete fibrillide moodustumise üldiseid molekulaarseid seaduspärasusi. Antud töö eesmärgiks oli uurida ja võrrelda erinevate keskkonnatingimuste, vedela faasi liikumise, Zn^{2+} ioonide ja madalmolekulaarsete ainete mõju insuliini fibrillisatsiooni kineetikale, kasutades spetsiifiliselt fibrillidega seonduvat fluorestseeruvat ligandi Tioflaviin T-d.

Pankrease beeta-rakkude sekretoorsetes graanulites on insuliin pakitud koos Zn^{2+} ioonidega heksameeridest moodustunud kristallidesse, mis tagab vesiikulite osmootilise stabiilsuse ja takistab fibrillide moodustumist. Vastuseta on küsimus, millised faktorid takistavad insuliini fibrillisatsiooni peale beetarakkudest vabanemist, kui insulin dissotseerub aktiivseteks monomeerideks, mis on väga fibrilleerumisaldid. Töös näidati, et Zn^{2+} ioonid inhibeerivad olulisel määral ka monomeerse insuliini fibrillisatsiooni, moodustades lahustuva Zn^{2+}-insuliin kompleksi. Zn^{2+} ioonide mõju oli väga tugev, inhibeerides insuliini fibrillisatsiooni väga madalatel kontsentratsioonidel (IC50 = 3.5 µM) ja juba nelja ekvivalendi Zn^{2+} lisamine insuliinile inhibeeris peaaegu täielikult fibrillide moodustumise. Tuginedes saadud tulemustele võib väita, et koos insuliiniga sekreteeritavad Zn^{2+} ioonid takistavad ka monomeerse insuliini fibrillisatsiooni pärast selle beetarakkudest vabanemist.

Lisaks uuriti kirjandusest teadaolevaid amüloidogeensete peptiidide, eelkõige Alzheimeri amüloidse peptiidi Aβ42, fibrillisatsiooni inhibiitorite toimet insuliini fibrillisatsioonile. Näidati, et mitmed oletatavad madalmolekulaarsed fibrillisatsiooni inhibiitorid hoopis konkureerivad ThT-ga sidumiskohtade pärast insuliini fibrillidel ja põhjustavad valepositiivseid tulemusi antud testimismeetodi kasutamisel. Seepärast tuleb ainult fluorestseeruvate värvainete meetodit kasutades leitud erinevate ühendite anti-amüloidogeensetesse omadustesse suhtuda ettevaatusega ja kriitiliselt.

Üldiselt arvatakse, et erinevates keskkonnatingimustes toimub insuliini fibrillisatsioon ühtse reaktsioonimehhanismi alusel. Antud töös uuriti insuliini kontsentratsiooni, pH, temperatuuri ja lahuse segamise intensiivsuse mõju fibrillisatsiooni kineetikale. Näidati, et happelises keskkonnas fibrilleerub insuliin ainult kõrgetel (> 10 µM) peptiidi kontsentratsioonidel, pH 7,4 juures oli aga fibrillisatsioon aeglasem kõrgematel (≥ 10 µM) insuliini kontsentratsioonidel. Selle tagajärjel on pH mõju insuliini erinevatel kontsentratsioonidel vastupidine: kõrgel (250 µM) kontsentratsioonil insuliini fibrillisatsiooni kiirus langes pH tõustes, samal ajal kui madalal (2,5 µM) kontsentratsioonil fibrillisatsiooni tase tõusis pH suurenedes. Leiti, et insuliini fibrillisatsiooni aktivatsiooni entalpia E_a väärtus pH 2.5 juures (33.8 kJ/mol) oli tunduvalt madalam, võrreldes pH 7.3 juures saadud E_a väärtusega 84 kJ/mol. See näitab,

et kiirust limiteeriva staadiumi mehhanism on erinev ja lubab oletada, et konformatsioonilised muutused, mis on vajalikud fibrillisatsiooni võimaldava struktuuri moodustamiseks, on oluliselt suuremad füsioloogiliste pH väärtuste juures. Samuti leiti, et pH 7,4 juures insuliini fibrillisatsioon peatus, kui segamine lõpetati, samal ajal kui pH 2,5 juures segamise peatamine fibrillisatsiooni kiirust ei mõjutanud. Keskkonnafaktorite erinev mõju insuliini fibrillisatsioonile näitab, et happeliste ja füsioloogiliste pH väärtuste juures mõjutavad reaktsioonikiirust erinevad molekulaarsed sündmused.

Kokkuvõtvalt saab järeldada, et saadud tulemused annavad üksikasjalikuma ülevaate amüloidsete fibrillide moodustumise molekulaarsetest mehhanismidest, mida tuleb arvestada, kasutades insuliini kui mudelit, fibrillisatsiooniprotsesside uurimises.

Appendix

Publication I

Noormägi, A., Gavrilova, J., Smirnova, J., Tõugu, V., Palumaa, P. "Zn(II) ions co secreted with insulin suppress inherent amyloidogenic properties of monomeric insulin" (2010) Biochem J.; 430(3): 511-518

BJ www.biochemj.org

Biochem. J. (2010) **430**, 511–518 (Printed in Great Britain) doi:10.1042/BJ20100627

Zn(II) ions co-secreted with insulin suppress inherent amyloidogenic properties of monomeric insulin

Andra NOORMÄGI, Julia GAVRILOVA, Julia SMIRNOVA, Vello TÕUGU and Peep PALUMAA[1]

Department of Gene Technology, Tallinn University of Technology, Akadeemia tee 15, Tallinn 12618, Estonia

Insulin, a 51-residue peptide hormone, is an intrinsically amyloidogenic peptide, forming amyloid fibrils *in vitro*. In the secretory granules, insulin is densely packed together with Zn(II) into crystals of $Zn_2Insulin_6$ hexamer, which assures osmotic stability of vesicles and prevents fibrillation of the peptide. However, after release from the pancreatic β-cells, insulin dissociates into active monomers, which tend to fibrillize not only at acidic, but also at physiological, pH values. The effect of co-secreted Zn(II) ions on the fibrillation of monomeric insulin is unknown, however, it might prevent insulin fibrillation. We showed that Zn(II) inhibits fibrillation of monomeric insulin at physiological pH values by forming a soluble Zn(II)–insulin complex. The inhibitory effect of Zn(II) ions is very strong at pH 7.3 ($IC_{50} = 3.5\ \mu M$), whereas at pH 5.5 it progressively weakens, pointing towards participation of the histidine residue(s) in complex formation. The results obtained indicate that Zn(II) ions might suppress fibrillation of insulin at its release sites and in circulation. It is hypothesized that misfolded oligomeric intermediates occurring in the insulin fibrillation pathway, especially in zinc-deficient conditions, might induce autoantibodies against insulin, which leads to β-cell damage and autoimmune Type 1 diabetes.

Key words: fibrillation, fluorescence spectroscopy, insulin, temperature dependence, thioflavin T (ThT), zinc.

INTRODUCTION

Insulin, a peptide hormone crucial for glucose metabolism, is produced in the islets of Langerhans by pancreatic β-cells. The peptide is synthesized in the endoplasmic reticulum and concentrated into secretory granules in the Golgi apparatus [1]. After processing by prohormone convertases PC1/3 and PC2 [2] insulin, with zinc, forms water-insoluble crystals of hexamer ($Zn_2Insulin_6$) in the slightly acidic environment (pH 5.5) of secretory granules [3,4]. Zn(II) content in the pancreatic β-cells is among the highest in the body, reaching 10 mmol per litre [5], and one third of it is localized in secretory granules together with insulin [6]. Zn(II) is uploaded to the granules with the assistance of a pancreas-specific zinc transporter ZnT8 localized on the membranes of the granules [7]. ZnT8-knockout mice, where secretory granules of insulin are zinc-depleted, show normal insulin biosynthesis, processing and release, which indicates that Zn(II) ions are not ultimately required in the processes upstream from insulin release [8].

Amyloidogenic properties of insulin have been known since the 1940s [9,10]. Fibrillation of insulin has been intensively studied at low pH values and high peptide concentration mostly as a suitable model of protein fibrillation [11]. However, insulin can also fibrillize at physiologically relevant neutral pH values [12, 13]. It is noteworthy that insulin does not form fibrils in the secretory granules, where its concentration is extremely high, reaching 21 mM [14]. Zn(II) ions, the concentration of which is approx. 11 mM in secretory granules [14], stabilize insulin at high peptide concentrations by forming crystals of $Zn_2Insulin_6$ [15,16]. However, insulin does not fibrillize in the Zn(II)-depleted secretory granules of transgenic ZnT8-knockout mice [8], indicating that Zn(II) is not the only factor preventing insulin fibrillation in secretory granules. In the absence of Zn(II), insulin still forms oligomeric structures, mainly hexamers, which may prevent insulin fibrillation at high peptide concentrations. Indeed, insulin fibrillation at high peptide concentrations is slower than that at low concentrations, indicating that oligomerization inhibits insulin fibrillation [17]. Insulin is a rare exception within the amyloidogenic peptides, since the propensity for fibrillation of other peptides increases at elevated concentrations. It has also been demonstrated that insulin oligomers must dissociate to monomers before fibrillation [18]. Dissociation of insulin crystals into monomers occurs immediately after secretion of the insulin and also after its injection. Thus a question may arise as to what factors prevent the fibrillation of considerably amyloidogenic insulin monomers in the pancreatic extracellular space, at sites of the injection and also in circulation.

It is noteworthy that, despite widespread use of insulin for treatment of Type 1 diabetes, the incidence of formation of insulin fibrillar deposits at the site of repeated injections is relatively rare. Such a condition, categorized as injection amyloidosis, has been observed at the sites of repeated injection of neutral porcine insulin [19,20]. As a rule, injection solutions of insulin are supplemented with approx. 0.3 molar equivalent of Zn(II) ions [12,21]. It has been suggested that co-injected Zn(II) ions might also suppress the fibrillation of monomeric insulin and formation of insulin fibril deposits at the sites of repeated injection as well as in circulation. The influence of Zn(II) on insulin at very low concentrations of the peptide would therefore be of great interest with regard to its action and metabolism.

It is known that metal ions such as Zn(II) and Cu(II) have pronounced effects on the fibrillation of a variety of amyloidogenic peptides such as Alzheimer's amyloid peptide [22], synuclein [23,24], tau protein and prion protein, whereas metal ions can enhance [23,24] or inhibit fibrillation [25]. In principle, the fibrillation of monomeric insulin can also be suppressed by metal ions, and its suppression by Zn(II) that is co-secreted with insulin can be physiologically relevant. Moreover, fibrillation

Abbreviations used: ESI–MS, electrospray ionization MS; SEC, size-exclusion chromatography; TEM, transmission electron microscopy; ThT, thioflavin T.

[1] To whom correspondence should be addressed (email peepp@staff.ttu.ee).

studies of monomeric insulin are also necessary for obtaining a better understanding about the mechanism of insulin fibrillation, as the critical amyloidogenic intermediate in fibrillation of insulin as well as other amyloidogenic peptides/proteins is a partially unfolded monomer [13,26,27]. In addition to Zn(II) ions, secretory granules of insulin also contain C-peptide [28] and amylin, which are present in equimolar and approx. 10-fold lower amounts than insulin respectively [29]. Insulin has been shown to interfere with amylin fibrillation [30], whereas C-peptide affects the pattern of insulin oligomerization [31,32] and suppresses amylin fibrillation [29]; however, the effects of the co-released peptides on the fibrillation of insulin have not been determined.

In the present work, we studied systematically the effects of Zn(II) ions, C-peptide, amylin and environmental conditions on the fibrillation of monomeric insulin at physiological pH and demonstrate that Zn(II) ions suppress fibrillation of monomeric insulin through differential stabilization of the monomeric ground state over the partially open transition state leading to amyloidogenesis. It is proposed that Zn(II) ions that are co-secreted together with insulin may prevent fibrillation of insulin at its release sites and in circulation. C-peptide and amylin did not influence the insulin fibrillation.

EXPERIMENTAL

Materials

Lyophilized insulin was purchased from Sigma–Aldrich, amylin was from rPeptide and C-peptide from Nordic BioSite. ThT (thioflavin T) and $CuCl_2 \cdot 2H_2O$ were from Sigma–Aldrich, and Hepes Ultrapure (molecular biology grade) was from USB Corporation. $ZnCl_2$ and NaCl (extra pure) were from Scharlau. All solutions were prepared in fresh Milli-Q water.

Sample preparation

A stock solution of insulin was prepared as follows. Insulin was dissolved in 20 mM Hepes, pH 7.3, and 100 mM NaCl at a concentration of 50 μM. After 30 min of incubation at 25 °C, the insulin stock solution was diluted with the same buffer and used for experiments. The oligomeric composition of insulin samples was determined by SEC (size-exclusion chromatography) on a Superdex™ 75 10/300 column (GE Healthcare) connected to an Äkta Purifier system (GE Healthcare) using 20 mM Hepes, pH 7.3, and 100 mM NaCl as the elution buffer.

Monitoring insulin fibrillation by ThT fluorescence

In a standard experiment, a freshly prepared stock solution of insulin was diluted to a final concentration of 2.5 μM in 20 mM Hepes, pH 7.3, and 100 mM NaCl containing 2.5 μM ThT and an appropriate amount of $ZnCl_2$. A 450-μl portion of each sample was incubated in a 0.5-cm-path-length quartz cell, equilibrated at 50 °C and agitated with a magnetic stirrer at 250 rev./min. The increase in ThT fluorescence was measured at 480 nm using a λ_{ex} of 440 nm on a PerkinElmer LS-45 fluorescence spectrophotometer equipped with a magnetic stirrer. When insulin was incubated without agitation under similar conditions, the fibrillation process was extremely slow and only a slight increase in ThT fluorescence was observed during prolonged incubation (5 days). Agitation at 250 rev./min was found to be optimal for monitoring the insulin fibrillation, and the effect of agitation was similar to that observed for Alzheimer's amyloid peptide fibrillation [25]. In temperature-dependence studies, temperature was varied from 35 °C to 50 °C. In a second series of experiments, the concentration of insulin was varied from 2.5 to 30 μM.

The kinetic curves of fibrillation were fitted to several sigmoidal functions including Avrami, Gompertz and Boltzmann using the Origin program (OriginLab) and it was found that the Boltzmann equation (eqn 1) provides the best fit of the experimental data and allows calculation of the kinetic parameters of fibrillation:

$$y = \frac{A_2 - A_1}{1 + e^{-(t-t_0)/\tau}} + A_2 \quad (1)$$

where A_1 is the initial fluorescence level, A_2 is the maximum fluorescence and t_0 is the time when fluorescence has reached half-maximum; $1/\tau$ is the apparent rate constant (k) of the fibril growth and lag time is approximated by $t_0 - 2\tau$ as suggested previously [33]. IC_{50} values were calculated according to hyperbolic dose–response curves as described in [25].

TEM (transmission electron microscopy)

TEM grids were placed on an adhesive solid surface and 3 μl of previously centrifuged (30 min, 12000 ***g***) peptide solution was pipetted on to each grid and allowed to air dry. Then, drops of 2 % uranylacetate were spotted on to a Parafilm plate and grids were placed on them with the upper side down (to bring the probe and the contrast solution in contact). Probes were kept in uranylacetate for 10 min, then removed and washed with Milli-Q water. After that, excess water was removed with a filter paper and the grids were placed into a special carrier. TEM images from the samples were created on a Selmi EM-125 instrument at 75 kV accelerating voltage and recorded on to high-resolution 60 × 90-mm negative film.

ESI–MS (electrospray ionization MS) measurements

Samples of 1–50 μM insulin in 100 mM ammonium acetate, pH 7.3, incubated for 10 min within a gas-tight syringe at 50 °C, were injected into the electrospray ion source of a QSTAR Elite ESI-Q-TOF (time-of-flight) MS instrument (Applied Biosystems) by a syringe pump at 10 μl/min, and ESI–MS spectra were recorded for up to 5 min in the m/z region 500–3000 Da using the following instrument parameters: ion-spray voltage, 5500 V; source gas, 45 litres/min; curtain gas, 20 litres/min; declustering potential, 60 V; focusing potential, 320 V; and detector voltage, 2300 V. ESI–MS spectra were analysed with the Bioanalyst program (Applied Biosystems).

Equilibrium dialysis

A dialysis experiment was performed with cellulose ester Spectra/Por dialysis-membrane tubing with a molecular-mass cut-off of 1000 Da (Spectrum Laboratories) containing 1.5 ml of 10 μM insulin dissolved in 20 mM Hepes, pH 7.3, and 100 mM NaCl. Dialysis tubing was equilibrated with 500 ml of dialysate solution containing 20 mM Hepes, pH 7.3, 100 mM NaCl and 5 μM $ZnCl_2$ under agitation for 24 h at 4 °C until equilibrium was achieved. At the end of the experiment, samples were taken from both the inside and outside solutions, acidified with 1 M HCl and analysed for zinc content by atomic absorption spectroscopy on a PerkinElmer 3100 instrument

RESULTS

Monitoring the *in vitro* formation of insulin fibrils

Insulin fibrillation experiments were performed with freshly solubilized peptide under continuous agitation by monitoring an increase in the fluorescence of the fibril-reactive dye ThT *in situ*. Under these conditions, a relatively fast increase in

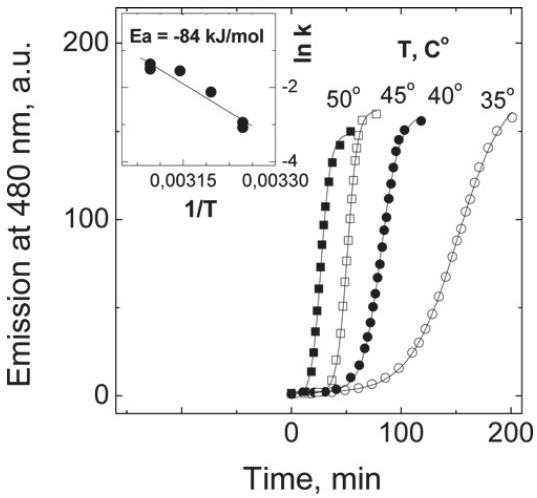

Figure 1 Temperature dependence of insulin fibrillation as followed by ThT fluorescence

Conditions: 2.5 μM insulin in 20 mM Hepes, pH 7.3, and 100 mM NaCl. Insulin was incubated at 50 °C (black squares), 45 °C (white squares), 40 °C (black circles) and 35 °C (white circles) in a quartz cell with continuous agitation in the presence of 2.5 μM ThT. Solid lines correspond to fits of the data to the Boltzmann equation (eqn 1). Inset: temperature dependence shown as Arrhenius coordinates. a.u., arbitrary units.

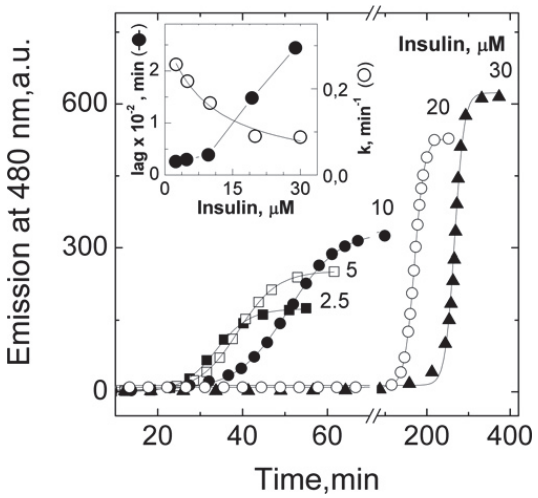

Figure 2 Effect of insulin concentration on its fibrillation

Conditions: 2.5 μM (black squares), 5 μM (white squares), 10 μM (black circles), 20 μM (white circles) and 30 μM (black triangles) insulin in 20 mM Hepes, pH 7.3, and 100 mM NaCl were incubated at 50 °C in a quartz cell with continuous agitation in the presence of 2.5 μM ThT. Solid lines correspond to fits of the data to the Boltzmann equation (eqn 1). Inset: dependence of the fibrillation rate constant on the insulin concentration. a.u., arbitrary units.

ThT fluorescence was observed in accordance with a typical two-phase growth curve (Figure 1). The kinetic curves of fibrillation fitted well to the Boltzmann equation (eqn 1), and the midpoint of fibril formation (t_0) and the rate constants for the fibrillation process were calculated. Fibrillation was monitored in the presence of 2.5 μM or 10 μM ThT. In a separate experiment, we demonstrated that ThT inhibits insulin fibrillation at concentrations higher than 10 μM. Experiments conducted with 2.5 μM insulin showed that the fibrillation rate constant increased and the duration of the lag phase decreased with increasing temperature (Figure 1). The enthalpy of activation E_a (-84 kJ/mol) was found from the slope in the Arrhenius plot (Figure 1, inset). In further experiments, insulin fibrillation was carried out at 50 °C for practical reasons. Fibrillation curves at 2.5 and 5 μM insulin exposed similar kinetics and lag phases, whereas at concentrations above 10 μM the lag phase increased and the values of the rate constant for fibril growth decreased (Figure 2).

Monomer–dimer equilibrium of insulin studied by ESI–MS

The ESI–MS spectrum of 2 μM insulin exposed $+4$ and $+5$ peaks of monomeric insulin (Figure 3a), whereas at higher peptide concentrations $+6$ and $+7$ peaks of dimeric insulin started increasing in the spectra (Figures 3b and 3c). Monomeric insulin was also the major peak in the spectrum at 50 μM insulin (Figure 3c), when a substantial proportion of the insulin is supposed to be dimeric. Such a behaviour is indicative of partial dissociation of insulin dimers to monomers during ESI. Moreover, in calculating the K_d for insulin dimers it should also be considered that the ionization efficiency of monomers and dimers is not equal in ESI–MS. To obtain the binding isotherm, the fractional content of insulin-dimer peaks was calculated by dividing the summarized area of all insulin-dimer peaks to the summarized areas of all insulin peaks in ESI–MS spectra, and the latter parameter was plotted against insulin concentration (Figure 3d). The curve obtained was fitted to the equation of the hyperbola and the maximal fractional content F_{max} (0.18 ± 0.03) indicated that 80 % of the insulin dissociated to monomers during ESI, which was expected as the insulin-dimer K_d is relatively high. The obtained K_d (18.9 ± 0.6 μM) describes the equilibrium of insulin-dimer dissociation. Our ESI–MS results at pH 7.3 are similar to previous nanospray ESI–MS studies; however, slightly different charge states for different species were observed at pH 3.3 [21]. On the basis of SEC and ESI–MS studies, we can conclude that at 2.5 μM insulin is prevalently monomeric and the effects of insulin oligomerization on the fibrillation kinetics are negligible.

Effects of Zn(II) on the fibrillation of insulin

The effect of Zn(II) on the fibrillation of 2.5 μM insulin was studied at pH 7.3 and 5.5. At pH 7.3, Zn(II) ions decreased the fibrillation rate constant and increased the lag phase of the process in a concentration-dependent manner, whereas the maximal level of ThT fluorescence was not affected (Figure 4a). The inhibitory effect of Zn(II) characterized by the IC_{50} [defined as the Zn(II) concentration at which a halving of the fibrillation rate constant was observed] was equal to 3.5 ± 0.9 μM (Figure 4a). At pH 5.5, the effect of Zn(II) was much weaker and only an insignificant (10 %) decrease in fibrillation rate was observed in the presence of 20 μM Zn(II) (Figure 4b).

Effects of C-peptide and amylin on the fibrillation of insulin

Fibrillation of 2.5 μM insulin at pH 7.3 and 50 °C was not affected by 2.5 and 5 μM C-peptide or by 1 μM amylin (Figure 5), indicating that micromolar concentrations of these peptides do not affect fibrillation of monomeric insulin.

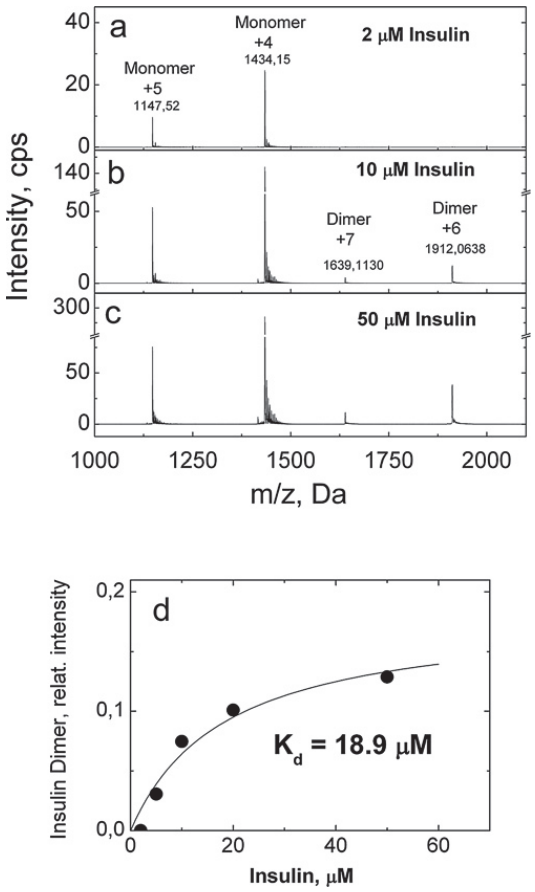

Figure 3 Determination of the apparent K_d for insulin dimers by ESI–MS

ESI–MS spectra of (**a**) 2 μM, (**b**) 10 μM and (**c**) 50 μM insulin in 100 mM ammonium acetate, pH 7.3; $T = 50\,^{\circ}C$. Monomeric insulin exposes charge states $+4$ and $+5$, and dimeric insulin exposes charge states $+6$ and $+7$. (**d**) Dependence of the relative intensity of insulin dimer peaks on the insulin concentration. The solid line shows the curve fitted for $K_d = 18.9$ μM. cps, c.p.s; relat., relative.

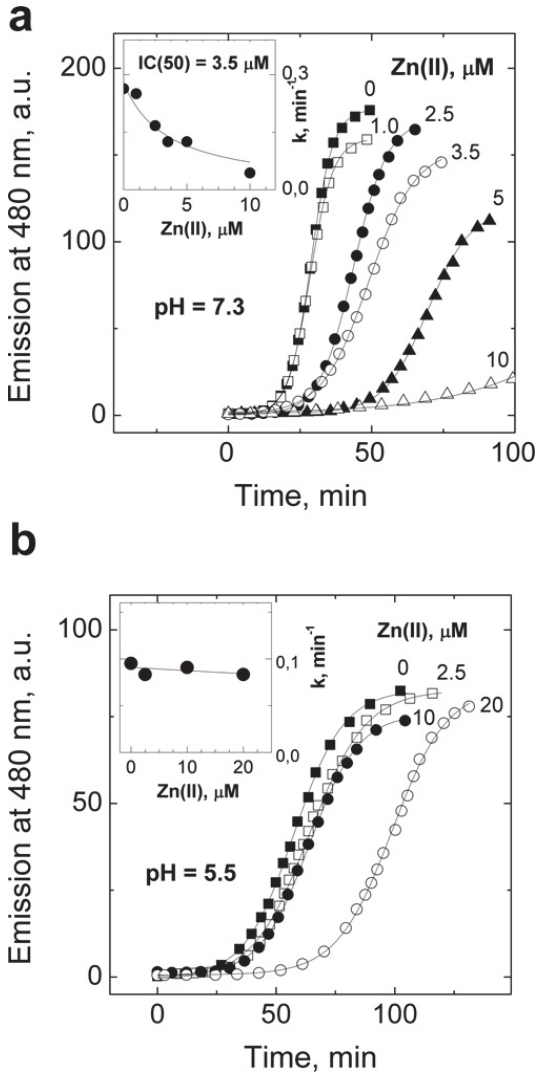

Figure 4 Effect of Zn(II) on fibrillation of insulin

Conditions: 2.5 μM of insulin in 20 mM Hepes and 100 mM NaCl at (**a**) pH 7.3 and (**b**) pH 5.5 was incubated at 50 °C in a quartz cell with continuous agitation in the presence of 2.5 μM ThT and various concentrations of Zn(II) as shown in the Figure. Solid lines correspond to fits of the data to the Boltzmann equation (eqn 1). Insets: dependence of the fibrillation rate constant on the concentration of Zn(II). a.u., arbitrary units.

SEC of insulin

SEC analysis showed that injection of 10 μM insulin exposed one peak with an elution volume of 14.5 ml (Figure 6a), whereas increasing the insulin concentration to 100 μM decreased the elution volume (Figure 6b), indicative of peptide oligomerization at higher concentrations in agreement with results in the literature [21,33]. SEC of aliquots of the fibrillation mixture showed that fibrillation is accompanied by the loss of insulin from the solution (Figure 6c). Fibrillation of 10 μM insulin is completely suppressed in the presence of 5 μM Zn(II) (Figure 4a) and SEC analysis of the fibrillation mixture in these conditions indicates that the peptide exposes a similar SEC peak as that for the initial solution of 10 μM insulin (Figure 6d). Moreover, the presence of 5 μM Zn(II) in elution buffer did not cause a shift of the insulin peak in SEC, confirming that 5 μM Zn(II) keeps insulin in a soluble state and does not induce changes in oligomers of insulin under our experimental conditions.

Equilibrium dialysis

Equilibrium dialysis of 10 μM insulin solution against 5 μM Zn(II) showed that in these conditions insulin binds 0.4 mol of Zn(II) per mol, which corresponds to the value of the K_{Zn} dissociation constant (7.5 μM).

Characterization of insulin fibrils by TEM

Insulin samples showing high ThT fluorescence (agitated for more than 30 min) showed the presence of fibrils in TEM, confirming

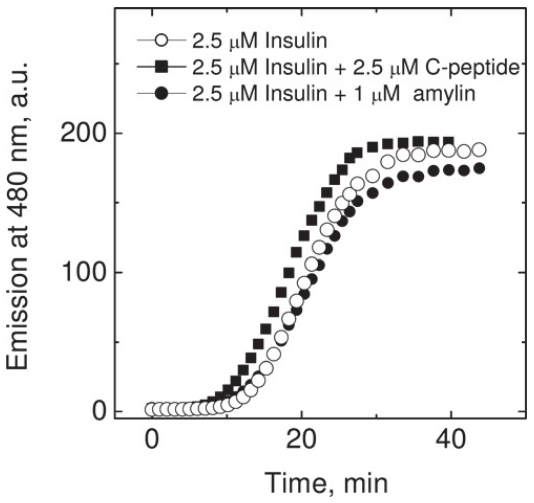

Figure 5 Effects of C-peptide and amylin on the fibrillation of insulin

Conditions: 2.5 μM insulin in 20 mM Hepes, pH 7.3, 100 mM NaCl and 2.5 μM ThT was incubated at 50 °C in a quartz cell with continuous agitation in the absence of other peptides (white circles) and in the presence of 2.5 μM C-peptide (black squares) or 1 μM amylin (black circles). a.u., arbitrary units.

that the increase of ThT fluorescence reflects peptide fibrillation in our assay. In the samples of 10 μM insulin with added 5 μM Zn(II), almost no aggregates were detected at pH 7.3 after 30 min of agitation; however, at pH 5.5, insulin fibrils were observed (Figure 6e), which confirms that 5 μM Zn(II) protects insulin from fibrillation at pH 7.3, but not at acidic pH values.

DISCUSSION

The fibrillation of insulin has been studied thoroughly for more than 60 years; however, the majority of studies have been performed with millimolar concentrations of Zn(II)–insulin, which fibrillizes at elevated temperatures and in acidic conditions [12]. Low pH is necessary for fibrillation since, at high millimolar concentrations and neutral pH, Zn(II)–insulin is predominantly in the form of hexamers resistant to fibrillation [18]. The addition of Zn(II) ions that stabilize the hexameric form is commonly used in injection solutions of insulin [12,21].

Zinc-free apo-insulin can fibrillize not only at acidic, but also at physiologically relevant, pH values, especially in the presence of chemical compounds such as ethanol, urea and guanidinium that are able to dissociate insulin to monomers [12,13]. Insulin is a rare exception within the amyloidogenic peptides since its dilution increases the propensity for fibrillation, whereas the fibrillation of other peptides is favoured at high peptide concentrations. Such a behaviour indicates that oligomerization inhibits insulin fibrillation [17]. Thus it follows that the fibrillation of the monomeric biologically active form of insulin, which is the most aggregation-prone form of the peptide, is insufficiently studied.

The behaviour of monomeric insulin can be studied at low peptide concentrations. According to the literature, insulin dimers begin to dissociate when diluted to concentrations below 100 μM [34,35] and 10 μM insulin is assumed to be essentially monomeric [21]. The K_d value for insulin dimers determined by static and dynamic laser light scattering is 12.5 μM at pH 7.3 and 25 °C [36]. Our present ESI–MS studies at 50 °C and pH 7.3 yielded a K_d of 18.9 μM, which is in good agreement with the literature.

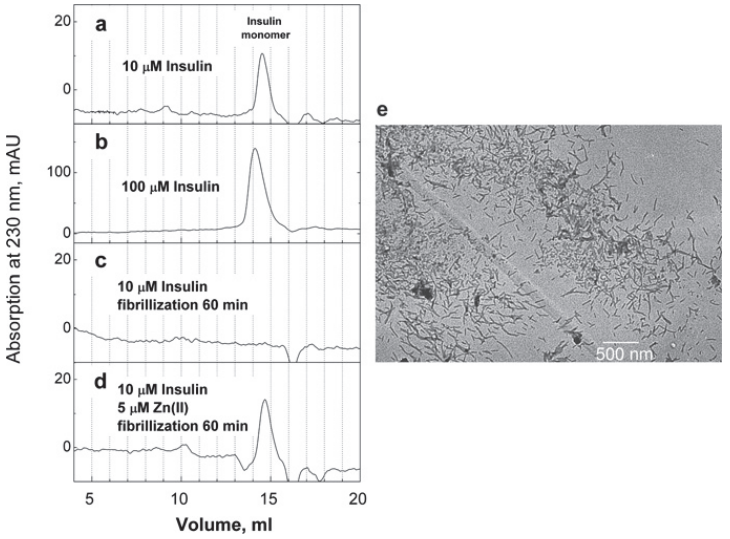

Figure 6 SEC of insulin samples and TEM image of insulin fibrils

(**a**) 10 μM insulin; (**b**) 100 μM insulin; (**c**) 10 μM insulin agitated at 50 °C for 60 min; and (**d**) 10 μM insulin agitated in the presence of 5 μM Zn(II) for 60 min; Superdex^{TM} 75 column; incubation and elution buffer, 20 mM Hepes, pH 7.3, and 100 mM NaCl; 25 °C. (**e**) TEM image of fibrils formed by agitation of 10 μM insulin in the presence of 5 μM Zn(II) for 60 min at pH 5.5. Scale bar, 500 nm. mAU, milli absorbance units.

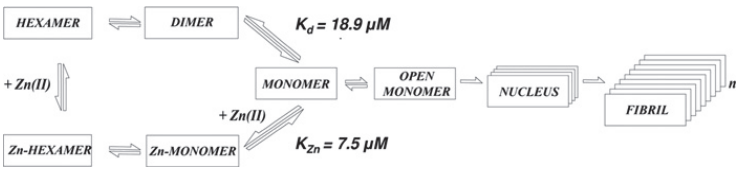

Scheme 1 Mechanism for assembly and fibrillogenesis of insulin in the presence of Zn(II) ions

Insulin is hexameric at high peptide concentrations both in the presence and absence of Zn(II). Insulin hexamers dissociate to dimers and monomers at low peptide concentrations, whereas peptide monomers can also bind Zn(II) ions. Monomeric insulin tends to fibrillize via a partially unfolded intermediate that is also assumed to be important for receptor binding. Zn(II)–insulin-monomer formation is off-pathway for fibrillation as it prevents opening of the conformation of monomeric insulin.

Accordingly, at 2.5 μM, insulin is prevalently monomeric and the equilibrium concentration of dimers is approx. 0.22 μM.

Our results demonstrated that fibrillation of insulin depends only slightly on the insulin concentration in the range 2.5–10 μM, whereas at higher concentrations the fibrillation lag time increases and the fibrillation rate decreases. The inhibition of fibril formation at higher insulin concentrations indicates that the formation of insulin oligomers is an off-pathway process for fibrillation. Secondly, as the rate constant for fibril growth at concentrations below 10 μM is constant, we can conclude that the rate-limiting step of fibril growth is most probably connected with some intramolecular event such as conformational change. Indeed, the fibrillation of monomeric insulin is characterized by a relatively large E_a value of -84 kJ/mol, indicating that the formation of a fibrillation-competent structure is accompanied by substantial conformational changes. The native conformation of insulin in $Zn(II)_2Insulin_6$ hexamers [37] as well as its monomers is essentially α-helical [38]. Multiple techniques including FTIR (Fourier-transform infrared) and CD demonstrate that insulin fibril formation is accompanied by extensive unfolding of the molecule to allow conversion from an α-helical into a β-sheet conformation [11,21], necessary to build up the cross-β framework of insulin fibrils [39]. Apparently, such a conformational change in disulfide-linked native insulin is causing the observed large E_a.

From the compounds co-released with insulin, only Zn(II) exposed a pronounced inhibitory effect upon the fibrillation of monomeric insulin at pH 7.3. An IC_{50} of 3.5 μM indicates that Zn(II) ions already inhibit fibrillation at a low micromolar concentration and the addition of a 4-fold excess of Zn(II) almost completely suppressed the formation of insulin fibrils. Equilibrium dialysis of insulin against 5 μM Zn(II) confirmed that the inhibitory effect is in the same range as the Zn(II) binding affinity of insulin, K_{Zn} (7.5 μM) at low concentrations. At pH 5.5, the inhibitory effect of Zn(II) was much weaker as 20 μM Zn(II) did not affect the fibrillation rate constant and caused only a slight increase of the lag phase. The pH-dependence points towards participation of histidine residue(s) in the Zn(II)-induced inhibition of insulin fibrillation. It is known that the histidine residue at position B10 that is located in the vicinity of the six-residue B-chain segment (B12–B17) contributing to the formation of cross-β structure [40] participates in the binding of Zn(II) ions. It could be suggested that binding of Zn(II) to His^{10} may hinder the formation of a β-sheet-rich conformation compatible for fibrillation nearby. Thus the interaction of Zn(II) with the monomeric insulin inhibits its fibrillation most probably through differential stabilization of the monomeric ground state over the partially open conformation that is necessary for fibrillation. A schematic model describing the effect of Zn(II) ions on the fibrillation of insulin is presented in Scheme 1.

Biological context

Insulin is present in the secretory granules at a extremely high concentration reaching 21 mM [14]. The main factor preventing insulin fibrillation in secretory granules is the formation of stable $Zn(II)_2Insulin_6$ hexamers (in zinc-enriched granules) or insulin oligomers (in zinc-depleted granules). Nevertheless, the fibrillation may also occur at the sites of its release, where insulin dissociates to monomers, which are the most fibrillation-prone form of the peptide. Based on the present results, we suggest that Zn(II) ions that are co-secreted with insulin from pancreatic β-cells might help insulin to avoid fibrillation at its release sites after dissociation of hexamers. Insulin fibrillation is a physiologically undesirable process for many reasons. First, fibrillation removes monomeric insulin out of secretion and prevents its interaction with insulin receptors. Secondly, insulin fibrillation occurs via intermediate misfolded oligomers [41,42] and prefibrillar aggregates, composed of 500 or more monomers and the dimensions of which might reach 14 Å (1 Å=0.1 nm) [43]. These intermediates might be cytotoxic, as demonstrated in the case of Alzheimer's amyloid peptides [44] and also in the case of many other peptides and proteins. Besides being cytotoxic, these large misfolded oligomeric intermediates can also be immunogenic if they occur in the circulation. Such a scenario is feasible in the case of insulin.

Type 1 diabetes is an autoimmune disease that is characterized by the presence of autoantibodies against insulin and some other pancreatic proteins. These diabetes-related autoantibodies are present already in the preclinical asymptomatic latent period of the disease, and several studies have shown that insulin autoantibodies are the first to appear in young children, implying that insulin may be the primary autoantigen in most cases of childhood Type 1 diabetes [45]. The reason why autoantibodies that attack and destroy pancreatic β-cells are generated is currently largely unknown. It cannot be ruled out that the pathology is related to the generation of antibodies against misfolded insulin oligomers occurring as on-pathway intermediates during insulin fibrillation. Based on the present results, it can be hypothesized that Zn(II) ions co-secreted from pancreatic β-cells protect the organism from insulin fibrillation and formation of intermediary non-native insulin oligomers/aggregates. It can also be hypothesized that disturbances in zinc metabolism and especially zinc deficiency might enhance insulin fibrillation with intermediary formation of misfolded oligomers, which are immunogenic and might induce the generation of insulin autoantibodies. Currently, there is no direct evidence confirming the suggested hypothesis;

however, epidemiological studies associate diabetes with zinc deficiencies, which is in good agreement with the suggested hypothesis.

AUTHOR CONTRIBUTION

Peep Palumaa and Vello Tõugu designed experiments, analysed data and wrote the paper, Andra Noormägi designed and performed experiments, analysed data and wrote the paper, and Julia Gavrilova and Julia Smirnova performed experiments and analysed data.

ACKNOWLEDGEMENTS

We thank Dr Valdek Mikli and Kairit Zovo for help with TEM experiments.

FUNDING

This work was supported by the Estonian Ministry of Education and Research [grant number SF0140055s08 (to P.P.)]; the Estonian Science Foundation [grant numbers 6840 (to V.T.) and 7191 (to P.P.)]; and a World Federation of Scientists scholarship (to A.N.).

REFERENCES

1 Orci, L., Ravazzola, M., Amherdt, M., Madsen, O., Vassalli, J. D. and Perrelet, A. (1985) Direct identification of prohormone conversion site in insulin-secreting cells. Cell **42**, 671–681

2 Creemers, J. W., Jackson, R. S. and Hutton, J. C. (1998) Molecular and cellular regulation of prohormone processing. Semin. Cell Dev. Biol. **9**, 3–10

3 Orci, L., Ravazzola, M., Storch, M. J., Anderson, R. G., Vassalli, J. D. and Perrelet, A. (1987) Proteolytic maturation of insulin is a post-Golgi event which occurs in acidifying clathrin-coated secretory vesicles. Cell **49**, 865–868

4 Dodson, G. and Steiner, D. (1998) The role of assembly in insulin's biosynthesis. Curr. Opin. Struct. Biol. **8**, 189–194

5 Clifford, K. S. and MacDonald, M. J. (2000) Survey of mRNAs encoding zinc transporters and other metal complexing proteins in pancreatic islets of rats from birth to adulthood: similar patterns in the Sprague–Dawley and Wistar BB strains. Diabetes Res. Clin. Pract. **49**, 77–85

6 Figlewicz, D. P., Forhan, S. E., Hodgson, A. T. and Grodsky, G. M. (1984) ^{65}Zinc and endogenous zinc content and distribution in islets in relationship to insulin content. Endocrinology **115**, 877–881

7 Chimienti, F., Devergnas, S., Pattou, F., Schuit, F., Garcia-Cuenca, R., Vandewalle, B., Kerr-Conte, J., Van Lommel, L., Grunwald, D., Favier, A. and Seve, M. (2006) *In vivo* expression and functional characterization of the zinc transporter ZnT8 in glucose-induced insulin secretion. J. Cell Sci. **119**, 4199–4206

8 Lemaire, K., Ravier, M. A., Schraenen, A., Creemers, J. W., Van de Plas, R., Granvik, M., Van Lommel, L., Waelkens, E., Chimienti, F., Rutter, G. A. et al. (2009) Insulin crystallization depends on zinc transporter ZnT8 expression, but is not required for normal glucose homeostasis in mice. Proc. Natl. Acad. Sci. U.S.A. **106**, 14872–14877

9 Waugh, D. F. (1946) A fibrous modification of insulin. I. The heat precipitate of insulin. J. Am. Chem. Soc. **68**, 247–250

10 Langmuir, I. and Waugh, D. F. (1940) Pressure-soluble and pressure displaceable components of monolayers of native and denatured proteins. J. Am. Chem. Soc. **62**, 2771–2793

11 Bouchard, M., Zurdo, J., Nettleton, E. J., Dobson, C. M. and Robinson, C. V. (2000) Formation of insulin amyloid fibrils followed by FTIR simultaneously with CD and electron microscopy. Protein Sci. **9**, 1960–1967

12 Brange, J., Andersen, L., Laursen, E. D., Meyn, G. and Rasmussen, E. (1997) Toward understanding insulin fibrillation. J. Pharm. Sci. **86**, 517–525

13 Ahmad, A., Millett, I. S., Doniach, S., Uversky, V. N. and Fink, A. L. (2004) Stimulation of insulin fibrillation by urea-induced intermediates. J. Biol. Chem. **279**, 14999–15013

14 Foster, M. C., Leapman, R. D., Li, M. X. and Atwater, I. (1993) Elemental composition of secretory granules in pancreatic islets of Langerhans. Biophys. J. **64**, 525–532

15 Brange, J., Havelund, S., Hommel, E., Sorensen, E. and Kuhl, C. (1986) Neutral insulin solutions physically stabilized by addition of Zn^{2+}. Diabet. Med. **3**, 532–536

16 Rasmussen, T., Kasimova, M. R., Jiskoot, W. and van de Weert, M. (2009) The chaperone-like protein α-crystallin dissociates insulin dimers and hexamers. Biochemistry **48**, 9313–9320

17 Nielsen, L., Khurana, R., Coats, A., Frokjaer, S., Brange, J., Vyas, S., Uversky, V. N. and Fink, A. L. (2001) Effect of environmental factors on the kinetics of insulin fibril formation: elucidation of the molecular mechanism. Biochemistry **40**, 6036–6046

18 Ahmad, A., Millett, I. S., Doniach, S., Uversky, V. N. and Fink, A. L. (2003) Partially folded intermediates in insulin fibrillation. Biochemistry **42**, 11404–11416

19 Dische, F. E., Wernstedt, C., Westermark, G. T., Westermark, P., Pepys, M. B., Rennie, J. A., Gilbey, S. G. and Watkins, P. J. (1988) Insulin as an amyloid-fibril protein at sites of repeated insulin injections in a diabetic patient. Diabetologia **31**, 158–161

20 Storkel, S., Schneider, H. M., Muntefering, H. and Kashiwagi, S. (1983) Iatrogenic, insulin-dependent, local amyloidosis. Lab. Invest. **48**, 108–111

21 Nettleton, E. J., Tito, P., Sunde, M., Bouchard, M., Dobson, C. M. and Robinson, C. V. (2000) Characterization of the oligomeric states of insulin in self-assembly and amyloid fibril formation by mass spectrometry. Biophys. J. **79**, 1053–1065

22 Bush, A. I., Pettingell, W. H., Multhaup, G., d Paradis, M., Vonsattel, J. P., Gusella, J. F., Beyreuther, K., Masters, C. L. and Tanzi, R. E. (1994) Rapid induction of Alzheimer Aβ amyloid formation by zinc. Science **265**, 1464–1467

23 Bharathi, Indi, S. S. and Rao, K. S. (2007) Copper- and iron-induced differential fibril formation in α-synuclein: TEM study. Neurosci. Lett. **424**, 78–82

24 Bharathi, K. S. and Rao, K. S. (2008) Molecular understanding of copper and iron interaction with α-synuclein by fluorescence analysis. J. Mol. Neurosci. **35**, 273–281

25 Tõugu, V., Karafin, A., Zovo, K., Chung, R. S., Howells, C., West, A. K. and Palumaa, P. (2009) Zn(II)- and Cu(II)-induced nonfibrillar aggregates of amyloid-β (1–42) are transformed to amyloid fibrils, both spontaneously and under the influence of metal chelators. J. Neurochem. **110**, 1784–1795

26 Nielsen, L., Frokjaer, S., Brange, J., Uversky, V. N. and Fink, A. L. (2001) Probing the mechanism of insulin fibril formation with insulin mutants. Biochemistry **40**, 8397–8409

27 Ahmad, A., Uversky, V. N., Hong, D. and Fink, A. L. (2005) Early events in the fibrillation of monomeric insulin. J. Biol. Chem. **280**, 42669–42675

28 Steiner, D. F. (2004) The proinsulin C-peptide – a multirole model. Exp. Diabesity Res. **5**, 7–14

29 Westermark, P., Li, Z. C., Westermark, G. T., Leckstrom, A. and Steiner, D. F. (1996) Effects of beta cell granule components on human islet amyloid polypeptide fibril formation. FEBS Lett. **379**, 203–206

30 Cui, W., Ma, J. W., Lei, P., Wu, W. H., Yu, Y. P., Xiang, Y., Tong, A. J., Zhao, Y. F. and Li, Y. M. (2009) Insulin is a kinetic but not a thermodynamic inhibitor of amylin aggregation. FEBS J. **276**, 3365–3371

31 Shafqat, J., Melles, E., Sigmundsson, K., Johansson, B. L., Ekberg, K., Alvelius, G., Henriksson, M., Johansson, J., Wahren, J. and Jornvall, H. (2006) Proinsulin C-peptide elicits disaggregation of insulin resulting in enhanced physiological insulin effects. Cell. Mol. Life Sci. **63**, 1805–1811

32 Jornvall, H., Lindahl, E., Astorga-Wells, J., Lind, J., Holmlund, A., Melles, E., Alvelius, G., Nerelius, C., Maler, L. and Johansson, J. (2010) Oligomerization and insulin interactions of proinsulin C-peptide: threefold relationships to properties of insulin. Biochem. Biophys. Res. Commun. **391**, 1561–1566

33 Jeffrey, P. D. and Coates, J. H. (1966) An equilibrium ultracentrifuge study of the self-association of bovine insulin. Biochemistry **5**, 489–498

34 Jeffrey, P. D., Milthorpe, B. K. and Nichol, L. W. (1976) Polymerization pattern of insulin at pH 7.0. Biochemistry **15**, 4660–4665

35 Roy, M., Lee, R. W., Brange, J. and Dunn, M. F. (1990) ^{1}H NMR spectrum of the native human insulin monomer. Evidence for conformational differences between the monomer and aggregated forms. J. Biol. Chem. **265**, 5448–5452

36 Kadima, W., Ogendal, L., Bauer, R., Kaarsholm, N., Brodersen, K., Hansen, J. F. and Porting, P. (1993) The influence of ionic strength and pH on the aggregation properties of zinc-free insulin studied by static and dynamic laser light scattering. Biopolymers **33**, 1643–1657

37 Adam, M. G., Coller, L., Hodgkin, D. C. and Dodson, G. G. (1966) X-ray crystallographic studies on zinc insulin crystals. Am. J. Med. **40**, 667–671

38 Bocian, W., Sitkowski, J., Bednarek, E., Tarnowska, A., Kawecki, R. and Kozerski, L. (2008) Structure of human insulin monomer in water/acetonitrile solution. J. Biomol. NMR **40**, 55–64

39 Burke, M. J. and Rougvie, M. A. (1972) Cross-protein structures. I. Insulin fibrils. Biochemistry **11**, 2435–2439

40 Ivanova, M. I., Sievers, S. A., Sawaya, M. R., Wall, J. S. and Eisenberg, D. (2009) Molecular basis for insulin fibril assembly. Proc. Natl. Acad. Sci. U.S.A. **106**, 18990–18995

41 Sorci, M., Grassucci, R. A., Hahn, I., Frank, J. and Belfort, G. (2009) Time-dependent insulin oligomer reaction pathway prior to fibril formation: cooling and seeding. Proteins **77**, 62–73

42 Nayak, A., Sorci, M., Krueger, S. and Belfort, G. (2009) A universal pathway for amyloid nucleus and precursor formation for insulin. Proteins **74**, 556–565
43 Smith, M. I., Sharp, J. S. and Roberts, C. J. (2008) Insulin fibril nucleation: the role of prefibrillar aggregates. Biophys. J. **95**, 3400–3406
44 Walsh, D. M. and Selkoe, D. J. (2007) Aβ oligomers – a decade of discovery. J. Neurochem. **101**, 1172–1184
45 Knip, M. (2002) Natural course of preclinical Type 1 diabetes. Horm. Res. **57** (Suppl. 1), 6–11

Received 22 April 2010/8 July 2010; accepted 15 July 2010
Published as BJ Immediate Publication 15 July 2010, doi:10.1042/BJ20100627

Publication II

Noormägi, A., Primar, K., Tõugu, V., Palumaa, P. "Interference of low-molecular substances with the thioflavin-T fluorescence assay of amyloid fibrils" (2011) J Pept Sci.; 18(1): 59-64

Research Article

Journal of PeptideScience

Received: 9 June 2011 Revised: 11 August 2011 Accepted: 18 August 2011 Published online in Wiley Online Library: 14 November 2011

(wileyonlinelibrary.com) DOI 10.1002/psc.1416

Interference of low-molecular substances with the thioflavin-T fluorescence assay of amyloid fibrils

Andra Noormägi,[a,b] Kateryna Primar,[a] Vello Tõugu[a] and Peep Palumaa[a,b]*

Abnormal fibrillization of amyloidogenic peptides/proteins has been linked to various neurodegenerative diseases such as Alzheimer's and Parkinson's disease as well as with type-II diabetes mellitus. The kinetics of protein fibrillization is commonly studied by using a fluorescent dye Thioflavin T (ThT) that binds to protein fibrils and exerts increased fluorescence intensity in bound state. Recently, it has been demonstrated that several low-molecular weight compounds like Basic Blue 41, Basic Blue 12, Azure C, and Tannic acid interfere with the fluorescence of ThT bound to Alzheimers' amyloid-β fibrils and cause false positive results during the screening of fibrillization inhibitors. In the current study, we demonstrated that the same selected substances also decrease the fluorescence signal of ThT bound to insulin fibrils already at submicromolar or micromolar concentrations. Kinetic experiments show that unlike to true inhibitors, these compounds did neither decrease the fibrillization rate nor increase the lag-period. Absence of soluble insulin in the end of the experiment confirmed that these compounds do not disaggregate the insulin fibrils and, thus, are not fibrillization inhibitors at concentrations studied. Our results show that interference with ThT test is a general phenomenon and more attention has to be paid to interpretation of kinetic results of protein fibrillization obtained by using fluorescent dyes.

Supporting information can be found in the online version of this article.

Keywords: insulin; aggregation; fibrillization; fluorescence; amyloid

Introduction

Abnormal accumulation of amyloidogenic peptides/proteins plays an important role in more than 40 human diseases, including Alzheimers and Parkinsons disease, and type-II diabetes mellitus [1,2]. Formation of protein fibrils is a physical process of the formation of insoluble highly ordered structures. Although the amino acid sequences of amyloidogenic peptides and proteins are diverse, they all adopt a similar structure in aggregates called cross-beta-spine, where the partially unfolded β-structure-rich polypeptides interact with each other via intermolecular hydrogen bonding. Recent studies indicate that the phenomenon of protein fibrillization seems to be a generic property of polypeptide as under appropriate conditions even otherwise stable peptides and proteins may form amyloid fibrils [1,3].

The fluorescence dye thioflavin T (ThT) (1), which binds to protein fibrils and exerts increased fluorescence intesity in bound state, is a defining probe for the identification and kinetic study of amyloid fiber formation [4].

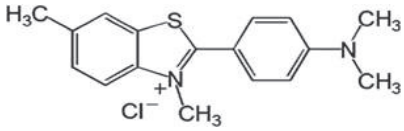

(1)

In a typical ThT fluorescence assay, ThT is added to samples containing fibril structures in micromolar concentration, and the ThT fluorescence intensity is monitored at 490 nm (excitation at 440 nm). Free ThT in an aqueous environment shows only weak fluorescence with lower (blue-shifted) excitation and emission maxima at 350 and 440 nm. As a rule, ThT does not affect the peptide fibrillation kinetics and has also been used for *in situ* monitoring of fibril formation [5,6].

The mechanism of interaction between ThT and amyloid fibrils involves the intercalation of ThT molecules within grooves between solvent-exposed side chains of the amyloid fibrils that run parallel to the fibril axis [4,7–9]. Binding within the channels is thought to provide rigidity of the molecule and the planar orientation of benzothiazole and benzene ring, which prevents the formation of a less-radiative twisted rotamers of the ThT molecule with the torsion angle between the benzothiazole and benzene ring from 37° to 90° [4,10]. The aromatic interaction with the protein is also contributing to the high quantum yield of fibril-bound ThT emission [4]. Because the interaction between ThT and amyloid is stoichiometric and reaches saturation at reasonably low ThT concentrations, the fluorescence signal from the amyloid–ThT complex provides a simple tool for the quantification of amyloid fibrils [11].

ThT test has also been used for the identification of fibrillization inhibitors applicable as tools for therapeutic intervention in

* *Correspondence to: Peep Palumaa, Department of Gene Technology, Tallinn University of Technology, Akadeemia 15, 12618, Tallinn, Estonia. E-mail: peepp@staff.ttu.ee*

a *Department of Gene Technology, Tallinn University of Technology, Akadeemia 15, 12618, Tallinn, Estonia*

b *Competence Center on Reproductive Medicine and BiologyTiigi 61b, Tartu 50410, Estonia*

Abbreviations: *ThT, thioflavine T.*

Table 1. Effect of tested substances on maximum fluorescence observed in fibrillization of insulin and on fluorescence intensity of ThT bound to fresh and old insulin fibrils (IC_{50}^{FI})

Substance	Fibrillization IC_{50}^{FI} value (μM)	Fresh fibrils IC_{50}^{FI} value (μM)	Old fibrils IC_{50}^{FI} value (μM)
Basic Blue 41	0.025 ± 0.006	0.041 ± 0.006	0.030 ± 0.016
Basic Blue 12	0.026 ± 0.003	0.048 ± 0.004	0.039 ± 0.008
Azure C	0.96 ± 0.21	1.64 ± 0.04	0.92 ± 0.14
Tannic acid	9.02 ± 3.85	5.82 ± 0.97	0.74 ± 0.35
$ZnCl_2$	3.49 ± 0.90 (ICk value [5])$_{50}$	n.a.	n.a.

Substance	Chemical structure
Basic Blue 41	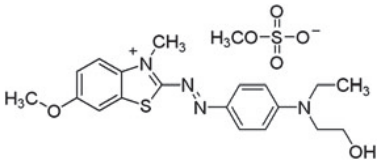
Nile blue Chloride (Basic Blue 12)	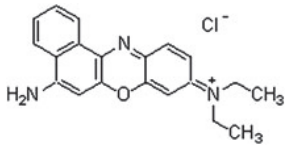
Azure C	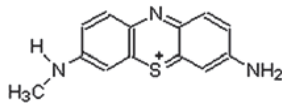
Tannic acid	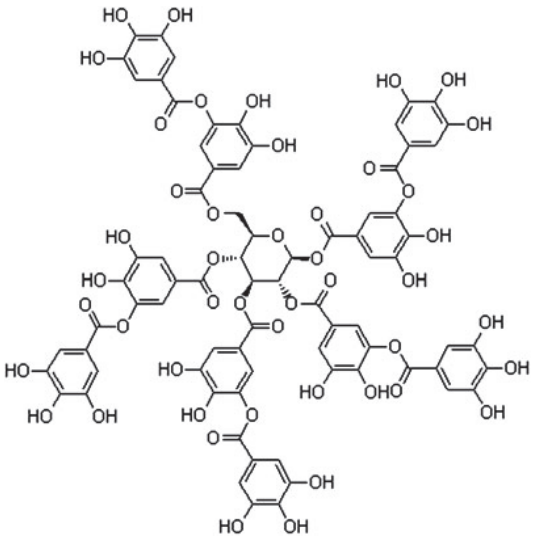

case of a variety of amyloidogenic diseases. However, in order to provide reliable data, the method for monitoring the fibril formation in the presence of a variety of substances *in vitro* should be reliable and free from artifacts. Recently, it has been demonstrated that low molecular weight substances may interfere with the ThT test and decrease ThT fluorescence in the case of Alzheimer's amyloid beta peptide (Aβ42), which may lead to false positive results in the screening of fibrillization inhibitors

Journal of PeptideScience

[12,13]. Interference with ThT test might be a rather general phenomenon that may disturb the fibrillization studies of all amyloidogenic peptides/proteins and lead to misinterpretation of experimental results obtained with application of ThT and its analogs.

Insulin is a 51-residue peptide hormone involved in glucose metabolism and universally used in diabetes treatment. Under specific conditions, that is, high temperature and low pH, it is very prone to fibrillization. Insulin fibrils exhibit common properties of amyloid fibrils, which have made insulin fibrillization a good model system for the study of protein fibrillization. There are also studies where inhibitors of insulin fibrillation at low pH have been studied using ThT fluorescence [14,15]. At the elevated temperatures and moderate agitation, zinc-free insulin aggregates rapidly at physiological pH values [5]. Considering that inhaled insulin forms toxic pulmonary amyloid aggregates [15] search for inhibitors of insulin fibrillization may also have a practical outcome.

The aim of this work was to test whether substances that have been studied as inhibitors of Aβ42 fibrillization [Tannic acid, Basic Blue 41, Basic Blue 12, Azure C (see Table 1), riboflavin, imidazole, ascorbic acid, phenolphtalein, and Zn(II)] compete with ThT for binding sites within insulin fibrils. We demonstrated that four substances (Tannic acid, Basic Blue 41, Basic Blue 12, Azure C) interfere with ThT test, which shows that interference with ThT test is a general phenomenon and more attention has to be paid to the interpretation of kinetic results of protein fibrillization obtained by using fluorescent dyes.

Materials and Methods

Lyophilized insulin, ThT, Basic Blue 41, Tannic acid, Azure C, Nile blue chloride (Basic Blue 12), riboflavin, imidazole, ascorbic acid, and phenolphtalein were from Sigma–Aldrich (St. Louis, USA). HEPES Ultrapure, MB Grade was from USB Corporation (Cleveland, USA). NaCl and $ZnCl_2$ were extra pure from Scharlau (Barcelona, Spain). All solutions were prepared in fresh MilliQ water. Stock solution of insulin was prepared as follows: Insulin was dissolved in 20 mM HEPES and 100 mM NaCl, pH 7.3 at a concentration of 50 μM. After 30 min incubation, the insulin stock solution was diluted with buffer and used for experiments. All test substances were dissolved in 20% ethanol.

Monitoring Insulin Fibrillization by ThT Fluorescence

Insulin fibrillation was monitored as described earlier [5]: in a standard experiment, the stock solution of insulin was diluted to a final concentration of 2.5 μM in 20 mM HEPES and 100 mM NaCl, pH 7.3 containing 2.5 μM of ThT and an appropriate amount of low-molecular weight substances [Basic Blue 41, Basic Blue 12, Azure C, Tannic acid, riboflavin, imidazole, phenolphtalein, ascorbic acid and ZnCl(II)]. A total of 450 μl of each sample was incubated in a 0.5 cm path length quartz cell, equilibrated to 50 °C and agitated with a magnetic stirrer at 250 rpm. The increase in the ThT fluorescence intensity at 480 nm (excitation at 440 nm) was monitored on a PerkinElmer LS-45 fluorescence

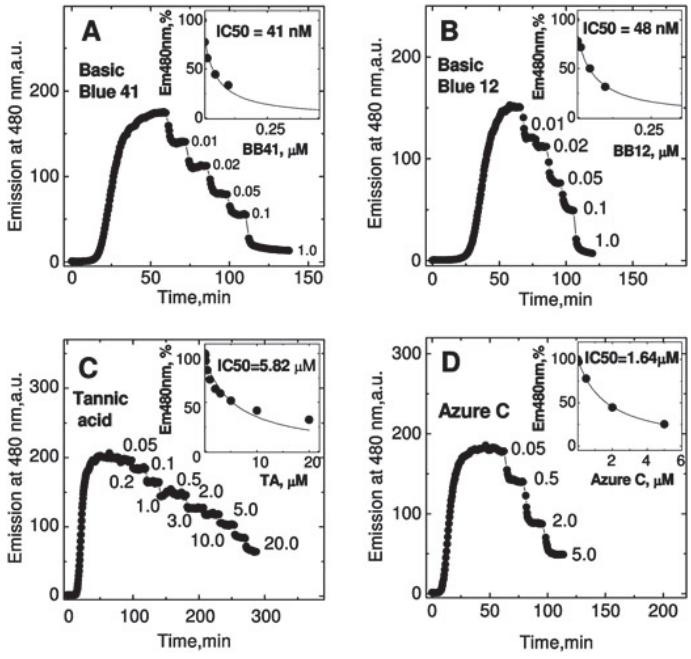

Figure 1. Effect of selected compounds on the ThT fluorescence emission in the presence of insulin fibrils. A total of 0.5 μmol/l of insulin in 20 mmol/l HEPES, 100 mmol/l NaCl at pH 7.3 was incubated at 50 °C in a quartz cell with continuous agitation at 250 rpm in the presence of 2.5 μM ThT; solid lines correspond to the fit of the data to Boltzmann equation; after completion of the fibrillization process, increasing amounts of selected compound was added. Inset – dependence of fibrillization rate constant from the concentration of selected compounds A – Basic Blue 41, B – Basic Blue 12, C – Tannic acid, D – Azure C.

spectrophotometer (PerkinElmer, Waltham, MA, USA) equipped with a custom magnetic stirrer.

The concentration of the low-molecular effectors was varied in the range 0.01–15.0 μM depending on the observed effects.

Determination of Soluble Insulin by SEC

Content of monomeric insulin in samples was determined by SEC on Superdex Peptide 10/300 column (GE Healthcare, Giles, United Kingdom) connected to an Äkta Purifier system (GE Healthcare, Giles, United Kingdom) by using 100 mM HEPES, pH 7.5 as elution buffer, flow rate 1 ml/min, sample volume 200 μl.

Calculation of Kinetic Parameters

The aggregation parameters were determined by fitting the fluorescence intensity *versus* time to Boltzmann sigmoid curve as described earlier [5]:

$$y = \frac{P_1 - P_0}{1 + e^{(t-t_0)\times k}} + P_0, \quad (2)$$

Where P_0 is the initial fluorescence level, P_1 is the maximum fluorescence, t_0 is the time t when fluorescence has reached half maximum, and k is the rate constant of the fibril elongation.

The half maximal inhibitory concentration (IC_{50}) values were calculated from the effects of substances on the final level of ThT fluorescence (IC_{50}^{FI}) and also from the effects on apparent rate constant of fibril formation (IC_{50}^{k}) according to hyperbolic dose-response curves:

$$y = P_1 - \frac{P_1 \cdot c}{IC_{50}^{FI} + c}, \quad (3)$$

where y is the fluorescence intensity of ThT, P_1 – the maximum value of ThT fluorescence, c – concentration of test substance, and IC_{50}^{FI}–concentration, which reduces ThT fluorescence by 50%.

Nonlinear regression analysis was carried out using a program Origin 6.1.

Results and Discussion

In the first set of experiments, the effect of Basic Blue 41, Basic Blue 12, Azure C, and Tannic acid on the ThT fluorescence intensity in the presence of pre-formed fibrils was estimated. Figure 1 shows typical fibrillization curves of insulin together with the decrease of the ThT fluorescence intensity upon addition the potential fibrillization inhibitors to the fibrils. The insets show the estimation of corresponding IC_{50}^{FI} values, presented also in Table 1. In principal, the abrupt decrease of fluorescence after addition of tested substances may result in (i) very fast disruption of the fibrils; (ii) competitive replacement of fibril bound ThT with the tested substances, or (iii) suppression of the ThT fluorescence. Quantitatively similar results were also obtained with matured fibrils that were incubated for 24 h before titration (Supplementary Figure 1).

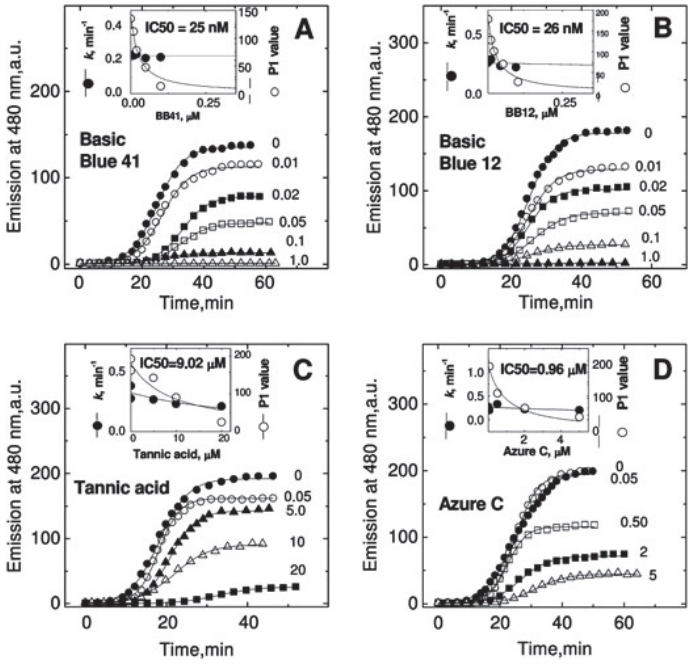

Figure 2. Effect of selected compounds on the fibrillization of insulin. A total of 2.5 μmol/l of insulin in 20 mmol/l HEPES, 100 mmol/l NaCl at pH 7.3 was incubated at 50 °C in a quartz cell with continuous agitation at 250 rpm in the presence of 2.5 μM ThT. Compounds added A: Basic Blue 41 concentrations: ● – 0 μM, ○ – 0.01 μM, ■ – 0.02 μM, □ – 0.05 μM, ▲ – 0.1 μM, – 1.0 μM. Basic Blue 12 concentrations: ● – 0 μM, ○ – 0.01 μM, ■ – 0.02 μM, □ – 0.05 μM, – 0.1 μM, ▲ – 1.0 μM. Tannic acid concentrations: ● – 0 μM, ○ – 0.05 μM, ▲ – 5.0 μM, – 10.0 μM, ■ – 20.0 μM. Azure C concentrations: ○ – 0 μM, ● – 0.05 μM, □ – 0.5 μM, ■ – 2.0 μM, – 5.0 μM. Solid lines correspond to the fit of the data to Boltzmann equation. Insets show the dependence of fibrillization rate constant k and maximal level of ThT fluorescence P1 on the concentration of effectors.

Journal of PeptideScience

Further, the kinetic curves of insulin fibrillization in the presence of Basic Blue 41, Basic Blue 12, Azure C, and Tannic acid were studied. Figure 2 shows that the maximal levels of ThT fluorescence is dropped with increasing concentration of the effector (IC^k_{50} values are presented in Table1), but neither the duration of the lag period nor the rate constant of fibril growth changed at the concentrations studied (Figure 2). This means that these compounds do not inhibit the insulin fibrillization process at low micromolar concentrations, but most probably compete with ThT for the same binding site in fibrils. After the addition of 1 μM Basic Blue 41 to insulin fibrils, peak of monomeric insulin was not detected by SEC in the supernatant (Figure 3), which confirms that the fibrils remain intact after addition of the compounds suppressing the ThT fluorescence. A weak inhibition of fibrillization rate was observed at elevated concentrations of Basic Blue, indicating that inhibition of fibrillization by the compounds studied occurs at higher micromolar concentration, but this cannot be determined using ThT fluorescence based methods.

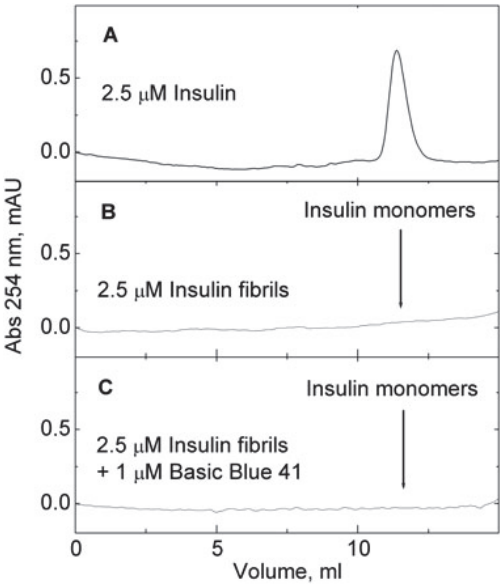

Figure 3. SEC analysis of the insulin solution before (A) and after (B) fibrillization and after addition of Basic Blue 41 to the fibrils (C).

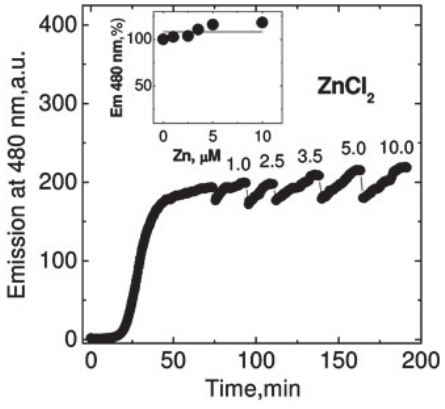

Figure 4. Effect of selected Zn(II) ions on the fibrils of insulin. A total of 2.5 μmol/l of insulin in 20 mmol/l HEPES, 100 mmol/l NaCl at pH 7.3 was incubated at 50 °C in a quartz cell with continuous agitation at 250 rpm in the presence of 2.5 μM ThT. Increasing amounts of ZnCl(II) (1.0 μM, 2.5 μM, 3.5 μM, 5.0 μM, 10.0 μM) were added. Inset shows the dependence of ThT fluorescence on the Zn(II) concentration.

It has been earlier shown in our laboratory that under similar conditions Zn(II) ions inhibit the fibrillization of monomeric insulin by decreasing the rate constant of fibril formation with $IC^k_{50} = 3.5$ μM [5]. Contrary to the compounds tested in this paper, Zn(II) did not decrease the fluorescence of preformed insulin fibrils (Figure 4). Riboflavin, imidazole, ascorbic acid, and phenolphthalein had also no effect on the fibrillization and ThT fluorescence.

It has been demonstrated that ThT binds to the grooves of the cross-beta structure of fibrils [4,7,9]. The binding stoichiometry of bound ThT inducing the characteristic fluorescence is about 0.09 moles of ThT per mole of insulin in fibril form [16]. Our results show that the apparent fluorescence quenching starts at very low submicromolar concentration of selected compounds and is completed at concentrations equal to 0.1 stoichiometry, which is in agreement with the binding stoichiometry for ThT determined earlier [16]. Compounds that interfere with ThT are similar to the structure of ThT (see Table 1), and, therefore, it is realistic that they compete with ThT for common binding sites on amyloid fibrils. Basic Blue 41 and Basic Blue 12 expose high, nanomolar affinity to the insulin fibrils, which is higher than affinity of ThT. This fact could be further exploited for design of novel amyloid probes or potential starting points for discovery of substances inhibiting protein fibrillization process, which are applicable as drug candidates for amyloidogenic diseases. We have to mention that Methylen Blue, which has similar structure to Basic Blue 41 and Basic Blue 12 is currently in clinical trials as disease modifying drug for Alzheimers disease [17,18].

Acknowledgements

This work was supported by the Estonian Ministry of Education, Research [SF0140055s08]; Estonian Science Foundation Grant 8811 both to Peep Palumaa, by the Enterprise Estonia Grant 30200 and by the World Federation of Scientists scholarship to Andra Noormägi.

References

1 Chiti F, Dobson CM. Amyloid formation by globular proteins under native conditions. *Nat. Chem. Biol.* 2009; **5**: 15–22.
2 Aguzzi A, O'Connor T. Protein aggregation diseases: pathogenicity and therapeutic perspectives. *Nat. Rev. Drug Discov.* 2010; **9**: 237–248.
3 Dobson CM. Protein folding and misfolding. *Nature* 2003; **426**: 884–890.
4 Wolfe LS, Calabrese MF, Nath A, Blaho DV, Miranker AD, Xiong Y. Protein-induced photophysical changes to the amyloid indicator dye thioflavin T. *Proc. Natl. Acad. Sci. U. S. A.* 2010; **107**: 16863–16868.
5 Noormagi A, Gavrilova J, Smirnova J, Tougu V, Palumaa P. Zn(II) ions co-secreted with insulin suppress inherent amyloidogenic properties of monomeric insulin. *Biochem. J.* 2010; **430**: 511–518.
6 Tougu V, Karafin A, Zovo K, Chung RS, Howells C, West AK, Palumaa P. Zn(II)- and Cu(II)-induced non-fibrillar aggregates of amyloid-beta (1–42) peptide are transformed to amyloid fibrils, both spontaneously and under the influence of metal chelators. *J. Neurochem.* 2009; **110**: 1784–1795.

7 Krebs MR, Bromley EH, Donald AM. The binding of thioflavin-T to amyloid fibrils: localisation and implications. *J. Struct. Biol.* 2005; **149**: 30–37.
8 Hawe A, Sutter M, Jiskoot W. Extrinsic fluorescent dyes as tools for protein characterization. *Pharm. Res.* 2008; **25**: 1487–1499.
9 Biancalana M, Koide S. Molecular mechanism of Thioflavin-T binding to amyloid fibrils. *Biochim. Biophys. Acta* 2010; **1804**: 1405–1412.
10 Stsiapura VI, Maskevich AA, Kuzmitsky VA, Turoverov KK, Kuznetsova IM. Computational study of thioflavin T torsional relaxation in the excited state. *J. Phys. Chem. A* 2007; **111**: 4829–4835.
11 Bolder SG, Sagis LMC, Venema P, van der Linden E. Thioflavin T and birefringence assays to determine the conversion of proteins into fibrils. *Langmuir* 2007; **23**: 4144–4147.
12 Zovo K, Helk E, Karafin A, Tougu V, Palumaa P. Label-free high-throughput screening assay for inhibitors of Alzheimer's amyloid-β peptide aggregation based on MALDI MS. *Anal. Chem.* 2010; **82**: 8558–8565.
13 Hudson SA, Ecroyd H, Kee TW, Carver JA. The thioflavin T fluorescence assay for amyloid fibril detection can be biased by the presence of exogenous compounds. *FEBS J.* 2009; **276**: 5960–5972.
14 Levy-Sakin M, Shreberk M, Daniel Y, Gazit E. Targeting insulin amyloid assembly by small aromatic molecules: toward rational design of aggregation inhibitors. *Islets* 2009; **1**: 210–215.
15 Lasagna-Reeves CA, Clos AL, Midoro-Hiriuti T, Goldblum RM, Jackson GR, Kayed R. Inhaled insulin forms toxic pulmonary amyloid aggregates. *Endocrinology* 2010; **151**: 4717–4724.
16 Groenning M, Norrman M, Flink JM, van de Weert M, Bukrinsky JT, Schluckebier G, Frokjaer S. Binding mode of Thioflavin T in insulin amyloid fibrils. *J. Struct. Biol.* 2007; **159**: 483–497.
17 Oz M, Lorke DE, Petroianu GA. Methylene blue and Alzheimer's disease. *Biochem. Pharmacol.* 2009; **78**: 927–932.
18 Gura T. Hope in Alzheimer's fight emerges from unexpected places. *Nat. Med* 2008; **14**: 894.

Publication III

Tiiman, A., **Noormägi, A.**, Friedemann, M., Krishtal, J., Palumaa, P., Tõugu, V. "Effect of agitation on the peptide fibrillization: Alzheimer´s amyloid-beta peptide 1-42 but no amylin and insulin fibrils can grow under quiescent conditions" (2013) J Pept Sci.; 19(6): 386-391

Research Article

Journal of PeptideScience

Received: 1 March 2013 Accepted: 11 March 2013 Published online in Wiley Online Library: 23 April 2013

(wileyonlinelibrary.com) DOI 10.1002/psc.2513

Effect of agitation on the peptide fibrillization: Alzheimer's amyloid-β peptide 1-42 but not amylin and insulin fibrils can grow under quiescent conditions

Ann Tiiman,[a]* Andra Noormägi,[a,b] Merlin Friedemann,[a] Jekaterina Krishtal,[a] Peep Palumaa[a,b] and Vello Tõugu[a]

Many peptides and proteins can form fibrillar aggregates *in vitro*, but only a limited number of them are forming pathological amyloid structures *in vivo*. We studied the fibrillization of four peptides – Alzheimer's amyloid-β (Aβ) 1-40 and 1-42, amylin and insulin. In all cases, intensive mechanical agitation of the solution initiated fast fibrillization. However, when the mixing was stopped during the fibril growth phase, the fibrillization of amylin and insulin was practically stopped, and the rate for Aβ_{40} substantially decreased, whereas the fibrillization of Aβ_{42} peptide continued to proceed with almost the same rate as in the agitated conditions. The reason for the different sensitivity of the *in vitro* fibrillization of these peptides towards agitation in the fibril growth phase remains elusive. Copyright © 2013 European Peptide Society and John Wiley & Sons, Ltd.

Keywords: Alzheimer's amyloid-β; insulin; amylin; fibrillization; agitation

Introduction

The formation of amyloid aggregates by peptides and proteins has attracted a great deal of attention because the presence of the resulting proteinaceous deposits with a fibrillar structure is characteristic to over 25 human diseases. Some of these amyloidogenic diseases, such as AD, Parkinson's disease and type II diabetes exert remarkable clinical relevance because of their dramatic prevalence in the elderly population [1]. The number of proteins that can misfold and aggregate into amyloid assemblies *in vitro* is considerably larger than the number of proteins involved in amyloid diseases. Moreover, it has been shown that most proteins can form fibrils under specific experimental conditions and fibrillization is suggested to be a generic property of polypeptide chains [2]. One of the most important questions in the studies of amyloid peptides/proteins is to find molecular and physicochemical characteristics that distinguish the peptides and proteins that are causing severe amyloid pathology from those that can fibrillize only in the *in vitro* conditions.

As a rule, protein fibrillization *in vitro* is characterized by a sigmoidal growth curve typical to autocatalytic processes [3,4]. The autocatalysis means that the addition of monomers to the ends of an existing fibril is faster than the formation of new fibrils from the monomers and, accordingly, the rate of the process depends on the number of fibril ends. Analysis of the kinetics of the self assembly of filamentous structures demonstrates that amyloid growth can often be dominated by secondary rather than primary nucleation events, for instance, fragmentation of early fibrils [5].

One of the important environmental factors that has a significant impact on the fibrillization kinetics and can also enhance fibril fragmentation is the agitation of the reaction mixture [6–8]. In this paper, we determined the effect of agitation on the different stages of fibrillization of four amyloidogenic peptides *in vitro*. The experimental conditions were similar for all four peptides, but optimized individually for each peptide, to obtain adequate fibrillization in the same time scale. For all the peptides studied, intensive agitation was required in the initial exponential phase of the reaction where the fibrillar 'seeds' and primary fibrils are formed that grow during the next elongation phase. Aβ_{42} was the only peptide that did not require agitation during this elongation phase as stopping of the agitation did not affect fibril elongation rate. Fibrillization of insulin and amylin stopped when agitation was stopped in this phase and fibrillization of Aβ_{40} proceeded with a significantly lower rate. We assume that the profound ability of Aβ_{42} fibrils to grow under quiescent

* *Correspondence to: Ann Tiiman, Department of Gene Technology, Tallinn University of Technology, Akadeemia 15, Tallinn 12618, Estonia. E-mail: ann.tiiman@ttu.ee*

a *Department of Gene Technology, Tallinn University of Technology, Akadeemia tee 15, Tallinn 12618, Estonia*

b *Competence Center on Reproductive Medicine and Biology, Tiigi 61 b, Tartu 50410, Estonia*

Abbreviations: *Aβ*, amyloid-β peptide; AD, Alzheimer's disease; ThT, Thioflavin T; HFIP, 1,1,1,3,3,3-hexafluoro-2-propanol

Journal of PeptideScience

conditions is responsible for their high propensity to form pathological aggregates *in vivo*.

Materials and Methods

Materials

Lyophilized Aβ_{42} peptide TFA salt, Aβ_{40} NaOH salt and amylin (ultrapure, recombinant) were purchased from rPeptide (Bogart, Georgia, USA). Lyophilized insulin was from Sigma-Aldrich (St. Louis, Missouri, USA). 4-(2-hydroxyethyl)-1-piperazineethanesulfonic acid (HEPES), Ultrapure, MB Grade was from USB Corporation (Cleveland, Ohio, USA). 1,1,1,3,3,3-hexafluoro-2-propanol (HFIP) and thioflavin T (ThT) were from Sigma-Aldrich. NaCl was extra pure from Scharlau (Barcelona, Spain). All solutions were prepared in fresh MilliQ water.

Sample Preparation

Stock solution of peptides was prepared as follows: 1 mg of the Aβ peptide was dissolved in HFIP at a concentration 500 μM to disassemble preformed aggregates [9]. The solution was divided into aliquots, HFIP was evaporated in vacuum, and the tubes with the peptide film were kept at −80 °C until used. Before usage, the Aβ HFIP film was dissolved in water containing 0.02% NH_3 at a concentration of 10–20 μM. After 5 min of incubation, the Aβ stock solution was filtrated through a 0.45 μm pore size Millex syringe-driven filter, dissolved with buffer and used for experiments. Insulin and amylin were dissolved in 20 mM HEPES and 100 mM NaCl, pH 7.4 at a concentration of 50 μM. After 30 min of incubation, the peptide stock solution was diluted with buffer and used for experiments.

Spectroscopy

Fluorescence spectra were collected on a Perkin–Elmer LS-45 fluorescence spectrophotometer equipped in house with a magnetic stirrer with constant stirring rate 250 rpm or equipped with a variable speed stirrer. Hellma semimicro cells were used. It is important to note that the stirring rate that is sufficient for a fast fibrillization depends not only on the stirrer speed but also varies with the cuvette and stirrer rod type used. We also noticed that in spectrofluorimeters equipped with built-in stirrers, the stirring speed should be 600–800 rpm to achieve fast aggregation (Figure 1). In our custom system, the movement of the stirrer rod was irregular because of a 2 mm shift of the rotation axis of the magnetic stirrer with respect to the center of the cell that caused the stirrer bar to flip against the walls of the quartz cell. Fibrillization was monitored using ThT fluorescence. If not otherwise stated, fresh Aβ stock solution was diluted in 20 mM HEPES and 100 mM NaCl, pH 7.4 containing 3.3 μM of ThT to a final concentration of 5 μM in the case of Aβ_{42} and 10 μM in the case of Aβ_{40}. The final concentration of insulin and amylin was 2.5 μM and 10 μM, respectively. Of each sample, 400 μl was incubated at constant temperature. ThT fluorescence was measured at 480 nm using excitation at 445 nm.

Bicine/Tris SDS-PAGE

The SDS-PAGE was performed using 15%T/5%C gel on *Mini-PROTEAN Tetra System* (Bio-Rad) over 1.5 h. Gel consisted of separation gel, stacking gel and comb gel, thickness, 0.75 mm, that were made according to Wiltfang J. *et al*. 1997 [10] with minor modifications: Separation gel was made without urea. Of samples containing 10 μM Aβ, 20 μl were mixed with 5 μl of 5× loading buffer (1.8 M bistris, 0.265 M bicine, 75% glycerol, 5% SDS, 0.02% bromophenol blue) and heated to 95 °C for 5 min. The SDS-PAGE gel was resolved in Cathode buffer with 0.1% SDS at 110 V for 1.5 h (room temperature). After electrophoresis, gel was fixed in glutaraldehyde/sodium borate/phosphate buffer solution for 45 min at room temperature (glutaraldehyde 0.25%). Silver staining was carried out by a modified Dunn, M. silver staining method [11].

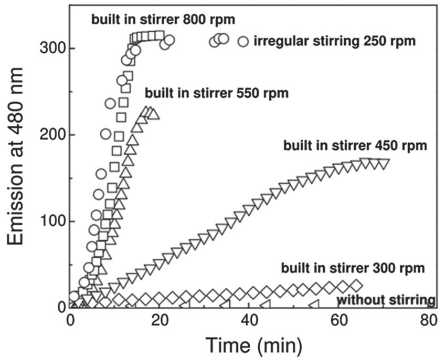

Figure 1. The effect of agitation on the Aβ fibrillization followed by ThT fluorescence. Aggregation of 5 μM Aβ_{42} in 20 mM HEPES and 100 mM NaCl, 25 °C, pH 7.4 with irregular stirring at a constant stirring rate of 250 rpm or with a built-in stirrer with various stirring speeds. Fluorescence measurement was carried out on a Perkin–Elmer LS-45 fluorescence spectrophotometer in a Hellma semimicro cells.

Data Analysis and Kinetics of Fibril Formation

The kinetics of Aβ fibrillization could be described as sigmoid curves, and the aggregation parameters were determined by fitting the plot of fluorescence intensity versus time to Boltzmann curve

$$y = \frac{A_2 - A_1}{1 + e^{(t-t_0)\times k}} + A_2 \quad (1)$$

where A_1 is the initial fluorescence level, A_2 corresponds to the fluorescence at maximal fibrillization level, t_0 is the time t when fluorescence is reached half maximum and k is the apparent rate constant for the growth of fibrils [12,13].

Results

Effect of Agitation on the Fibrillization of Aβ Peptides

The time curves of Aβ_{42} fibrillization are presented in Figures 1 and 2. As a rule, the lyophilized Aβ_{42} preparations without HFIP pretreatment showed comparably high initial ThT-fluorescence levels indicating high content of fibrillar material (Figure 2). Different peptide preparations with different counterions had similar fibrillization curves after pretreatment of lyophilized peptides with HFIP (Figure 2). Aβ peptides, pretreated with HFIP to disassemble preformed aggregates, form stable solutions where the formation of ThT reactive material was not observed during several (2–4) days. The changes in the ThT fluorescence of Aβ_{40} were parallel to changes on the light scattering (Figure 3)

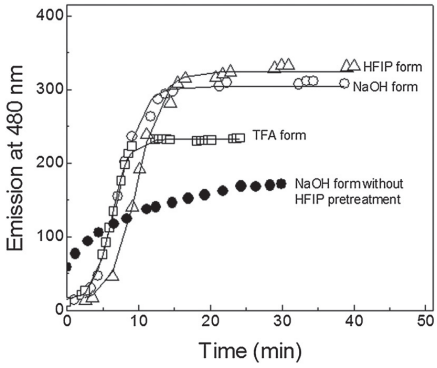

Figure 2. The effect of Aβ preparation on the fibrillization. The aggregation of 5 μM Aβ_{42} in 20 mM HEPES and 100 mM NaCl, pH 7.4, at 25 °C in the presence of 3.3 μM ThT with irregular stirring at a constant stirring rate of 250 rpm. Open symbols – different Aβ preparations with HFIP pretreatment, closed symbols – Aβ_{42} NaOH form without HFIP pretreatment.

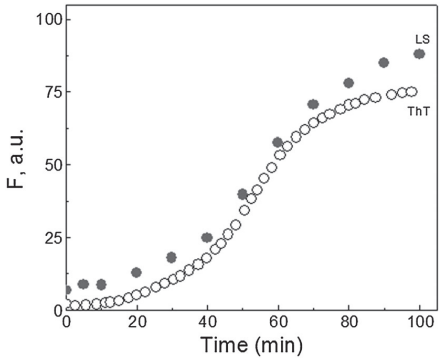

Figure 3. The fibrillization of Aβ_{40} followed by ThT fluorescence and light scattering. Aggregation of 10 μM Aβ_{40} in 20 mM HEPES and 100 mM NaCl, pH 7.4 at 50 °C in the presence of 3.3 μM ThT with irregular stirring at a constant stirring rate of 250 rpm. Fluorescence measurements were carried out on a Perkin–Elmer LS-45 fluorescence spectrophotometer in a Hellma semimicro cells. ThT fluorescence was measured at 480 nm using excitation at 445 nm. Light scattering measured at 90° angle at 540 nm using excitation at 270 nm.

demonstrating that the aggregation is parallel to the formation of β-structures. The aggregates were centrifugated at 21 130 g for 30 min, and the SDS-PAGE analysis shows that all the peptide is sedimented (Figure 4). This means that there is no detectable amounts of soluble peptide either in monomeric or in oligomeric form after fibrillization is completed. It has been shown earlier that a fast fibrillization of the HFIP treated Aβ_{42} peptide can be initiated by stirring [12] or by the addition of preformed fibrillar seeds [14]. A typical sigmoidal fibrillization curve observed under the conditions of intensive stirring is presented in Figure 5A occurring with $t_0 = 10$ min and $k = 0.50\ \text{min}^{-1}$ (average values given in Table 1). Figure 5A shows that in the case of Aβ_{42}, stopping the stirrer after the fluorescence has achieved 25% of its maximum value had no effect on the rate of the process: In some experiments, a small 10% decrease in the rate of increase of ThT fluorescence was detected, which is presumably caused by sedimentation of larger aggregates.

Thus, for the fibrillization of Aβ_{42}, the agitation is crucial only in the initial exponential phase of the process, where new fibrils are forming and stirring is not required in the following first-order growth phase, where the major process is fibril elongation. When the stirrer was turned off earlier, for instance, at the level of 5% of the final fluorescence intensity, the exponential phase and the increase in the fibrillization rate ended abruptly, and the fibril growth continued with the rate achieved at that time point. These results show clearly that in the case of Aβ_{42}, agitation affects the formation of new seeds and/or fibrils but not the fibril growth.

Similar to Aβ_{42}, the Aβ_{40} peptide was also stable under quiescent conditions at pH 7.4 for several days, and its fast fibrillization was induced by stirring with a magnetic stirrer. However, the response of Aβ_{40} to the stopping of agitation in the fibril growth phase was different from that of Aβ_{42}. Figure 5B shows that stopping the stirring almost halted the fibril growth independently of the depth of the reaction; thus, Aβ_{40} needed agitation for fibrillization throughout the whole process including the fibril growth phase. From the rates of Aβ_{40} fibrillization after stopping the stirrer, it was estimated that in nonagitated conditions, reaction proceeded with 5%–20% of the rate in agitated conditions. When the stirring was turned on again, the fibrillization rate quickly returned to the value it had before the stirrer was turned off. It has been demonstrated that the fibrillization of Aβ_{40} initiated by shearing continues when shearing was stopped, however at a much slower (approximately fourfold to fivefold)

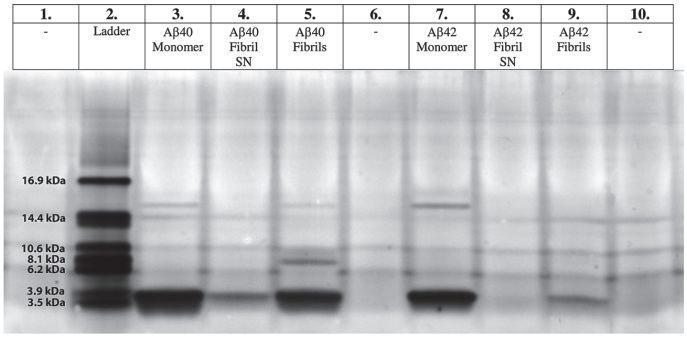

Figure 4. The SDS-PAGE analysis of Aβ fibrils. Monomers – HFIP treated Aβ_{40} and Aβ_{42} was dissolved in 10 mM NaOH and diluted two times with 40 mM HEPES and 200 mM NaCl buffer, pH 7.4 with concentration of 10 μM. Fibrils – 10 μM Aβ_{40} and Aβ_{42} fibrils were centrifuged for 30 min, 21 130 g. Supernatant (SN) was collected, and precipitate (fibrils) was dissolved in equal amounts of 10 mM NaOH and 40 mM HEPES buffer containing 200 mM NaCl, pH 7.4 with concentration of 10 μM. SDS-PAGE was performed using 15%T/5%C gel on *Mini-PROTEAN Tetra System* (Bio-Rad) over 1.5 h and visualized by silver staining.

Journal of PeptideScience

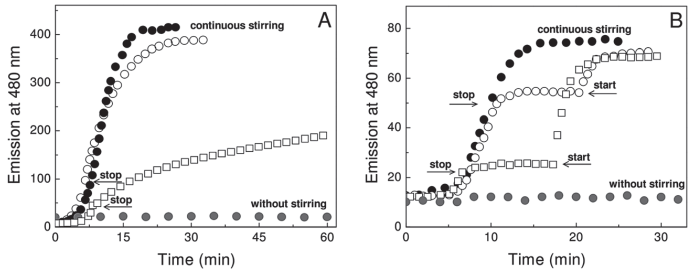

Figure 5. The effect of agitation on the Aβ fibrillization followed by ThT fluorescence. Fluorescence measurement was carried out on a Perkin–Elmer LS-45 fluorescence spectrophotometer equipped in house with a magnetic stirrer with constant stirring rate 250 rpm in a Hellma semimicro cells. Closed symbols – continuous stirring, open symbols – stirrer was turned off on at the points indicated by the first arrow and turned on again at the points indicated by the second arrow; gray symbols correspond to quiescent conditions. (A) Aggregation of 5 μM $A\beta_{42}$ in 20 mM HEPES and 100 mM NaCl, 25 °C, pH 7.4; other conditions and sample preparation as described earlier [12]. (B) Aggregation of 10 μM $A\beta_{40}$ in 20 mM HEPES and 100 mM NaCl, 50 °C pH 7.4. The decrease of the fibrillization rate after stopping the agitation was estimated from the slopes of the kinetic curves.

Table 1. The fibrillization parameters of $A\beta_{40}$, $A\beta_{42}$, insulin and amylin.

Peptide	Reaction conditions	k (per minute)	t_0 (min)
$A\beta_{42}$ ($n=9$)	5 μM peptide; 25 °C	0.45 ± 0.09	11.5 ± 4.9
$A\beta_{40}$ ($n=3$)	10 μM peptide; 50 °C	1.11 ± 0.37	7.6 ± 1.5
Insulin ($n=5$)	2.5 μM peptide; 50 °C	4.00 ± 0.71	26.4 ± 5.2
Amylin ($n=4$)	10 μM peptide; 40 °C	2.51 ± 0.83	13.4 ± 0.6

pace than with continuous shearing [15]. However, the lag period of the shear-induced fibrillization was several hours under similar temperature and pH, and the overall process was slower.

Effect of Stirring on the Fibrillization of Insulin and Amylin

It has been shown recently that fast insulin fibrillization may occur at physiologically relevant pH, temperature and ionic strength under agitated conditions without added denaturating agents [16]. Figure 6A and B show that insulin and amylin are forming fibrils under agitated conditions in the same time scale as Aβ peptides. No fibril formation was observed during the incubation of these peptides under quiescent conditions at the same temperature and pH for at least 2–3 days. Insulin and amylin behaved similarly to $A\beta_{40}$, where intensive agitation was necessary during the whole fibrillization process, e.g. the fibril growth when the stirrer was turned off was 11% and 5%, respectively, of the rate in agitated conditions. Fibrillization continued with high rate at the point where stirrer was turned on again (Figure 6A and B).

Discussion

It has been generally accepted that the agitation of the solution substantially accelerates the peptide and protein fibrillization; however, the origin of the accelerating effect has remained elusive. Historically, the first explanation for this rate enhancement was that mixing causes the fragmentation of fibrils and increases the number of fibril ends available for monomer addition. This explanation links the acceleration with a phenomenon called secondary (e.g., fibril depending) nucleation that is crucial in the exponential phase of the fibrillization. It has been demonstrated

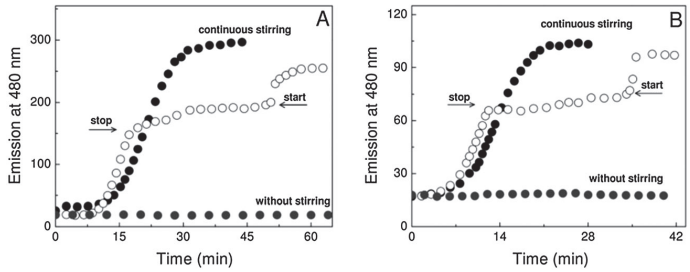

Figure 6. The effect of agitation on the fibrillization of insulin (A) and amylin (B) followed by ThT fluorescence. (A) Insulin concentration 2.5 μM 50 °C. (B) Amylin concentration 10 μM, 40 °C; 20 mM HEPES and 100 mM NaCl, pH 7.4, stirring speed 250 rpm. Closed symbols – continuous stirring; open symbols– stirrer was turned off at the points indicated by the first arrow and turned on again at the points indicated by the second arrow, gray symbols correspond to the process in quiescent conditions. The decrease of fibrillization rate after stopping the agitation was estimated from the slopes of the kinetic curves.

that the fibrillization curves for several peptides cannot be described without assuming intensive secondary nucleation during fibrillization [5,17–20]; thus, secondary nucleation is a common phenomenon in peptide fibrillization in agitated as well as in nonagitated conditions. The fibril fragmentation by agitation is not the only mechanism that can lead to secondary nucleation. Interactions of peptide/protein fibrils with water–air and water–solid interfaces may also be involved in the acceleration of fibrillization because of catalyzing both secondary and primary nucleation events *in vitro* [8]. Our experiments also demonstrated the importance of interface effects because a regular stirring vortex generated by magnetic stirrer at 250 rpm had a significantly lower impact on the fibrillization rate than putative 'grinding' of fibrils when stirrer contacts the cell walls. However, as the fibrillization process is also accelerated by shear generated by Couette flow [6], the secondary nucleation can also occur in bulk solution. The origin of primary nucleation both *in vitro* and *in vivo* remains unknown. As the duration of lag phase is relatively insensitive to the increase in the peptide concentration [21,22] and the process is enhanced by stirring, it is reasonable to speculate that in practice, the primary fibrils start to grow on the interface of the test tube. *In vivo* the process can be triggered by metal ions [12,23,24] or, for instance, by lipid membranes [25].

The impact of agitation on the fibrillization of Aβ_{42} can be described assuming that the enhanced secondary nucleation is the only impact of agitation; however, it remains elusive why the fibrils of other peptides required agitation throughout the whole process. It can be hypothesized that they need secondary nucleation because of some kind on extensive 'autoinhibition', which may result from accidental association of peptide molecules to the fibril end in a 'nonproductive' way or incorrect or slow 'locking' (in the framework of docking and locking model) that blocks the growth of the individual fibrils temporarily. This assumption is based on the finding that assembly of individual amyloid fibrils is discontinuous: Bursts of rapid growth phases are interrupted with pauses, e.g. the process involves fluctuation between fast-growing and blocked states in which fibril is somehow kinetically trapped [26]. It might be suggested that in agitated conditions, the pauses between bursts are shorter as compared with the fibrillization in nonagitated conditions. The *in vitro* fibrillization rates of the peptides studied were relatively similar in the agitated conditions (Table 1). However, only Aβ_{42}, which has the highest amyloidogenity among these peptides *in vivo*, showed high fibrillization rate in the absence of intensive agitation in the fibril growth phase. We suggest that the high *in vivo* amyloidogenity of Aβ_{42} might be causatively related to the ability of Aβ_{42} fibrils to growth under quiescent conditions.

Acknowledgements

This work was supported by the Estonian Ministry of Education and Research (grant SF0140055s08), Estonian Science Foundation grants no. 9318 (V.T.) and 8811 (P.P.) and World Federation of Scientists scholarships to A.T. and A.N.

References

1 Harrison RS, Sharpe PC, Singh Y, Fairlie DP. Amyloid peptides and proteins in review. *Rev. Physiol. Biochem. Pharmacol.* 2007; **159**: 1–77.
2 Dobson CM. Protein folding and misfolding. *Nature* 2003; **426**(6968): 884–90.
3 Harper JD, Lansbury PT, Jr. Models of amyloid seeding in Alzheimer's disease and scrapie: mechanistic truths and physiological consequences of the time-dependent solubility of amyloid proteins. *Annu. Rev. Biochem.* 1997; **66**: 385–407.
4 Lomakin A, Chung DS, Benedek GB, Kirschner DA, Teplow DB. On the nucleation and growth of amyloid beta-protein fibrils: detection of nuclei and quantitation of rate constants. *Proc. Natl. Acad. Sci. USA* 1996; **93**(3): 1125–1129.
5 Knowles TPJ, Waudby CA, Devlin GL, Cohen SIA, Aguzzi A, Vendruscolo M, Terentjev EM, Welland ME, Dobson CM. An analytical solution to the kinetics of breakable filament assembly. *Science* 2009; **326**(5959): 1533–1537.
6 Dunstan DE, Hamilton-Brown P, Asimakis P, Ducker W, Bertolini J. Shear flow promotes amyloid-{beta} fibrilization. *Protein Eng. Des. Sel.* 2009; **22**(12): 741–746.
7 Mahler HC, Friess W, Grauschopf U, Kiese S. Protein aggregation: pathways, induction factors and analysis. *J. Pharm. Sci.* 2009; **98**(9): 2909–2934.
8 Morinaga A, Hasegawa K, Nomura R, Ookoshi T, Ozawa D, Goto Y, Yamada M, Naiki H. Critical role of interfaces and agitation on the nucleation of abeta amyloid fibrils at low concentrations of abeta monomers. *Biochim. Biophys. Acta* 2010; **1804**(4): 986–95.
9 Stine WB, Jr., Dahlgren KN, Krafft GA, LaDu MJ. *In vitro* characterization of conditions for amyloid-beta peptide oligomerization and fibrillogenesis. *J. Biol. Chem.* 2003; **278**(13): 11612–22.
10 Wiltfang J, Smirnov A, Schnierstein B, Kelemen G, Matthies U, Klafki HW, Staufenbiel M, Hüther G, Rüther E, Kornhuber J. Improved electrophoretic separation and immunoblotting of beta-amyloid (a beta) peptides 1-40, 1-42, and 1-43. *Electrophoresis* 1997; **18**(3-4): 527–32.
11 Dunn M. Detection of proteins in polyacrylamide gels by silver staining. In *The Protein Protocols Handbook*, Walker J (ed.). Humana Press, New York, 1996; 229-233.
12 Tõugu V, Karafin A, Zovo K, Chung RS, Howells C, West AK, Palumaa P. Zn(II)- and Cu(II)-induced non-fibrillar aggregates of amyloid-beta (1-42) peptide are transformed to amyloid fibrils, both spontaneously and under the influence of metal chelators. *J. Neurochem.* 2009; **110**(6): 1784–95.
13 Nielsen L, Frokjaer S, Brange J, Uversky VN, Fink AL. Probing the mechanism of insulin fibril formation with insulin mutants. *Biochemistry* 2001; **40**(28): 8397–409.
14 Zovo K, Helk E, Karafin A, Tougu V, Palumaa P. Label-free high-throughput screening assay for inhibitors of Alzheimer's amyloid-beta peptide aggregation based on MALDI MS. *Anal. Chem.* 2010; **82**(20): 8558–8565.
15 Hamilton-Brown P, Bekard I, Ducker WA, Dunstan DE. How does shear affect a beta fibrillogenesis? *J. Phys. Chem. B* 2008; **112**(51): 16249–16252.
16 Noormägi A, Gavrilova J, Smirnova J, Tõugu V, Palumaa P. Zn(II) ions co-secreted with insulin suppress inherent amyloidogenic properties of monomeric insulin. *Biochem. J.* 2010; **430**: 511–518.
17 Hofrichter J. Kinetics of sickle hemoglobin polymerization. III. Nucleation rates determined from stochastic fluctuations in polymerization progress curves. *J. Mol. Biol.* 1986; **189**(3): 553–71.
18 Larson JL, Miranker AD. The mechanism of insulin action on islet amyloid polypeptide fiber formation. *J. Mol. Biol.* 2004; **335**(1): 221–231.
19 Librizzi F, Rischel C. The kinetic behavior of insulin fibrillation is determined by heterogeneous nucleation pathways. *Protein Sci.* 2005; **14**(12): 3129–34.
20 Padrick SB, Miranker AD. Islet amyloid: phase partitioning and secondary nucleation are central to the mechanism of fibrillogenesis. *Biochemistry* 2002; **41**(14): 4694–703.
21 Hellstrand E, Boland B, Walsh DM, Linse S. Amyloid beta-protein aggregation produces highly reproducible kinetic data and occurs by a two-phase process. *ACS Chem. Neurosci.* 2010; **1**(1): 13–18.
22 Karafin A, Palumaa P, Tõugu V. Monitoring of amyloid-beta fibrillization using an improved fluorimetric method. In *New Trends in Alzheimer and Parkinson Related Disorders: ADPD 2009*, Fisher A, Hanin I (eds). Medimond International Proceedengs: Bologna, Italy, 2009; 255–261.
23 Sarell CJ, Wilkinson SR, Viles JH. Substoichiometric levels of Cu2+ ions accelerate the kinetics of fiber formation and promote cell toxicity of amyloid-beta from Alzheimer disease. *J. Biol. Chem.* 2010; **285**(53): 41533–41540.

24 Bush AI, Pettingell WH, Multhaup G, d Paradis M, Vonsattel JP, Gusella JF, Beyreuther K, Masters CL, Tanzi RE. Rapid induction of Alzheimer a beta amyloid formation by zinc. *Science* 1994; **265**(5177): 1464–7.
25 Murray IV, Liu L, Komatsu H, Uryu K, Xiao G, Lawson JA, Axelsen PH. Membrane-mediated amyloidogenesis and the promotion of oxidative lipid damage by amyloid beta proteins. *J. Biol. Chem.* 2007; **282**(13): 9335–45.
26 Kellermayer MS, Karsai A, Benke M, Soos K, Penke B. Stepwise dynamics of epitaxially growing single amyloid fibrils. *Proc. Natl. Acad. Sci. U.S.A.* 2008; **105**(1): 141–4.

Publication IV

Noormägi, A.; Valmsen, K.; Tõugu, V.; Palumaa, P. "Insulin fibrillization at acidic and physiological pH values is controlled by different molecular mechanisms" (2015) The Protein Journal.; 34(6): 398-403

Protein J (2015) 34:398–403
DOI 10.1007/s10930-015-9634-x

Insulin Fibrillization at Acidic and Physiological pH Values is Controlled by Different Molecular Mechanisms

Andra Noormägi[1] · Karin Valmsen[1] · Vello Tõugu[1] · Peep Palumaa[1]

Published online: 22 October 2015

Abstract Formation of amyloid-like fibrils by insulin was studied at different insulin concentrations, pH and temperatures. At low pH (pH 2.5) the insulin fibrillization occurred only at high (>10 μM) peptide concentrations, whereas at physiological pH values the fibril formation is inhibited at higher insulin concentrations. The enthalpy of activation Ea of the fibril growth at pH 2.5 equals to 33 kJ/mol, which is considerably lower than 84 kJ/mol at physiological pH. The fibrillization rate of insulin decreases with increasing pH at high, 250 μM concentration, which was opposite to the pH effect observed in 2.5 μM insulin solutions. The latter effect indicates that protonation of histidine residues seems to be important for the fibrillization of monomeric insulin, whereas the pH effect at high concentration may result from off-pathway oligomerization propensity. Together, the different effect of environmental factors on the insulin fibrillization suggest that the reaction rate is controlled by different molecular events in acidic conditions and at physiological pH values.

Keywords Amyloid · Fibrillization · Insulin

Abbreviations

ThT	Thioflavin T
TEM	Transmission electron microscopy
Hepes	2-[4-(2-hydroxyethyl)-piperazin-1-yl]ethane-1-sulfonic acid

1 Introduction

Protein aggregation and accumulation in the form of amyloid fibrils is associated with more than 40 human pathologies, including the most common neurodegenerative diseases and Type 2 diabetes [1]. Moreover, the formation of amyloid is assumed to be a generic property of a polypeptide chain [2, 3]. During the amyloid formation evolutionarily and structurally unrelated proteins obtain similar structural characteristics, they form elongated non-branching structures with fibrillar morphology and dominant β-sheet content organized in a cross-β fashion [4, 5].

Insulin is one of the peptides that easily forms amyloid-like fibrils in vitro. The fibrillization of insulin poses a variety of concerns in the production, storage, and transport of the artificially produced hormone [6]. Insulin is also used as a good model molecule in the studies of protein fibrillization in general [7]. Pathologies related with insulin fibrillization in humans are relatively uncommon: small amounts of insulin fibrils have been observed in the organisms of patients with type II diabetes and in normal elder people and in rare cases insulin fibers appear after subcutaneous insulin infusion and repeated injection [8–10]. However, inhaled insulin readily forms fibrils in the lungs, causing a significant reduction in pulmonary air flow, which excludes the use of insulin inhalators [11].

Electronic supplementary material The online version of this article (doi:10.1007/s10930-015-9634-x) contains supplementary material, which is available to authorized users.

✉ Vello Tõugu
vello.tougu@ttu.ee

Peep Palumaa
peep.palumaa@ttu.ee

[1] Department of Gene Technology, Tallinn University of Technology, Akadeemia 15, 12816 Tallinn, Estonia

The rate of insulin fibrillization depends on various environmental factors—pH, temperature, peptide concentration, agitation, availability of hydrophobic surfaces, etc. The majority of insulin fibrillization studies have been performed at acidic pH values using high peptide concentrations [12–14] and only few studies have been performed at physiological pH values. It is generally believed [15] that insulin fibrillization occurs via a uniform reaction mechanism under various conditions, however, this has been never proved experimentally. For instance, at low pH values an increase in the insulin concentrations resulted the shortening of the lag phase and an increase in the apparent rate constant of the fibril formation in nonagitated solutions but not in vigorously agitated solutions [16]. In contrast, under physiological pH values an increase in the insulin concentration leads to longer lag phase, which has been explained by insulin oligomerization and formation of off-pathway oligomers [17]. Insulin fibrillization occurs through the dissociation of oligomers into active monomers, which undergo a structural change to a conformation having strong propensity to fibrillate [14, 16, 18], however, the different influence of peptide concentration to the process may suggest, that insulin fibrillization at acidic and physiological pH values proceed via different reaction mechanism.

Our aim was to compare the kinetics of insulin fibrillization at different pH, temperature and peptide concentrations. The results suggest that fibrillization of insulin at low and physiological pH values are controlled by different molecular events.

2 Materials and Methods

2.1 Materials

Lyophilized bovine insulin, ThT (thioflavin T) and acetic acid were purchased from Sigma-Aldrich. 2-[4-(2-hydroxyethyl)-piperazin-1-yl]ethane-1-sulfonic acid (Hepes) Ultrapure (molecular biology grade) was from USB Corporation. NaCl (extra pure) was from Scharlau and formic acid was from Riedel-deHaen. All solutions were prepared in fresh Milli-Q water.

2.2 Sample Preparation

A stock solution of insulin was prepared by dissolving an appropriate amount of lyophilized insulin in either 20 mM Hepes and 100 mM NaCl at pH 7.3; 50 mM ammonium acetate and 100 mM NaCl at pH values from 5.5 to 8.5; or 0.1 % formic acid and 100 mM NaCl at pH 2.5 at a concentration of 50 or 500 μM. After 30 min of incubation at 25 °C, the insulin stock solution was diluted with the same buffer and used for further experiments.

2.3 Monitoring Insulin Fibrillation by ThT Fluorescence

Insulin fibrillation was monitored as described earlier [17]: in a standard experiment, a freshly prepared stock solution of insulin was diluted to a final concentration of 250 μM in 0.1 % formic acid, pH 2.5 and 100 mM NaCl containing 50 μM ThT. A 500-μl sample was incubated in a 0.5-cm-path-length semi-micro quartz cell (Hellma), equilibrated at 50 °C and equipped with a magnetic stirrer. The increase in ThT fluorescence was measured at 470 nm using excitation at 430 nm on a Perkin-Elmer LS-55 fluorescence spectrophotometer, and the "fast" stirring regime was used. For studying the effect of pH, 2.5 μM or 250 μM insulin were dissolved in 0.1 % formic acid and 100 mM NaCl at pH 2.5–4.0, 50 mM ammonium acetate and 100 mM NaCl at pH 5.5–8.5 or 20 mM Hepes and 100 mM NaCl at pH 7.3. The k values were estimated from the slopes of the linear region in the middle of the fibrillation growth curve by simple linear regression, since systematic deviations were observed when the time curves were fitted to the Boltzmann equation describing the fibrillization at high pH values (See Supplementary Figure 1).

2.4 Transmission Electron Microscopy

3 μl of centrifuged (30 min, 12,000g) peptide solution was pipetted on to TEM grids placed at adhesive surface and allowed to air dry. 2 % uranylacetate water solution was spotted on to a Parafilm plate and grids were placed on them with the upper side down. Probes were incubated in uranylacetate for 10 min and washed with Milli-Q water. Excess water was removed with a filter paper and the grids were placed into a special carrier. TEM images from the samples were recorded to a high-resolution 60 × 90-mm negative film using a Selmi EM-125 instrument at 75 kV accelerating voltage.

3 Results

3.1 Effect of Temperature on Insulin Fibrillization

At low pH and high insulin concentration the insulin fibrillization is characterized by time-curves typical for autocatalytic amyloid formation and the overall process is consisting of an initial lag phase, a subsequent growth phase, and a final equilibrium phase. Insulin fibrillization was significantly enhanced with increasing temperature (Fig. 1). No amyloid formation was observed at

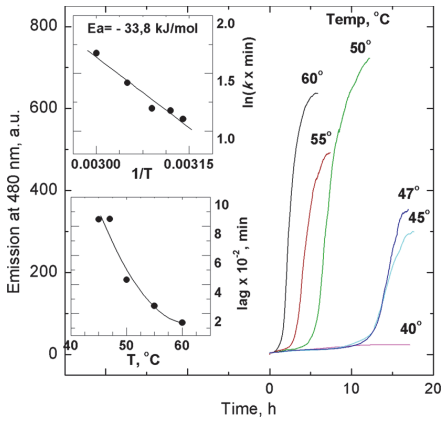

Fig. 1 The effect of temperature on the insulin fibrillization at pH 2.5 followed by ThT fluorescence. Fibrillization of 250 μM insulin in 0.1 % formic acid and 100 mM NaCl at pH 2.5. Insulin was incubated at 60 °C (*black squares*), 55 °C (*white squares*), 50 °C (*black circles*), 47 °C (*white circles*), 45 °C (*black triangles*) and 40 °C (*white triangles*) in the presence of 50 μM ThT with continuous agitation. *Insets* temperature dependence shown in Arrhenius coordinates and dependence of lag time on temperature. *a.u.* arbitrary units

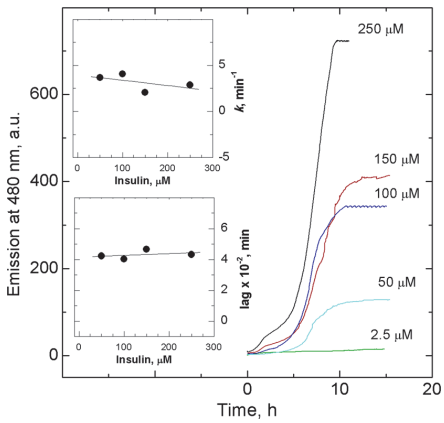

Fig. 2 The effect of insulin concentration on the fibril formation. Insulin in 0.1 % formic acid and 100 mM NaCl (pH 2.5) was incubated at 50 °C with continuous agitation and peptide concentration was varied from 2.5 to 250 μM. *Insets* dependence of the fibrillization rate constant and lag time on the insulin concentration. *a.u.* arbitrary units. Relative SD ± 11 % for the k value was determined at 100 μM insulin concentration (n = 6)

temperatures below 40 °C, at higher temperatures the fibrillization rate constant increased and lag period was decreased. The enthalpy of activation $E_a = 33.8$ kJ/mol was found from the slope of the Arrhenius plot (Fig. 1, inset). The fibrillization rate at 50 °C was optimal for measurements and further experiments were carried out at that temperature.

3.2 Effect of Insulin Concentration on Fibrillization

At pH 2.5 under the final ThT florescence levels increased with increasing peptide concentration (Fig. 2). No significant changes in the duration of lag periods and rate constants were observed in the concentration range of 50–250 μM, however, at low (2.5 μM) insulin concentration no amyloid formation was observed. The maximal levels of ThT fluorescence were reasonably well proportional to the peptide concentrations. When we carried out the fibrillization of 2.5 μM insulin at pH 7.3 and lowered the pH to 2.5 by adding formic acid after the fibrils were already formed, the sample showed similar fluorescence intensity than that at pH 7.3 (Fig. 3).

3.3 Effect of pH on Insulin Fibrillization

The influence of pH on the kinetics of fibril formation was studied at "low" 2.5 μM and "high" 250 μM insulin concentrations. Fibrillation curves of 2.5 μM insulin in the pH range of 7.0–7.8 exposed shorter lag times and faster growth rates than those measured at acidic or basic pH values (Fig. 3a). An increase in pH from 5.5 to 7.8 resulted in a 1.5-fold reduction in lag time and an increase in the value of the rate constant, no fibrils were formed at pH 2.5. The fibrillation of 250 μM insulin, on the contrary, was enhanced by low pH: the lag period was significantly shorter at acidic pH, and the rate constant was increased almost threefold (Fig. 3b). No significant changes were observed in lag times and rate constants in the pH range of 2.5–4.0. The fibrillization of 250 μM of insulin could not be studied at intermediate pH values due to the low solubility of the peptide near its pI value.

Figure 4 shows, that the rate of insulin fibrillization at low pH is not sensitive towards agitation, stopping the stirrer did not affect the fibrillization rate. In a similar experiment at physiological pH the process stopped with ending the agitation [19].

The presence of insulin fibrils in the samples was confirmed by TEM. The samples were taken from 250 μM insulin agitated for 10 h at pH 2.5 and from the solution of 2.5 μM insulin agitated for 75 min at pH 7.4. Representative examples of TEM images from fibrils are shown in Fig. 5a, b. At low pH short fibrils were formed whereas "networks" of longer fibrils were detected at physiological pH.

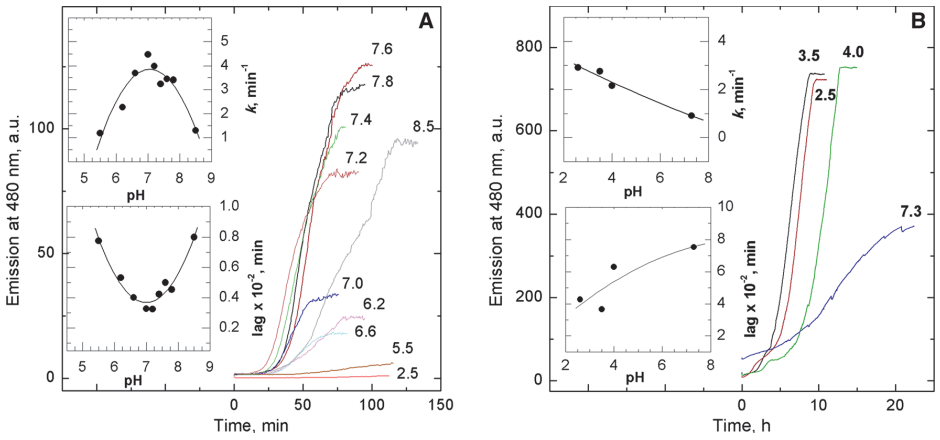

Fig. 3 The effect of pH on the fibrillization of insulin. 2.5 μM (**a**) or 250 μM (**b**) of insulin in 0.1 % formic acid and 100 mM NaCl (pH 2.5–4.0) or in 20 mM Hepes and 100 mM NaCl (pH 7.3) was incubated at 50 °C with continuous agitation in the presence of 50 μM ThT and at various pH values as shown in the figure. *Insets* dependence of the fibrillization rate constant and lag time on the pH value. *a.u.* arbitrary units

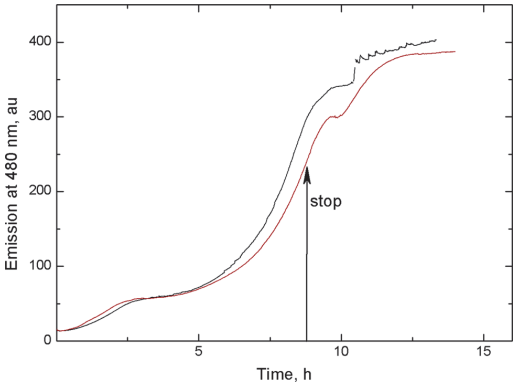

Fig. 4 The effect of agitation on the fibrillization of insulin at low pH. 100 μM of insulin in 0.1 % formic acid and 100 mM NaCl (pH 2.5) was incubated at 50 °C. *Open symbols* continuous agitation, *filled symbols* agitation was turned off at the point indicated with an *arrow*

4 Discussion

Insulin is often used as a suitable model peptide in fibrillization studies, whereas elevated temperatures, low pH, high peptide concentration, and high ionic strength usually associate with accelerated fibril formation [20, 21]. However, insulin can also fibrillize at physiological pH values [16, 17]. We have shown earlier [17] that the insulin fibrillization at pH 7.3 in vitro is characterized by a "reverse" dependence on peptide concentration—the fibrillization is fastest at low peptide concentration and higher peptide concentration inhibit the process. We suggest that the insulin fibrillization mechanisms at physiological and acidic pH values are rather different. At low pH the lag period and rate constants of fibril growth did not depend on the insulin concentration in the range of 50–150 μM. The fibrillization of 250 μM insulin exposed slightly shorter lag time and faster growth whereas formation of fibrils was not observed at low (1 and 2.5 μM) peptide concentrations. Thus, the effects of peptide concentration were clearly opposite at pH 2.5 and pH 7.3. Taking into account that IC50 for insulin dimerization is approx. 30 μM at pH 3.3 [22], it can be speculated that at low pH insulin dimerization is required for fibril growth. The inhibition of fibril formation at higher insulin concentrations at physiological pH values is most likely caused by insulin oligomerization into species that suppress fibrillization, for instance dimers and hexamers [17]. At acidic pH values insulin can form fibrils both in quiescent and agitated solutions [16]. However, at pH 7.3 the fibrillization of insulin stops when the agitation is stopped [19], whereas the fibrillization at low pH the fibrillization continues proceed with the same rate after stopping the agitation, which points to differences in the mechanism of fibrilllization.

The different shapes of the ThT emission versus time curves at neutral and acidic pH also indicate a difference between the insulin fibrillization at low and high pH. At pH 7.3 the fibrillization curves were symmetrical and could be well fitted to the Boltzmann equation, which is commonly used for the determination of the rate constant k values for growth rate and lag period durations [16, 17]. However, the fibrillization at low pH was characterized by a relatively

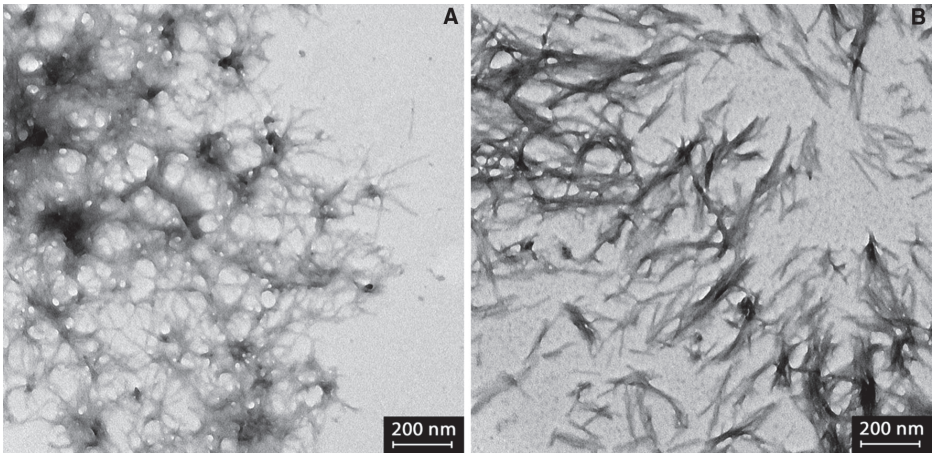

Fig. 5 TEM images of insulin fibrils. **a** TEM image of fibrils formed by agitation of 2.5 μM insulin for 75 min at pH 7.4. *Scale bar* 200 nm. **b** TEM image of fibrils formed by agitation of 250 μM insulin for 10 h at pH 2.5. *Scale bar* 200 nm

slow increase in the reaction rate after the lag-period and very sharp decrease of the rate at the end of the reaction demonstrating clear systematic deviation of residuals from the Boltzmann curve (Supplementary Figure). What causes this difference is not known, moreover, it is not known, why the fibrillization curves for several amyloid peptides are symmetrical and can be fitted to the Boltzmann equation widely used for the description of experimental data.

The enthalpy of activation of the insulin fibrillization E_a at pH 2.5 was equal to 33.8 kJ/mol. At pH 7.3, the E_a value was considerably larger: 84 kJ/mol [17], which indicates that fibrillization mechanisms are different under the acidic conditions and at the physiological pH values. It can be assumed that the conformational changes necessary for the formation of fibrillization-competent structure are much more prominent at neutral pH values.

TEM analysis demonstrated that the morphology of fibrils formed at neutral and acidic pH is also somewhat different.

In order to determine when the "high pH" fibrillization mechanism is replaced by a "low pH mechanism" we studied the pH effects on the insulin fibrillization at low and high peptide concentrations. The fibrillization of 2.5 μM insulin exposed shorter lag times and faster growth of fibrils at physiological pH range compared to those measured at acidic pH values (Fig. 3). Insulin is partially unfolded at low pH [23], however, it seems that the stabilization of partially unfolded forms on the peptide does not result in higher fibrillization rate. The maximal ThT fluorescence values were also higher at higher pH values, however, when the solution containing preformed fibrils and ThT was acidified to pH 2,5, its emission intensity was not changed, suggesting that the pH dependence of maximal ThT level changes due to different ThT binding or spectral properties of ThT bound to "high pH" and low pH" fibrils. The fluorescence of ThT bound to insulin fibrils formed at acidic pH has been shown to be tenfold lower [24]. The inhibition of fibril formation at low concentration is controlled by side chains in the peptide with pKa value close to 6, which is indicative to imidazole groups. It is known that the histidine residue at position B10 contributes to the formation of cross-β structure [7]. According to the amylin fibril model, where His18 participates in the intermolecular hydrogen-bonded β-sheet of amylin fibrils [25], the lowered pK_a of His18 in the fibrils indicates that that positive charges at the histidine residues inhibit fibril formation [26]. It can be suggested that the protonation of B10 His residue plays a similar role in insulin: histidine protonation at low pH results in electrostatic repulsion between positive charges in adjacent monomers in fibril. At high, 250 μM, concentration the pH effect was opposite to that observed at low insulin concentration: the rate constant decreased and the duration of the lag phase increased with increasing pH (Fig. 4). This difference demonstrates again that the processes limiting the fibrillization rate at high and low concentration of insulin are different.

The inhibition of fibril formation at higher insulin concentrations at physiological pH values is caused by insulin oligomerization, most likely by dimerization [17]. We observed the highest rate of insulin fibrillization at physiological pH and low peptide concentration. At low pH

values the fibrillization is slower, however, due to weaker insulin oligomerization, high rates are achieved at high peptide concentration

Taken together, the results indicate that fibrillization of insulin at high and low pH values occur via different mechanisms, which should be considered in using of insulin fibrillization as model for fibrillization processes.

Acknowledgments This work was supported by the Estonian Research Council (Grant IUT 19-8) and the Estonian Science Foundation Grants 8811 to PP and 9318 to VT.

Compliance with Ethical Standards

Conflict of interest The authors declare that they have no conflict of interest.

References

1. Castillo V, Ventura S (2009) Amyloidogenic regions and interaction surfaces overlap in globular proteins related to conformational diseases. PLoS Comput Biol 5:e1000476
2. Kurouski D, Washington J, Ozbil M, Prabhakar R, Shekhtman A, Lednev IK (2012) Disulfide bridges remain intact while native insulin converts into amyloid fibrils. PLoS One 7:e36989
3. Dobson CM (1999) Protein misfolding, evolution and disease. Trends Biochem Sci 24:329–332
4. Sipe JD, Cohen AS (2000) Review: history of the amyloid fibril. J Struct Biol 130:88–98
5. Jimenez JL, Nettleton EJ, Bouchard M, Robinson CV, Dobson CM, Saibil HR (2002) The protofilament structure of insulin amyloid fibrils. Proc Natl Acad Sci USA 99:9196–9201
6. Ahmad A, Millett IS, Doniach S, Uversky VN, Fink AL (2003) Partially folded intermediates in insulin fibrillation. Biochemistry 42:11404–11416
7. Ivanova MI, Sievers SA, Sawaya MR, Wall JS, Eisenberg D (2009) Molecular basis for insulin fibril assembly. Proc Natl Acad Sci USA 106:18990–18995
8. Dische FE, Wernstedt C, Westermark GT, Westermark P, Pepys MB, Rennie JA, Gilbey SG, Watkins PJ (1988) Insulin as an amyloid-fibril protein at sites of repeated insulin injections in a diabetic patient. Diabetologia 31:158–161
9. Swift B (2002) Examination of insulin injection sites: an unexpected finding of localized amyloidosis. Diabet Med 19:881–882
10. Shikama Y, Kitazawa J, Yagihashi N, Uehara O, Murata Y, Yajima N, Wada R, Yagihashi S (2010) Localized amyloidosis at the site of repeated insulin injection in a diabetic patient. Intern Med 49:397–401
11. Lasagna-Reeves CA, Clos AL, Midoro-Hiriuti T, Goldblum RM, Jackson GR, Kayed R (2010) Inhaled insulin forms toxic pulmonary amyloid aggregates. Endocrinology 151:4717–4724
12. Bryant C, Spencer DB, Miller A, Bakaysa DL, McCune KS, Maple SR, Pekar AH, Brems DN (1993) Acid stabilization of insulin. Biochemistry 32:8075–8082
13. Hua QX, Weiss MA (1991) Comparative 2D NMR studies of human insulin and des-pentapeptide insulin: sequential resonance assignment and implications for protein dynamics and receptor recognition. Biochemistry 30:5505–5515
14. Bouchard M, Zurdo J, Nettleton EJ, Dobson CM, Robinson CV (2000) Formation of insulin amyloid fibrils followed by FTIR simultaneously with CD and electron microscopy. Protein Sci 9:1960–1967
15. Li SH, Leblanc RM (2014) Aggregation of insulin at the interface. J Phys Chem B 118:1181–1188
16. Nielsen L, Khurana R, Coats A, Frokjaer S, Brange J, Vyas S, Uversky VN, Fink AL (2001) Effect of environmental factors on the kinetics of insulin fibril formation: elucidation of the molecular mechanism. Biochemistry 40:6036–6046
17. Noormagi A, Gavrilova J, Smirnova J, Tougu V, Palumaa P (2010) Zn(II) ions co-secreted with insulin suppress inherent amyloidogenic properties of monomeric insulin. Biochem J 430:511–518
18. Nielsen L, Frokjaer S, Brange J, Uversky VN, Fink AL (2001) Probing the mechanism of insulin fibril formation with insulin mutants. Biochemistry 40:8397–8409
19. Tiiman A, Noormägi A, Friedemann M, Krishtal J, Palumaa P, Tõugu V (2013) Effect of agitation on the peptide fibrillization: Alzheimer's amyloid-β peptide 1–42 but not amylin and insulin fibrils can grow under quiescent conditions. J Pept Sci 19:386–391
20. Brange J, Andersen L, Laursen ED, Meyn G, Rasmussen E (1997) Toward understanding insulin fibrillation. J Pharm Sci 86:517–525
21. Dzwolak W, Ravindra R, Lendermann J, Winter R (2003) Aggregation of bovine insulin probed by DSC/PPC calorimetry and FTIR spectroscopy. Biochemistry 42:11347–11355
22. Nettleton EJ, Tito P, Sunde M, Bouchard M, Dobson CM, Robinson CV (2000) Characterization of the oligomeric states of insulin in self-assembly and amyloid fibril formation by mass spectrometry. Biophys J 79:1053–1065
23. Hua QX, Weiss MA (2004) Mechanism of insulin fibrillation—the structure of insulin under amyloidogenic conditions resembles a protein-folding intermediate. J Biol Chem 279:21449–21460
24. Mishra R, Sjolander D, Hammarstrom P (2011) Spectroscopic characterization of diverse amyloid fibrils in vitro by the fluorescent dye Nile red. Mol Biosyst 7:1232–1240
25. Alexandrescu AT (2013) Amide proton solvent protection in amylin fibrils probed by quenched hydrogen exchange NMR. PLoS One 8:e56467
26. Jha S, Snell JM, Sheftic SR, Patil SM, Daniels SB, Kolling FW, Alexandrescu AT (2014) pH dependence of amylin fibrillization. Biochemistry 53:300–310

Curriculum vitae

Name: Andra Noormägi
Date of birth: 05.03.1984
Citizenship: Estonian

CONTACT INFORMATION

Address: Tallinn University of Technology, Institute of Chemistry and Biotechnology, Department of Gene Technology, Akadeemia tee 15, 12618 Tallinn, Estonia
Phone: +372 620 4412
E-mail: andra.noormagi@gmail.com

EDUCATION

2009-2018	Tallinn University of Technology, PhD student
2006-2008	M.Sc., Tallinn University of Technology, Department of Gene Technology“Cleavage of amyloid-β fused proteins with cyanogen bromide”
2003-2006	B.Sc., Tallinn University of Technology, Department of Gene Technology “A novel method for the cleavage of amyloid-β fused proteins with cyanogen bromide”

SUPPLEMENT COURSES

September 2013	Crystallography course, introduction of the new X-ray diffractometer; Tallinn, Estonia
September 2009	EBA Roadshow "Proteomics Course"; Tartu, Estonia
May 2006	Technological Course of Experimental Animal; Tallinn, Estonia

AWARDS

2010	World Federation of Scientists scholarship
2010	Estoninan National Competition of Student Research Works, Letter of thanks

CONFERENCES

May 2018	Oral presentation "Mechanisms of insulin fibrillization" in the Estonian Biochemical Society Spring School, Paunküla Welfare centre; Harjumaa, Estonia
October 2012	Annual Conference of the Estonian Society of Human Genetics "An overview of genetics and a precise view of heart disease"; Haapsalu, Estonia
October 2011	Annual Conference of the Estonian Society of Human Genetics "An overview of genetics and a precise view of neurogenetics"; Pärnu, Estonia
June 2010	Poster presentation "Zinc (II) ions inhibit fibrillation of monomeric insulin", 35th FEBS Congress "Molecules of Life"; Gothenburg, Sweden

EMPLOYMENT

01.08.2006-01.03.2018	Tallinn University of Technology, Department of Gene Technology, specialist

PUBLICATIONS

Noormägi, A.; Valmsen, K.; Tõugu, V.; Palumaa, P. "Insulin fibrillization at acidic and physiological pH values is controlled by different molecular mechanisms" (2015) The Protein Journal.; 34(6): 398-403

Tiiman, A., **Noormägi, A.**, Friedemann, M., Krishtal, J., Palumaa, P., Tõugu, V. "Effect of agitation on the peptide fibrillization: Alzheimer´s amyloid-beta peptide 1-42 but no amylin and insulin fibrils can grow under quiescent conditions" (2013) J Pept Sci.; 19(6): 386-391

Taler-Vercic, A., Kirsipuu, T., Friedemann, M., **Noormägi, A.**, Polajnar, M., Smirnova, J., Znidaric, M. T., Zganec, M., Skarabot, M.,Vilfan, A., Staniforth, R. A., Palumaa, P.,Zerovnik, E. "The role of initial oligomers in amyloid fibril formation by human stefin B" (2013) Int J Mol Sci.; 14(9): 18362-18384

Noormägi, A., Primar, K., Tõugu, V., Palumaa, P. "Interference of low-molecular substances with the thioflavin-T fluorescence assay of amyloid fibrils" (2011) J Pept Sci.; 18(1): 59-64

Noormägi, A., Gavrilova, J., Smirnova, J., Tõugu, V., Palumaa, P. "Zn(II) ions co secreted with insulin suppress inherent amyloidogenic properties of monomeric insulin" (2010) Biochem J.; 430(3): 511-518

Elulookirjeldus

Nimi:	Andra Noormägi
Sünniaeg:	05.03.1984
Kodakondsus:	Eesti

KONTAKTANDMED

Aadress:	Tallinna Tehnikaülikool, Keemia ja biotehnoloogia instituut, Geenitehnoloogia osakond, Akadeemia tee 15, 12618, Tallinn, Eesti
Telefon:	+372 620 4412
E-post:	andra.noormagi@gmail.com

HARIDUS

2009-2018	Tallinna Tehnikaülikool, doktorant
2006-2008	M.Sc., Tallinna Tehnikaülikool, Geenitehnoloogia instituut "Amüoid-β liitvalkude lagundamine tsüanogeen bromiidiga"
2003-2006	B.Sc., Tallinna Tehnikaülikool, Geenitehnoloogia instituut "Uudne metoodika amüloid-β liitvalkude lagundamiseks tsüonogeen bromiidiga"

TÄIENDKOOLITUS

September 2013	Kristallograafia kursus, uue X-kiirte difraktomeetri tutvustus; Tallinn, Eesti
September 2009	EBI Roadshow "Proteoomika kursus"; Tartu, Eesti
Mai 2006	Katseloomade tehnika kursus; Tallinn, Eesti

TUNNUSTUS

2010	World Federation of Scientists stipendium
2010	Üliõpilaste teadustööde riikliku konkursi tänukiri

OSALEMINE KONVERENTSIDEL

Mai 2018	Suuline ettekanne "Mechanisms of insulin fibrillization" Eesti Biokeemia Seltsi Kevadkooli raames, Paunküla Heaolukeskus; Harjumaa, Eesti
Oktoober 2012	Eesti Inimesegeneetika Ühingu Aastakonverents "Ülevaade geneetikast ja lähivaade südamehaigustele"; Haapsalu, Eesti
Oktoober 2011	Eesti Inimesegeneetika Ühingu Aastakonverents "Ülevaade geneetikast ja lähivaade neurogeneetikale"; Pärnu, Eesti
Juuni 2010	Posterettekanne "Zinc (II) ions inhibit fibrillization of monomeric insulin", 35th FEBS Congress "Molecules of life"; Göteborg, Rootsi

TÖÖKOGEMUS

01.08.2006-01.03.2018	Tallina Tehnikaülikool, Keemia ja biotehnoloogia instituut, spetsialist

PUBLIKATSIOONID

Noormägi, A.; Valmsen, K.; Tõugu, V.; Palumaa, P. "Insulin fibrillization at acidic and physiological pH values is controlled by different molecular mechanisms" (2015) The Protein Journal.; 34(6): 398-403

Tiiman, A., **Noormägi, A.**, Friedemann, M., Krishtal, J., Palumaa, P., Tõugu, V. "Effect of agitation on the peptide fibrillization: Alzheimer´s amyloid-beta peptide 1-42 but no amylin and insulin fibrils can grow under quiescent conditions" (2013) J Pept Sci.; 19(6): 386-391

Taler-Vercic, A., Kirsipuu, T., Friedemann, M., **Noormägi, A.**, Polajnar, M., Smirnova, J., Znidaric, M. T., Zganec, M., Skarabot, M.,Vilfan, A., Staniforth, R. A., Palumaa, P.,Zerovnik, E. "The role of initial oligomers in amyloid fibril formation by human stefin B" (2013) Int J Mol Sci.; 14(9): 18362-18384

Noormägi, A., Primar, K., Tõugu, V., Palumaa, P. "Interference of low-molecular substances with the thioflavin-T fluorescence assay of amyloid fibrils" (2011) J Pept Sci.; 18(1): 59-64

Noormägi, A., Gavrilova, J., Smirnova, J., Tõugu, V., Palumaa, P. "Zn(II) ions co secreted with insulin suppress inherent amyloidogenic properties of monomeric insulin" (2010) Biochem J.; 430(3): 511-518